

# An Update of the Parton Distributions for the LHC

Robert Thorne

October 30th, 2007



University College London

Royal Society Research Fellow

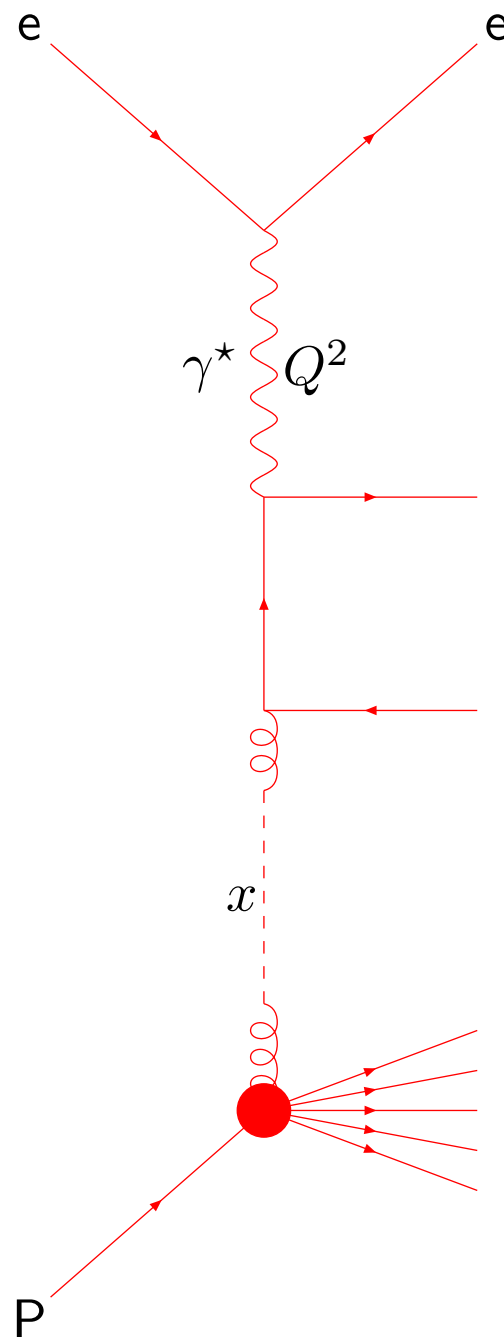
Strong force makes it difficult to perform analytic calculations of scattering processes involving hadronic particles.

The weakening of  $\alpha_s(\mu^2)$  at higher scales  $\rightarrow$  the **Factorization Theorem**.

Hadron scattering with an electron factorizes.

$Q^2$  – Scale of scattering

$x = \frac{Q^2}{2m\nu}$  – Momentum fraction of Parton ( $\nu$ =energy transfer)



perturbative  
calculable  
coefficient function  
 $C_i^P(x, \alpha_s(Q^2))$

nonperturbative  
incalculable  
parton distribution  
 $f_i(x, Q^2, \alpha_s(Q^2))$

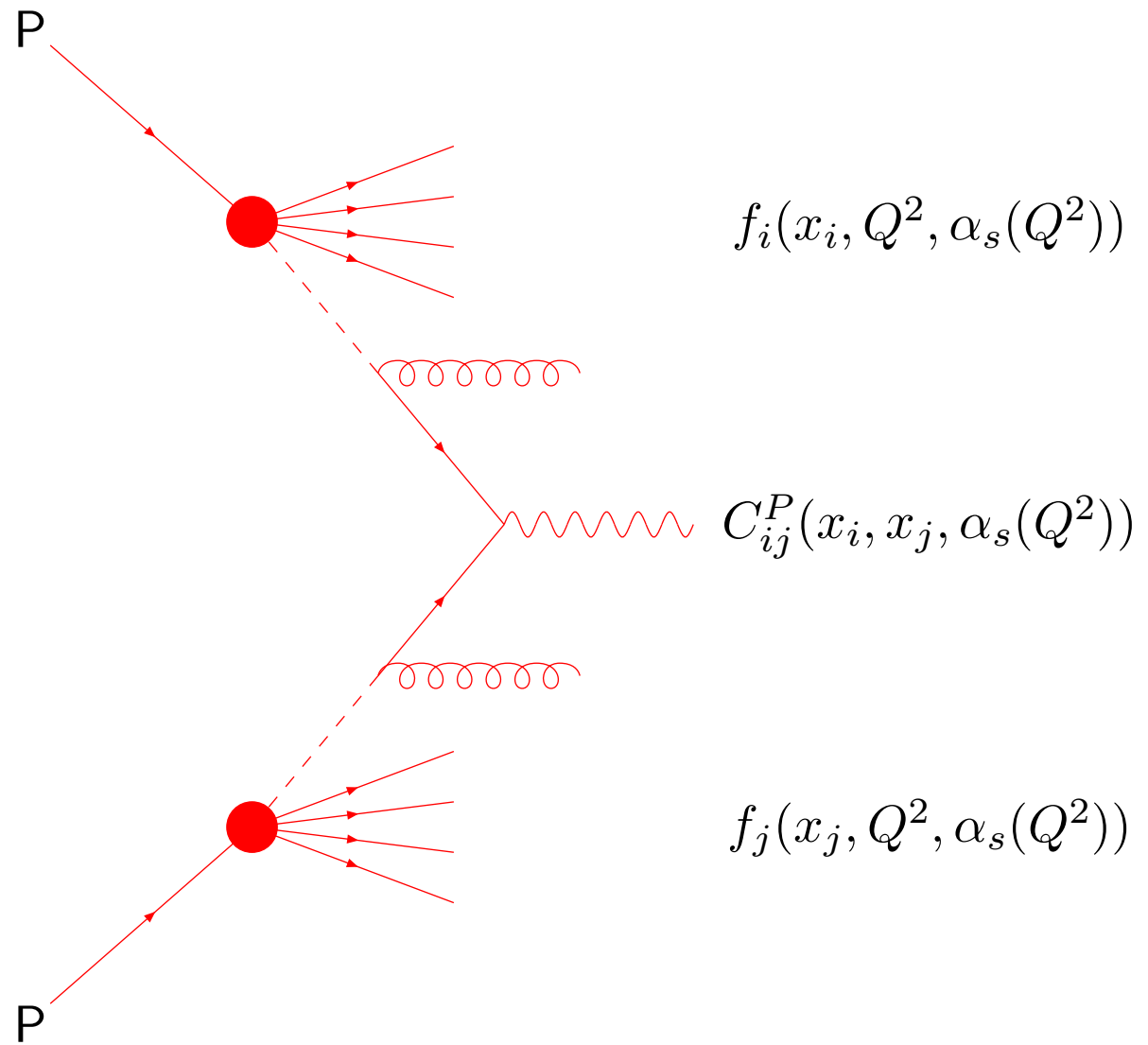
The coefficient functions  $C_i^P(x, \alpha_s(Q^2))$  are process dependent (**new physics**) but are calculable as a power-series in  $\alpha_s(Q^2)$ .

$$C_i^P(x, Q^2) = \sum_k C_i^{P,k}(x) \alpha_s^k(Q^2).$$

Since the parton distributions  $f_i(x, Q^2, \alpha_s(Q^2))$  are process-independent, i.e. **universal**, once they have been measured at one experiment, one can predict many other scattering processes.

Moreover, once  $Q^2$  is large enough they evolve with  $Q^2$  in a perturbative manner.

$$\frac{df_i(x, Q^2, \alpha_s(Q^2))}{d \ln Q^2} = \sum_j P_{ij} \otimes f_j.$$



Evolve partons upwards using **NLO** (or **NNLO**) **DGLAP** equations. Fit data for scales above  $2 - 5\text{GeV}^2$ . Need many different types of experiment for full determination.

**H1**  $F_2^{e^+p}(x, Q^2)$  1996-97 moderate  $Q^2$  and 1996-97 high  $Q^2$ , and  $F_2^{e^-p}(x, Q^2)$  1998-99 high  $Q^2$  small  $x$ . **ZEUS**  $F_2^{e^+p}(x, Q^2)$  1996-97 small  $x$  wide range of  $Q^2$ . 1999-2000 high  $Q^2$ . **H1** and **ZEUS**  $F_2^{c,b}(x, Q^2)$ .

**NMC**  $F_2^{\mu p}(x, Q^2)$ ,  $F_2^{\mu d}(x, Q^2)$ ,  $(F_2^{\mu n}(x, Q^2)/F_2^{\mu p}(x, Q^2))$ , **E665**  $F_2^{\mu p}(x, Q^2)$ ,  $F_2^{\mu d}(x, Q^2)$  medium  $x$ .

**BCDMS**  $F_2^{\mu p}(x, Q^2)$ ,  $F_2^{\mu d}(x, Q^2)$ , **SLAC**  $F_2^{\mu p}(x, Q^2)$ ,  $F_2^{\mu d}(x, Q^2)$  large  $x$ .

**CCFR**  $F_2^{\nu(\bar{\nu})p}(x, Q^2)$ ,  $F_3^{\nu(\bar{\nu})p}(x, Q^2)$  large  $x$ , singlet, valence.

**E605**, **E866**  $pN \rightarrow \mu\bar{\mu} + X$  large  $x$  sea.

**E866** Drell-Yan asymmetry  $\bar{u}, \bar{d}$   $\bar{d} - \bar{u}$ .

**CDF** W-asymmetry  $u/d$  ratio at high  $x$ .

**CDF D0** Inclusive jet data high  $x$  gluon.

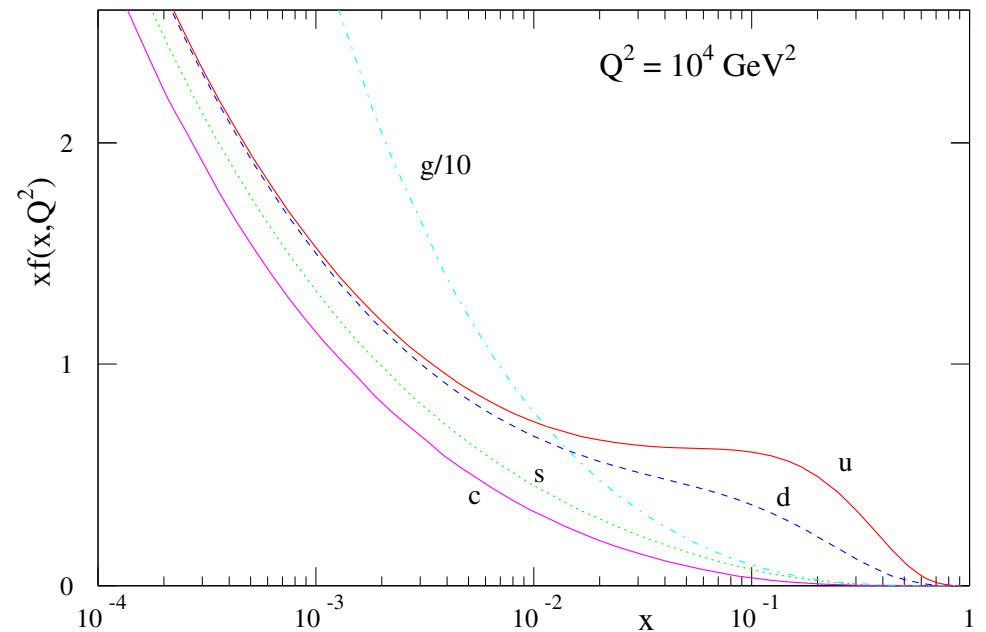
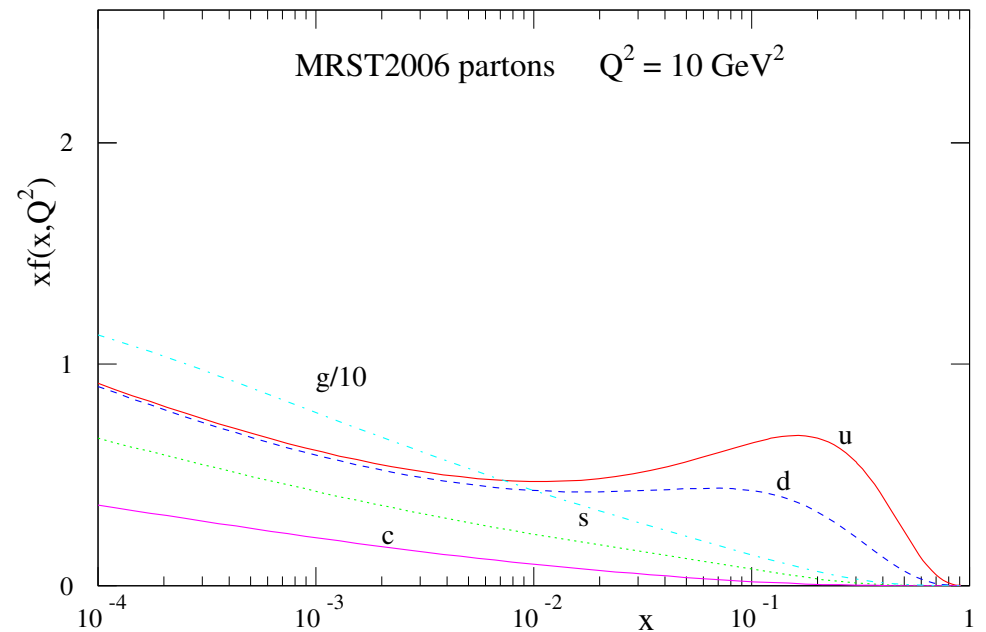
This procedure is generally successful and is part of a large-scale, ongoing project.

Results in partons of the form shown.

Various choices of partons – MRST (MSTW), CTEQ, Alekhin, ZEUS, H1

.....

All hadron collider (HERA, Tevatron, LHC) cross-sections rely on our understanding of these partons.



## Major update in people involved.

Dick Roberts completely retired from project.

Graeme Watt started as Responsive RA on parton distributions from April 1st 2006. Now making major contribution to project – responsible for many of these new results.

## Major changes in theory.

Implementation of updated heavy flavour VFNS, particularly at NNLO.

Already used a general VFNS since 1998 but change in details.

Inclusion of NNLO corrections (Anastasiou, Dixon, Melnikov, Petriello) Drell-Yan ( $W, Z$  and  $\gamma^*$ ) data using Vrap and FEWZ.

Change in definition of  $\alpha_S$ .

Improved nuclear corrections.

Some important changes as NLO  $\rightarrow$  NNLO. Most important change compared to previous NNLO – new VFNS.  $\rightarrow$  significant change in partons.

Implementation of fastNLO – fast perturbative QCD calculations Kluge, Rabbertz, Wobisch. Allows easy inclusion of new jet data.

## New data included.

NuTeV and CHORUS data on  $F_2^{\nu, \bar{\nu}}(x, Q^2)$  and  $F_3^{\nu, \bar{\nu}}(x, Q^2)$  replacing CCFR.

NuTeV and CCFR dimuon data included directly. Leads to a direct constraint on  $s(x, Q^2) + \bar{s}(x, Q^2)$  and on  $s(x, Q^2) - \bar{s}(x, Q^2)$ . Affects other partons.

CDFII lepton asymmetry data in two different  $E_T$  bins –  $25\text{GeV} < E_T < 35\text{GeV}$  and  $35\text{GeV} < E_T < 45\text{GeV}$ . D0II data for  $E_T > 20\text{GeV}$ .

CDFII (prel) and D0II data on  $d\sigma(Z)/dy$  for  $0 < y < 2.5$ .

HERA inclusive jet data (in DIS).

New CDFII high- $E_T$  jet data.

Direct high- $x$  data on  $F_L(x, Q^2)$ .

Update to include all recent charm structure function data.

Would like averaged HERA structure function data.

## Intermediate Update at NNLO

Recently updated partons at NNLO - officially MRST06. Fit to same data as MRST04 Produced for two reasons.

Previously only central values. No NNLO partons with uncertainties due to experimental errors.

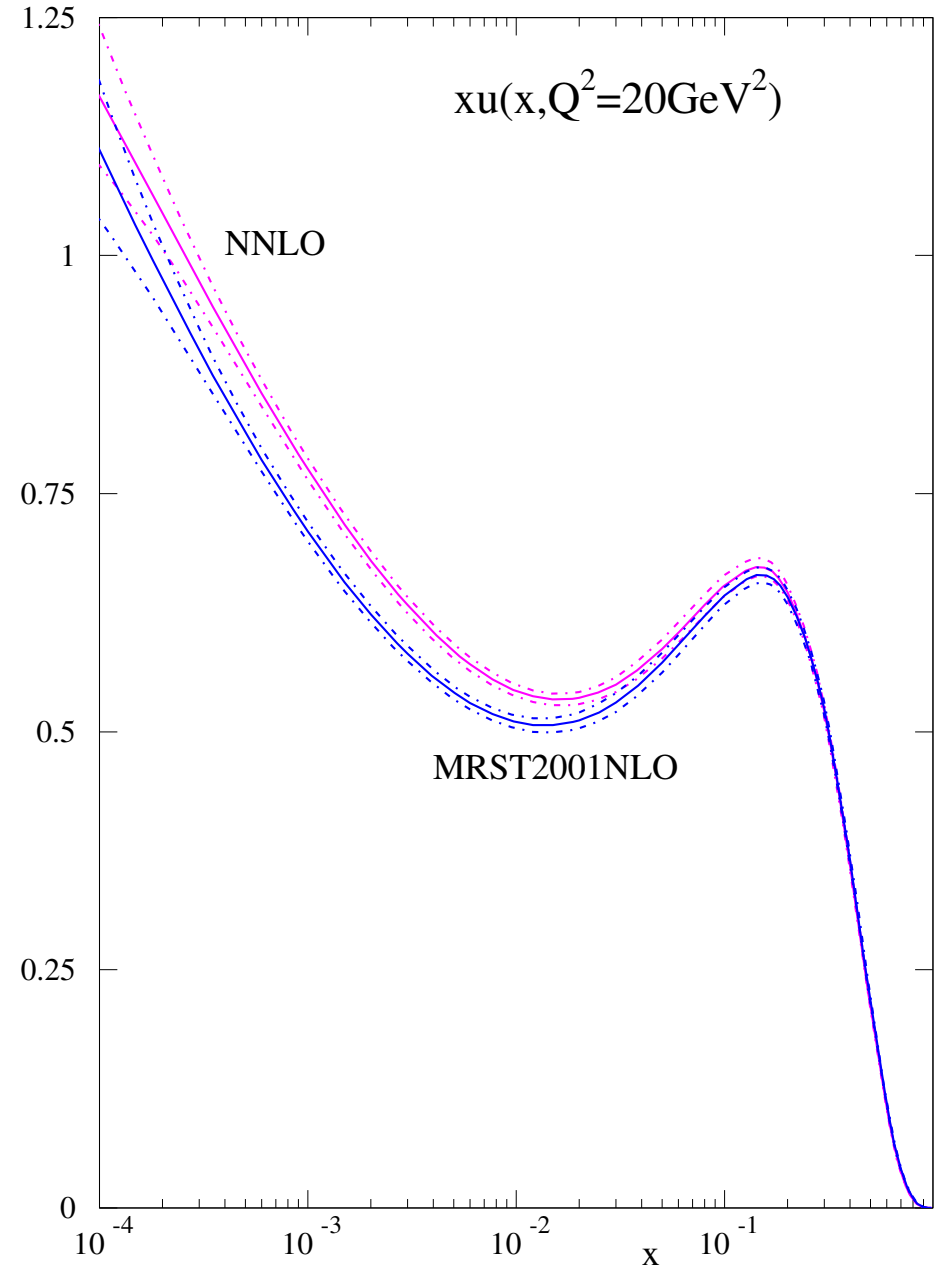
Same procedure as before – 15 eigenvector sets of partons and  $\Delta\chi^2 = 50$  for 90% confidence limit.

Example,  $u(x, Q^2)$  at NNLO compared to NLO.

Size of uncertainties similar to at NLO.

At small  $x$  effect of coefficient functions, particularly  $C_{2,g}(x, Q^2)$ , important.

Change from NLO to NNLO greater than uncertainty in each.



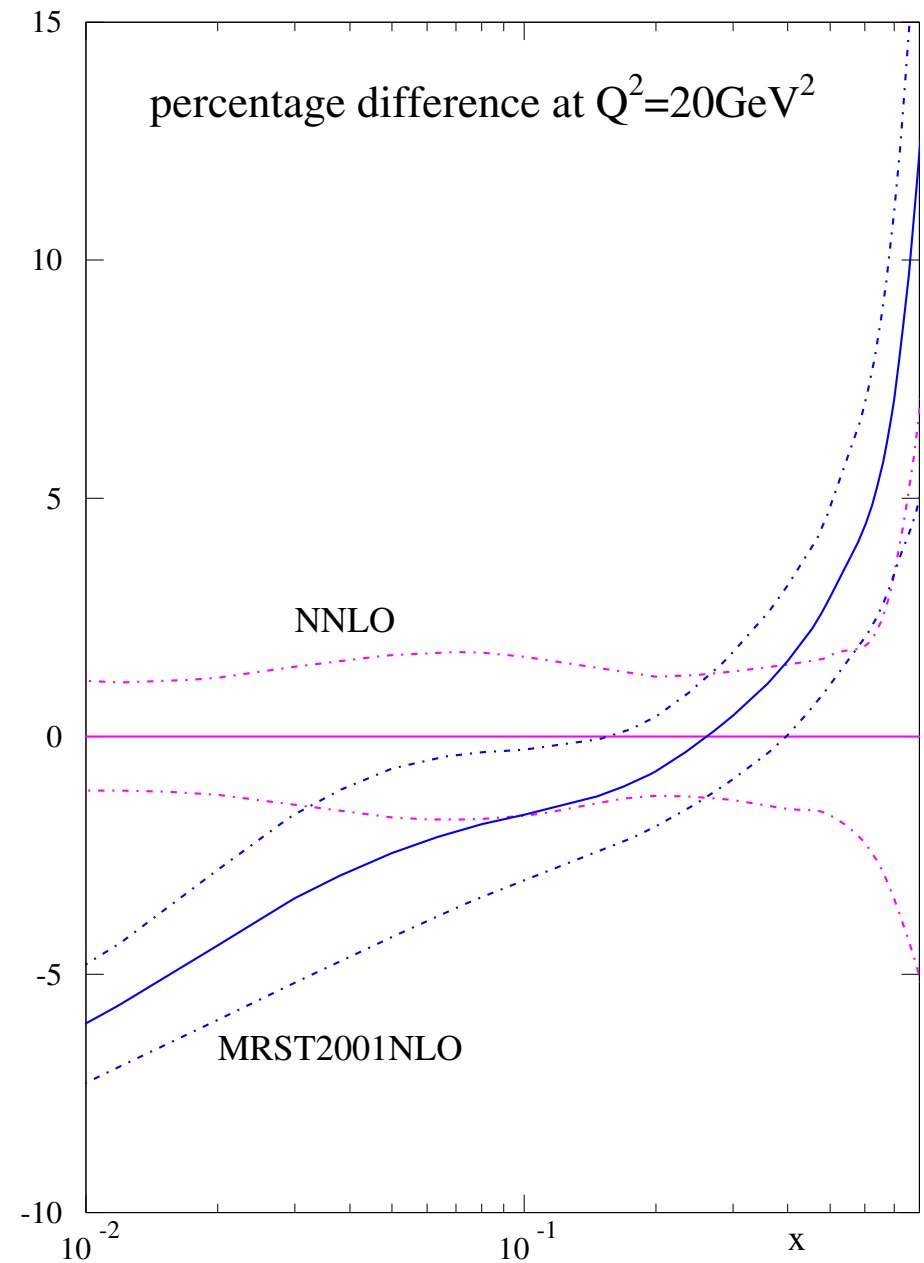


At large  $x$  coefficient functions important again,

$$C_{2,q}^{(2)}(x) \sim \left( \frac{\ln^3(1-x)}{1-x} \right)_+$$

Change from **NLO** to **NNLO** again larger than uncertainty in each.

No real change from **MRST2004NNLO** partons.

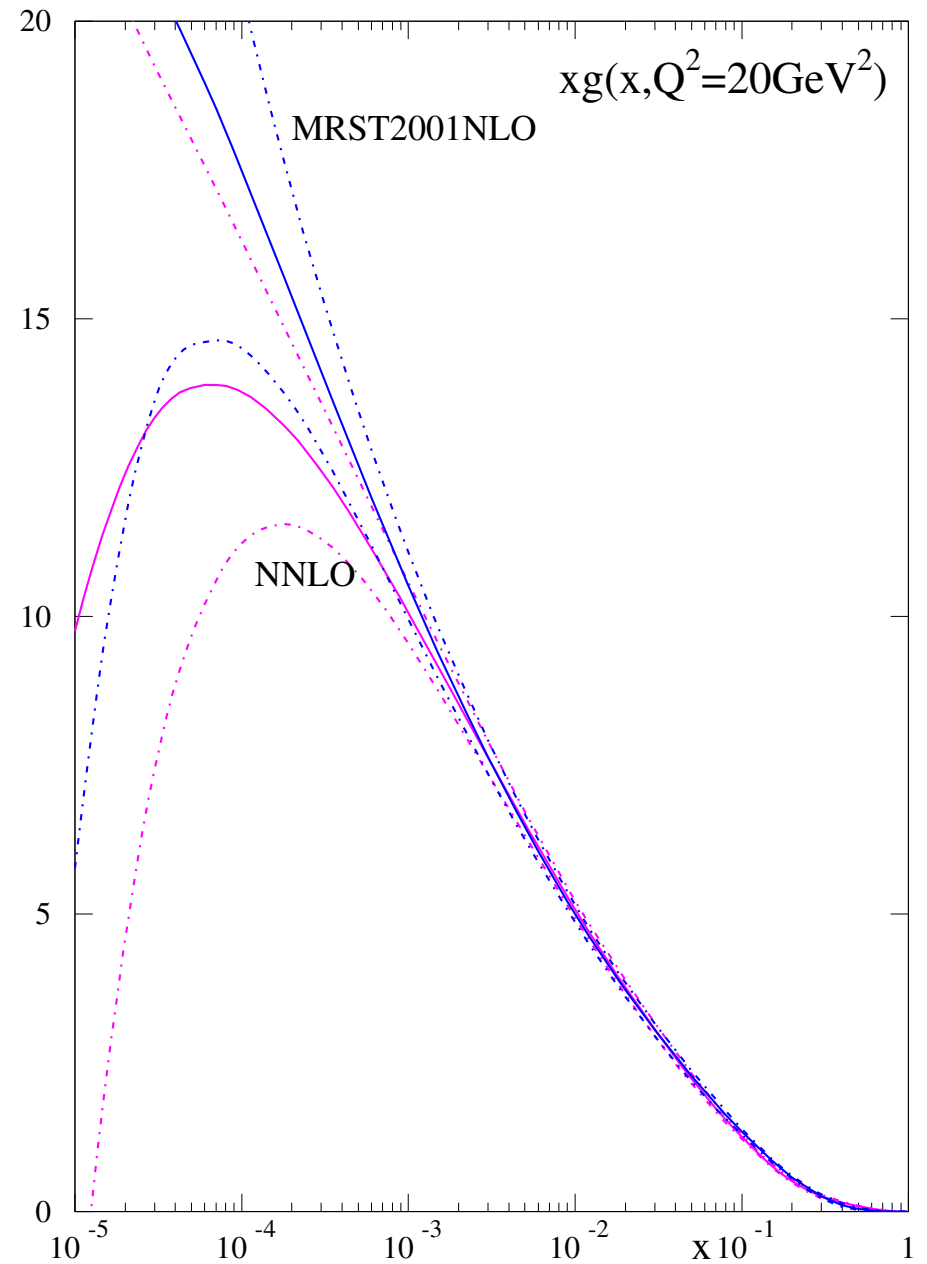


At small  $x$  effect of splitting functions particularly  $P_{qg}^{(2)}(x, Q^2)$  important.

Positive  $\ln(1/x)/x$  contribution at low  $x$ .

Affects gluon by fitting  $dF_2(x, Q^2)/d \ln Q^2$ .

Smaller at very low  $x$ .



Second reason for intermediate update of **NNLO** partons due to improvement to previous approximate treatment of heavy flavour.

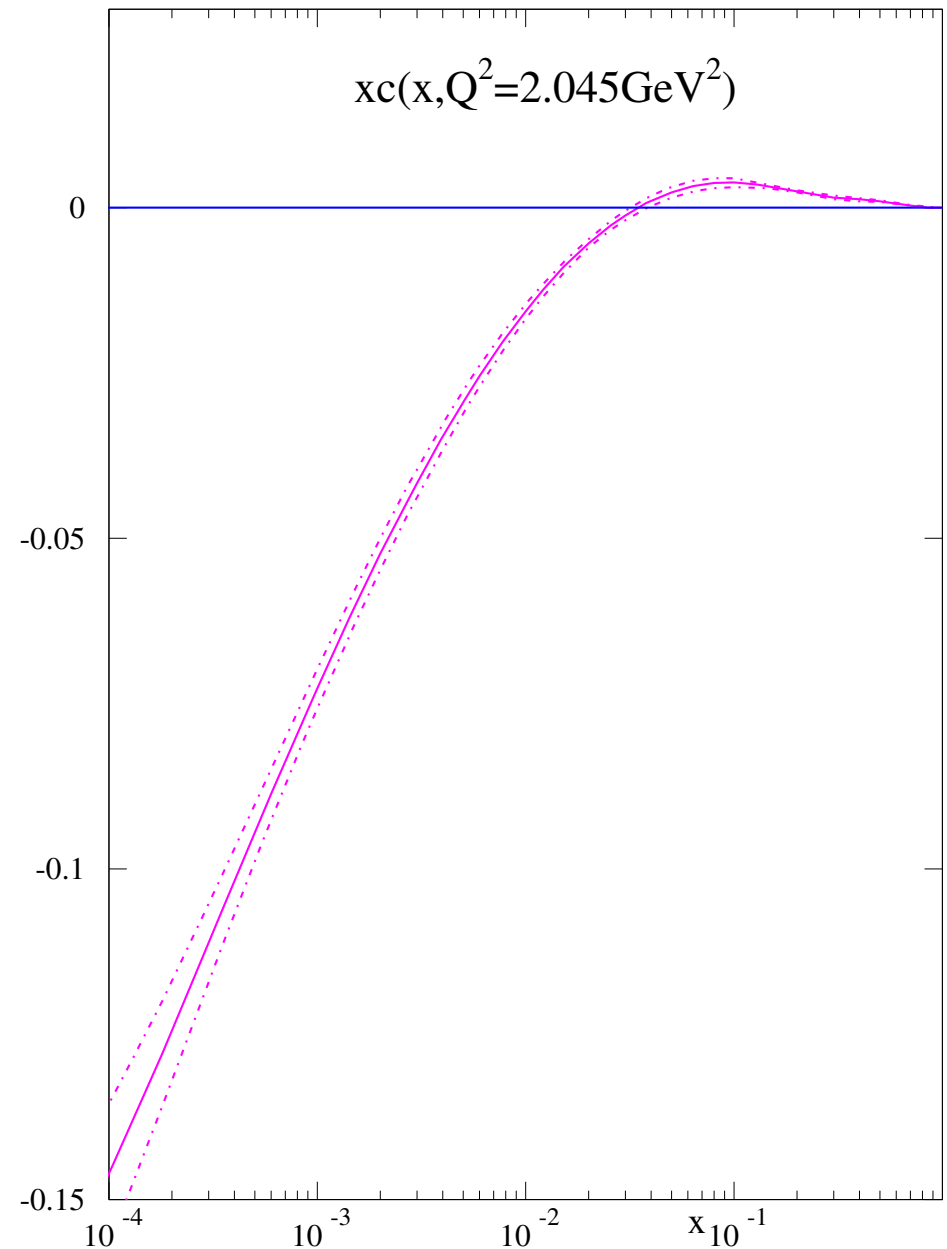
In reality at **NNLO** heavy flavour no longer turns on from zero at  $\mu^2 = m_c^2$

$$(c + \bar{c})(x, m_c^2) = A_{Hg}^{(2)}(m_c^2) \otimes g(m_c^2)$$

In practice turns on from negative value (for general gluon).

Also, previous approximation had no  $\mathcal{O}(\alpha_s^3)$  heavy quark coefficient functions.

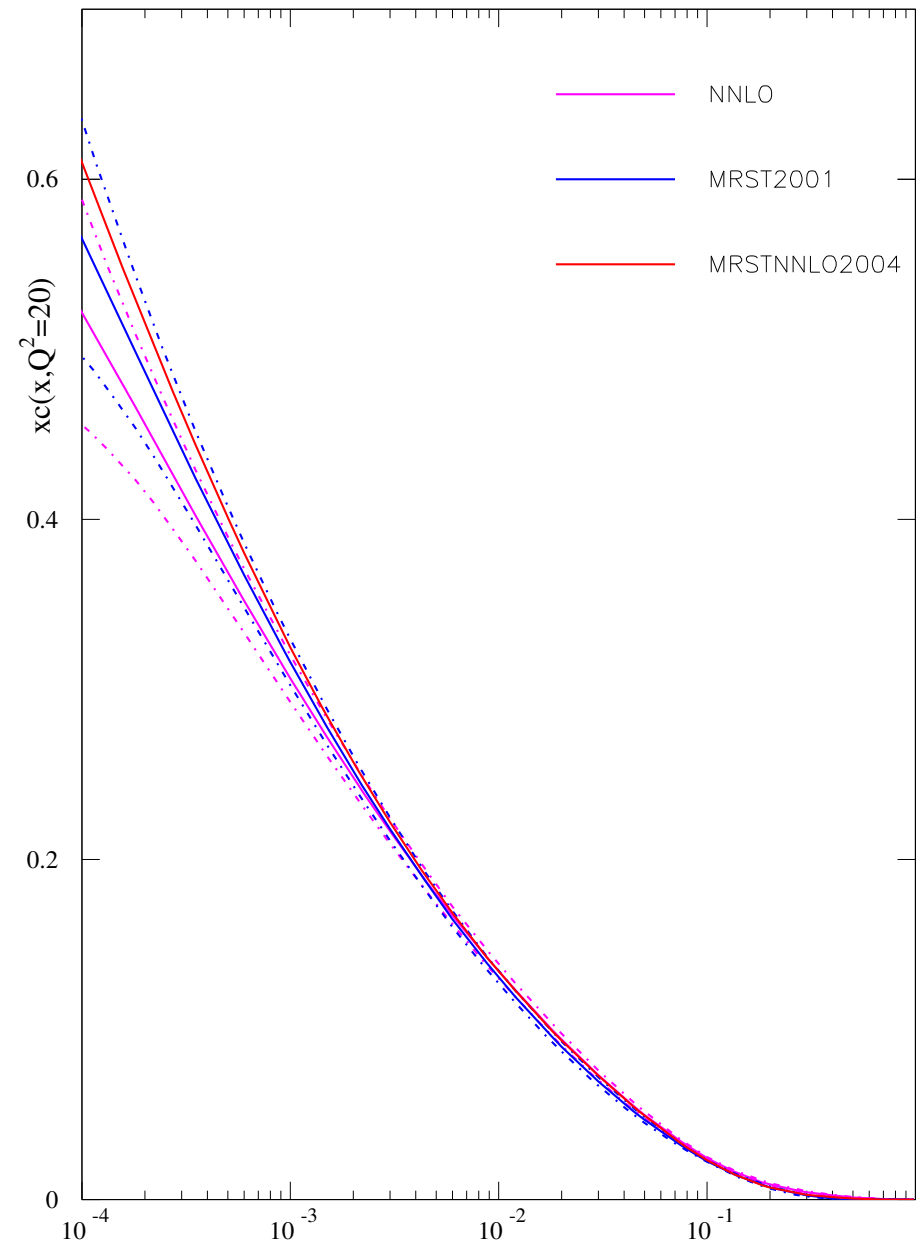
Now modelled using high and small- $x$  limits. Additional positive contribution at low  $Q^2$ .



At small  $x$  increased evolution from NNLO splitting function allows charm to catch up a bit with NLO which starts from zero at  $m_c^2$ .

Always lags a little at higher  $Q^2$

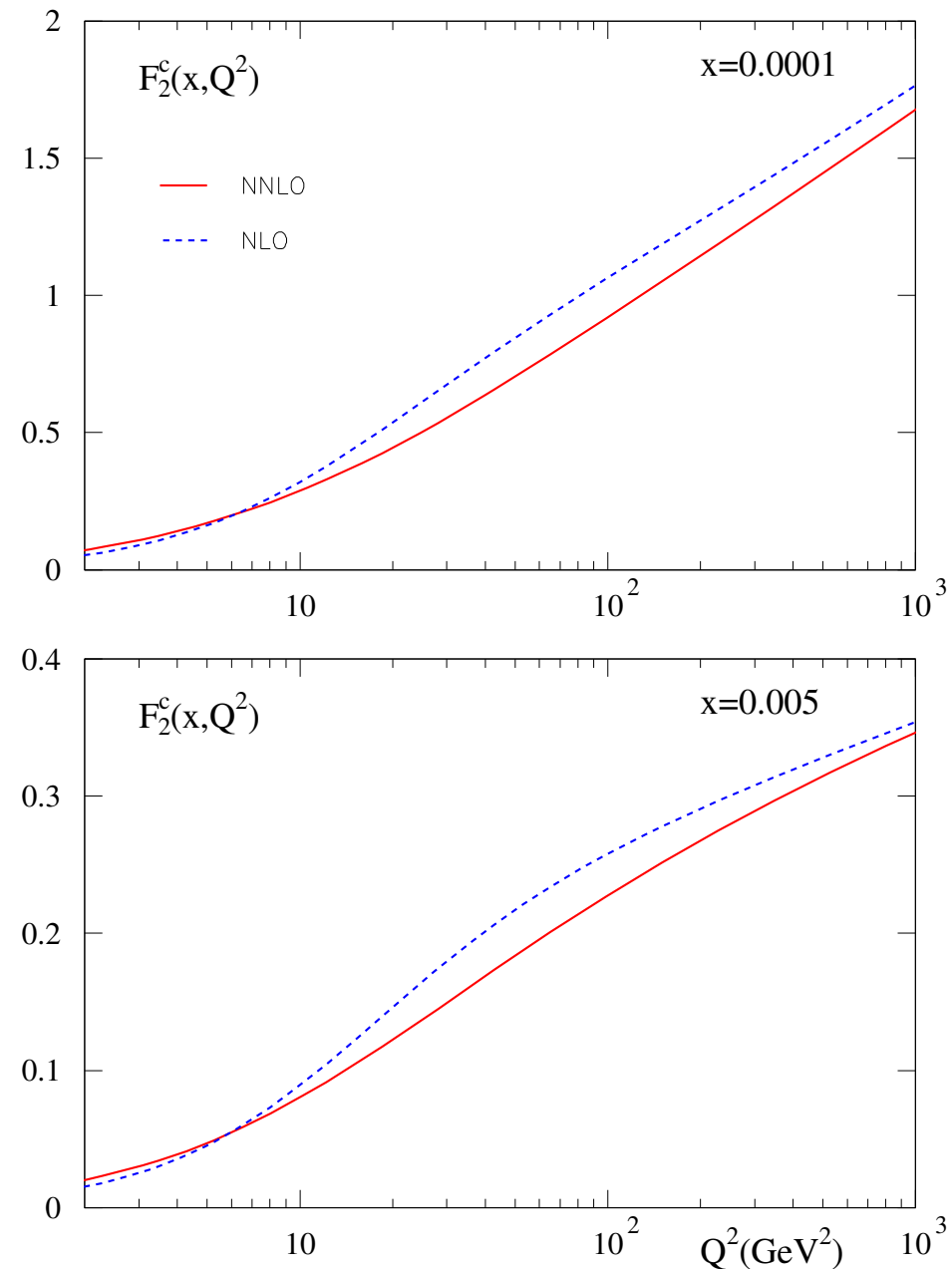
Significantly lags old approx MRST2004 distribution which turned on from zero.



NNLO  $F_2^c(x, Q^2)$  starts from higher value at low  $Q^2$ .

At high  $Q^2$  dominated by  $(c + \bar{c})(x, Q^2)$ . This has started evolving from negative value at  $Q^2 = m_c^2$ . Remains lower than at NLO for similar evolution.

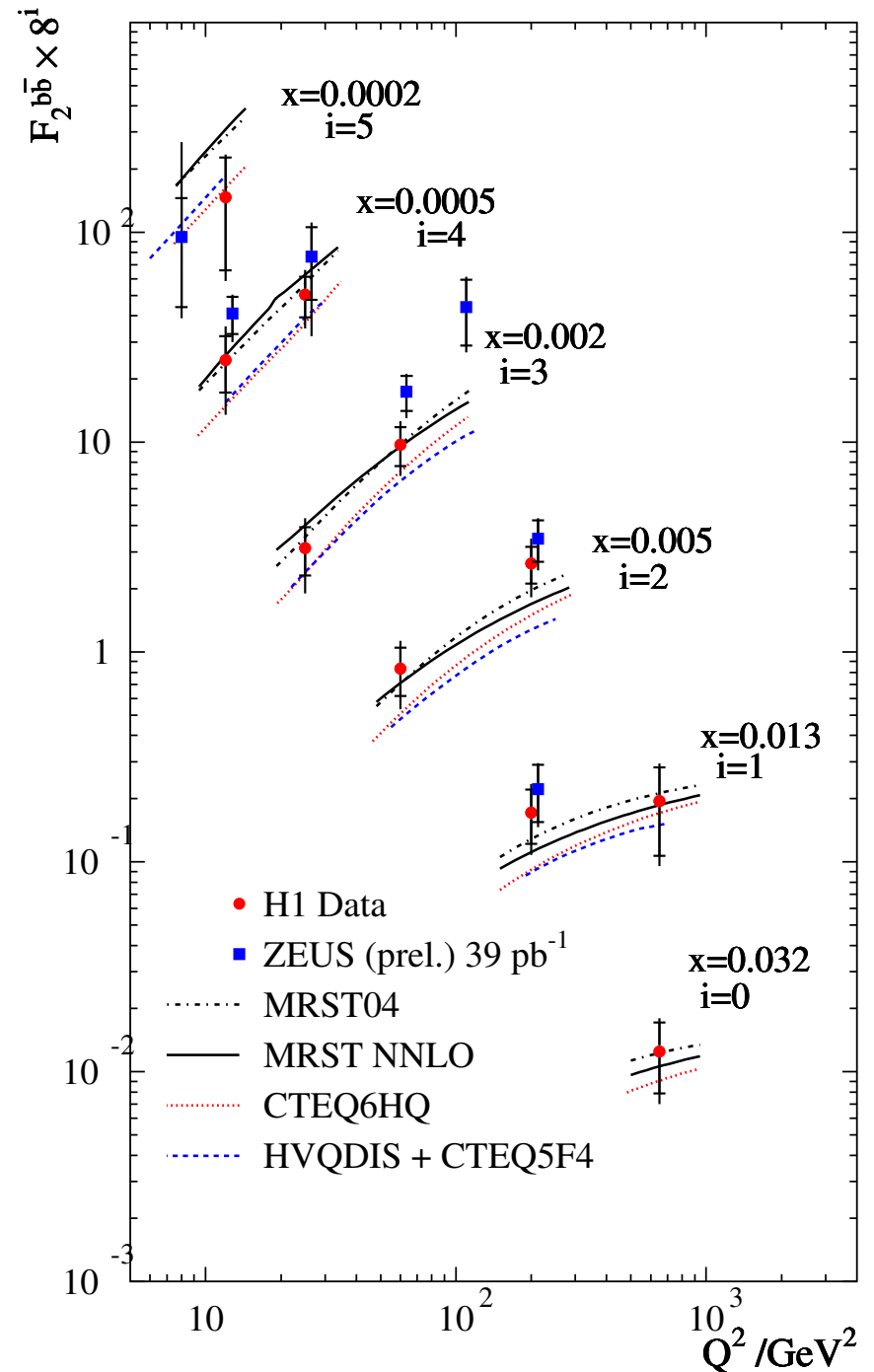
General trend –  $F_2^c(x, Q^2)$  flatter in  $Q^2$  at NNLO than at NLO. Important effect on gluon distribution going from one to other.



Good comparison to both H1 and ZEUS data on  $F_2^b(x, Q^2)$

The difference in the NLO predictions from MRST and CTEQ is due to details of definition of VFNS near threshold.

Both VFNS curves for  $m_b = 4.3\text{GeV}$ . Should be corrected to  $m_b = 4.75\text{GeV}$ . Lowers both prediction slightly, particularly at low  $Q^2$ .

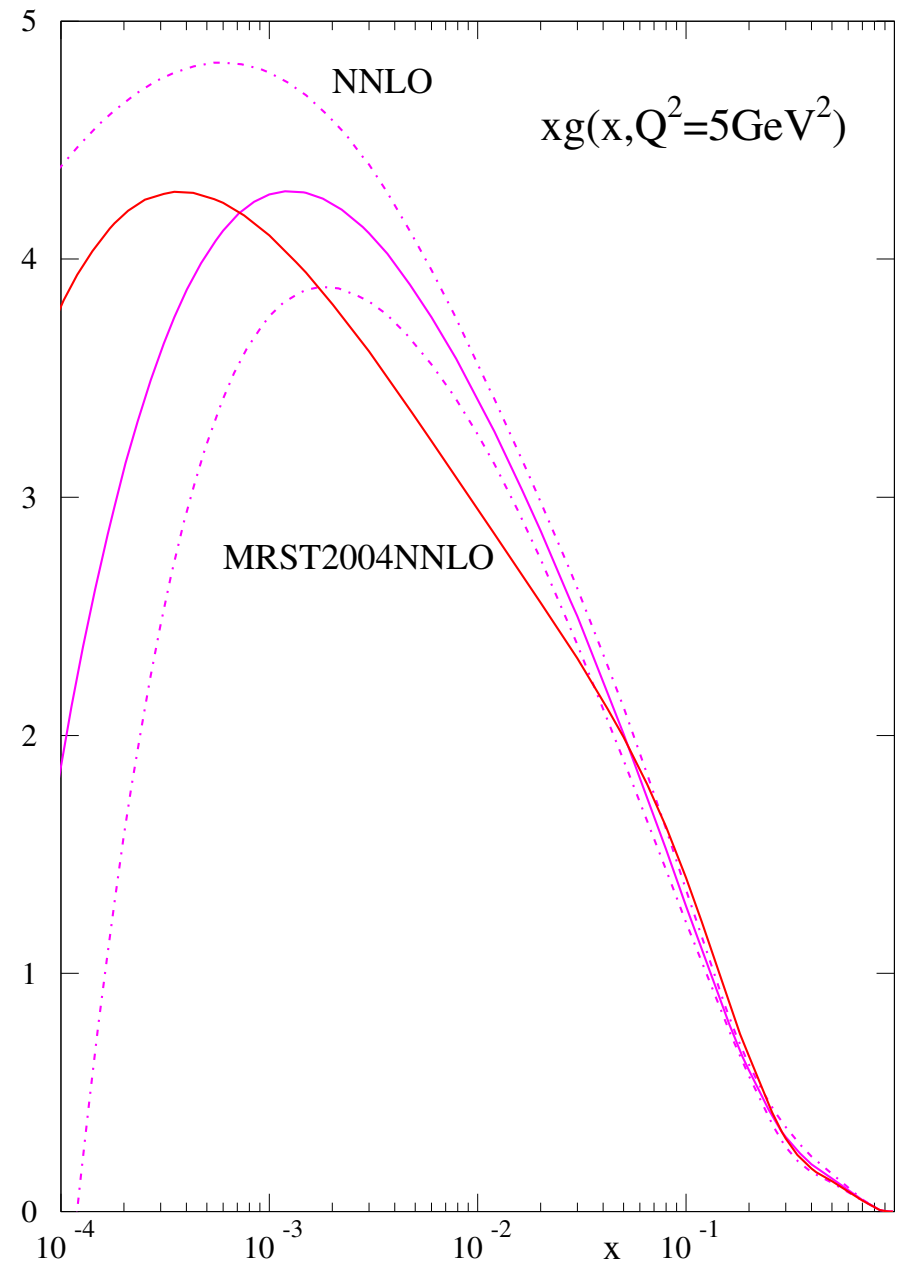


Difference in charm procedure affects gluon compared to approx MRST2004 NNLO fit.

Far more of a turnover at small  $x$ .

Change greater than uncertainty in some places. Correct heavy flavour treatment vital.

Requires larger coupling for increased evolution –  $\alpha_S(M_Z^2) = 0.119$ .



Comparison to other (Alekhin) NNLO gluon.

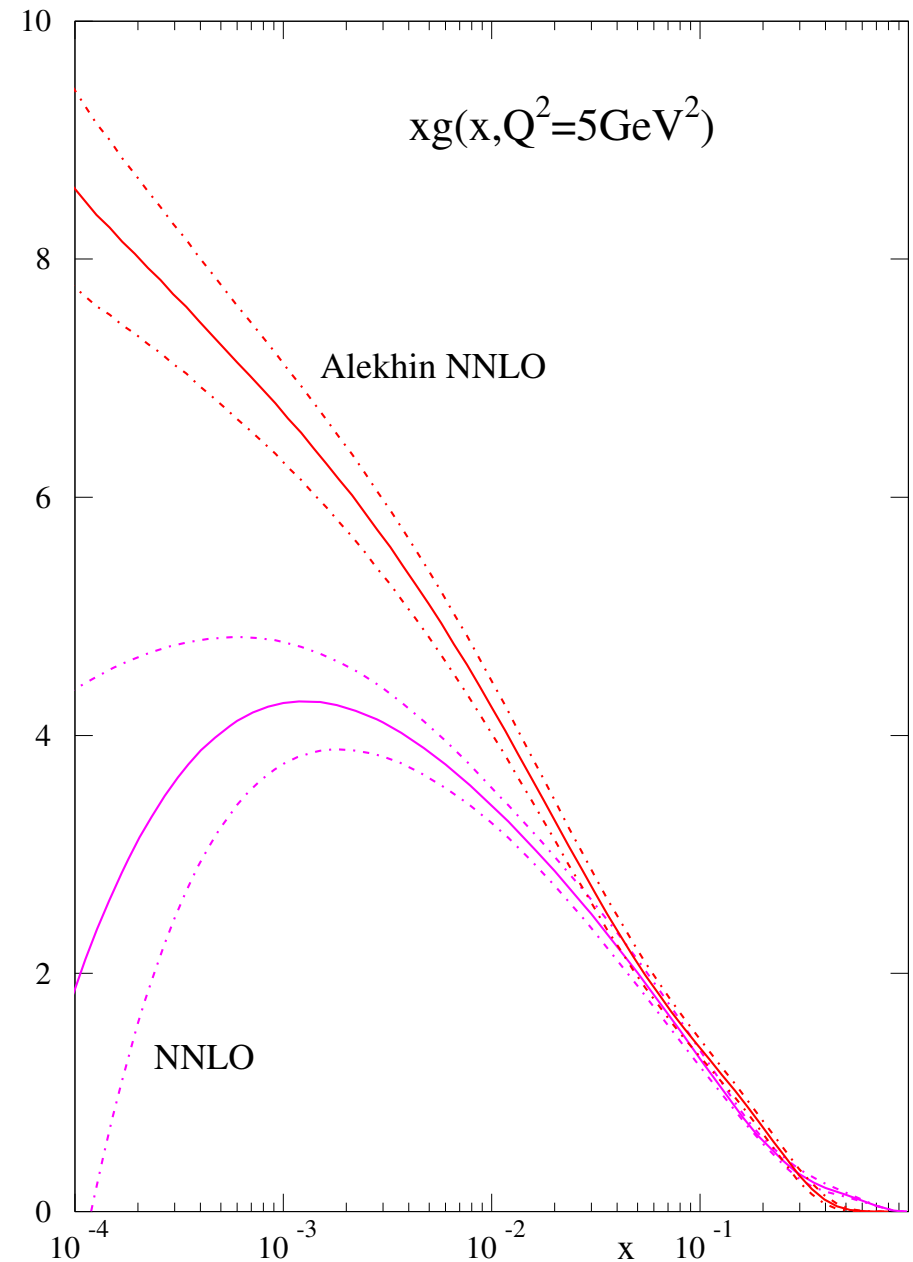
Hugely different at small  $x$ .

Differences much bigger than uncertainties.

Differences in heavy flavour treatments - disagreement on what constitutes definition of NNLO.

Differences in data fit and also in  $\alpha_S(M_Z^2)$  ( $\alpha_S(M_Z^2) = 0.114$ ).

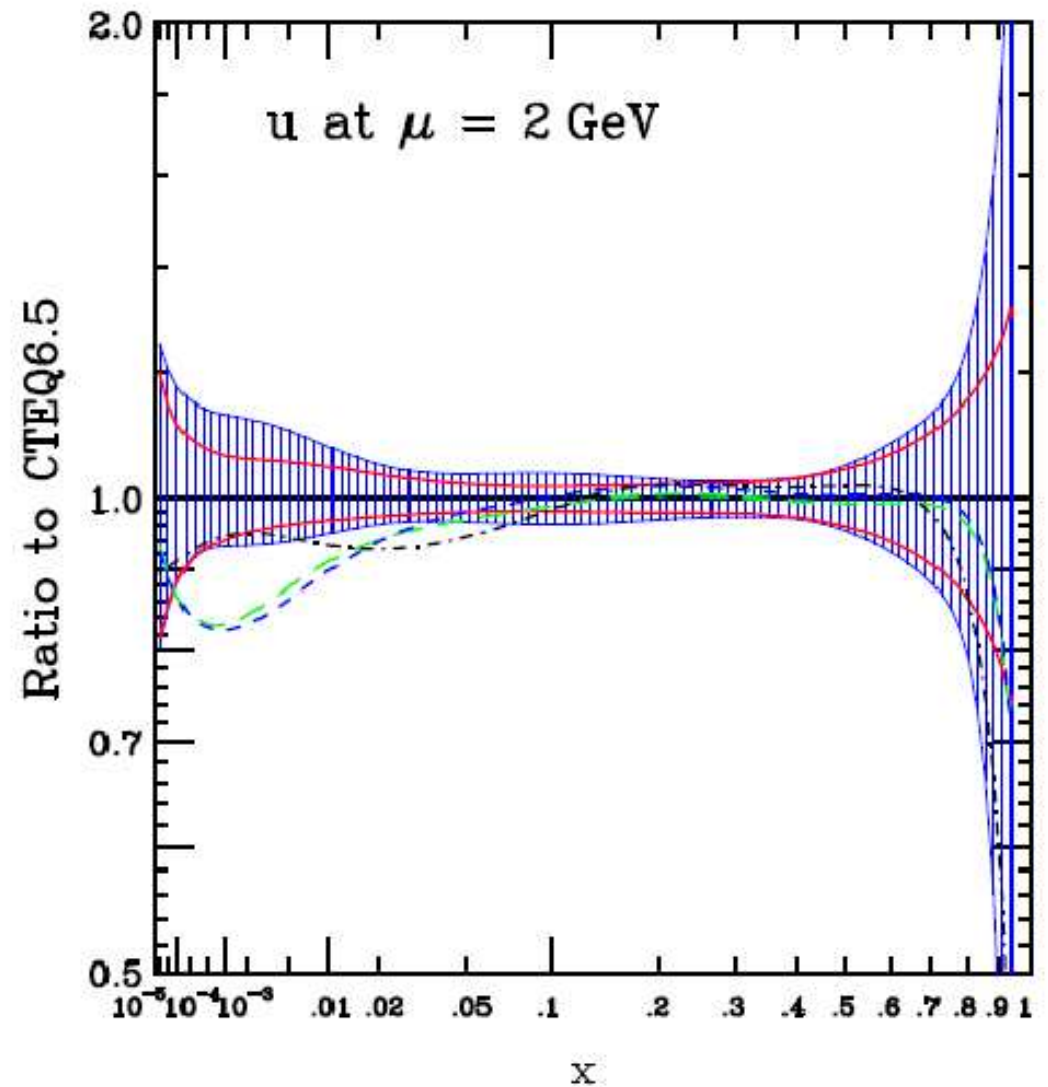
Note difference in uncertainty at low  $x$  not just in shape.



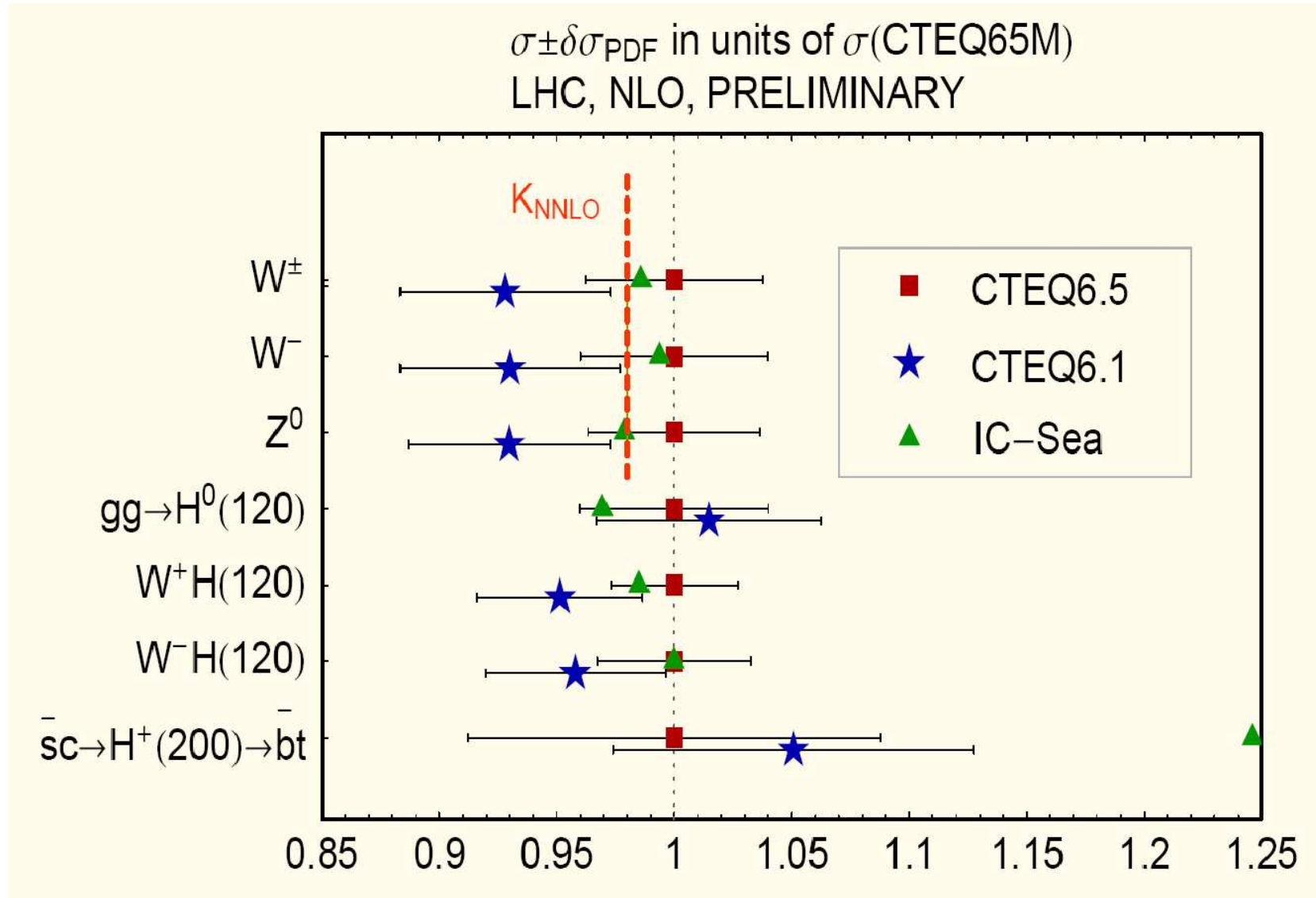


Importance of treating heavy flavour correctly illustrated by CTEQ6.5 up quark with uncertainties compared with previous versions, e.g. CTEQ6 in green.

MRST in dash-dot line. Reasonable agreement. Already used heavy flavour treatment in default sets.



Leads to large change in predictions using CTEQ partons at LHC



Some disagreements with MRST partons due to different gluon distributions.

Similar effect at NNLO with MRST partons.

Previous approximate NNLO sets used (declared) approximate VFNS at flavour thresholds.

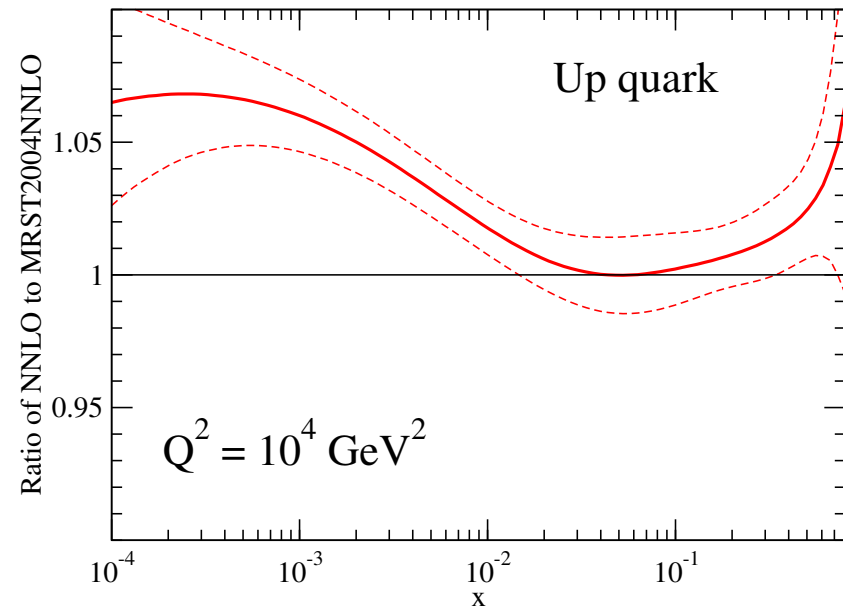
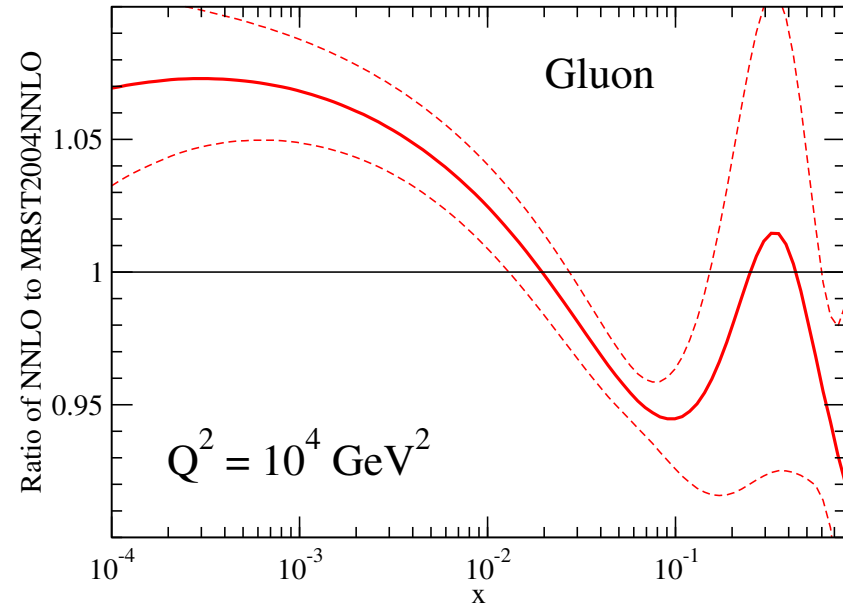
Full VFNS → flatter evolution of charm

→ bigger gluon and more evolution of light sea.

→ 6% increase in  $\sigma_W$  and  $\sigma_Z$  at the LHC.

With hindsight this and CTEQ result are corrections not uncertainty.

Very important changes nonetheless.



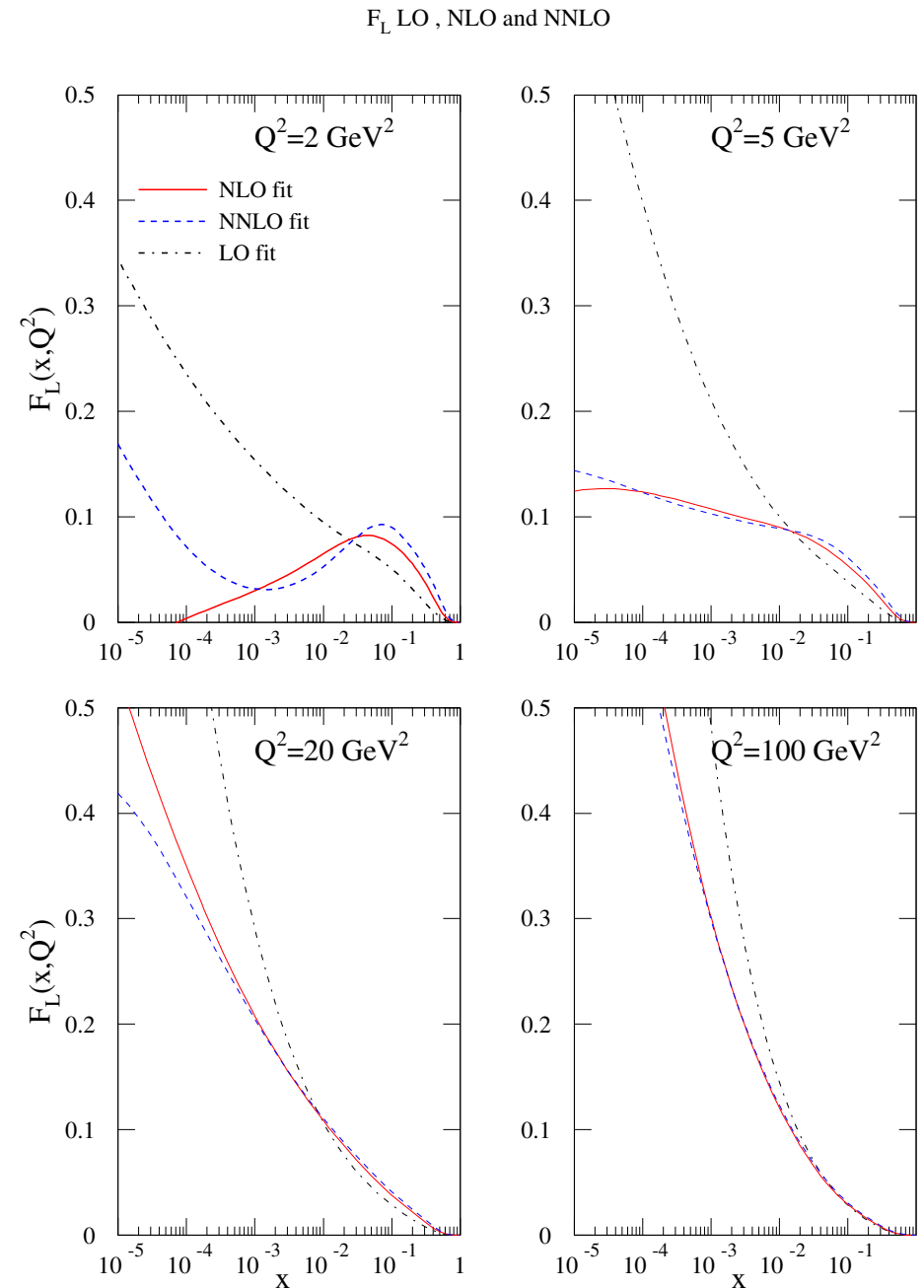
Instability in physical, gluon dominated, quantity  $F_L(x, Q^2)$  going from **LO**  $\rightarrow$  **NLO**  $\rightarrow$  **NNLO**.

Gluon at **NLO**  $\rightarrow$   $F_L(x, Q^2)$  dangerously small at smallest  $x, Q^2$ .

Note very large effect of exact **NNLO** coefficient function.

Possible sign of required  $\ln(1/x)$  corrections.

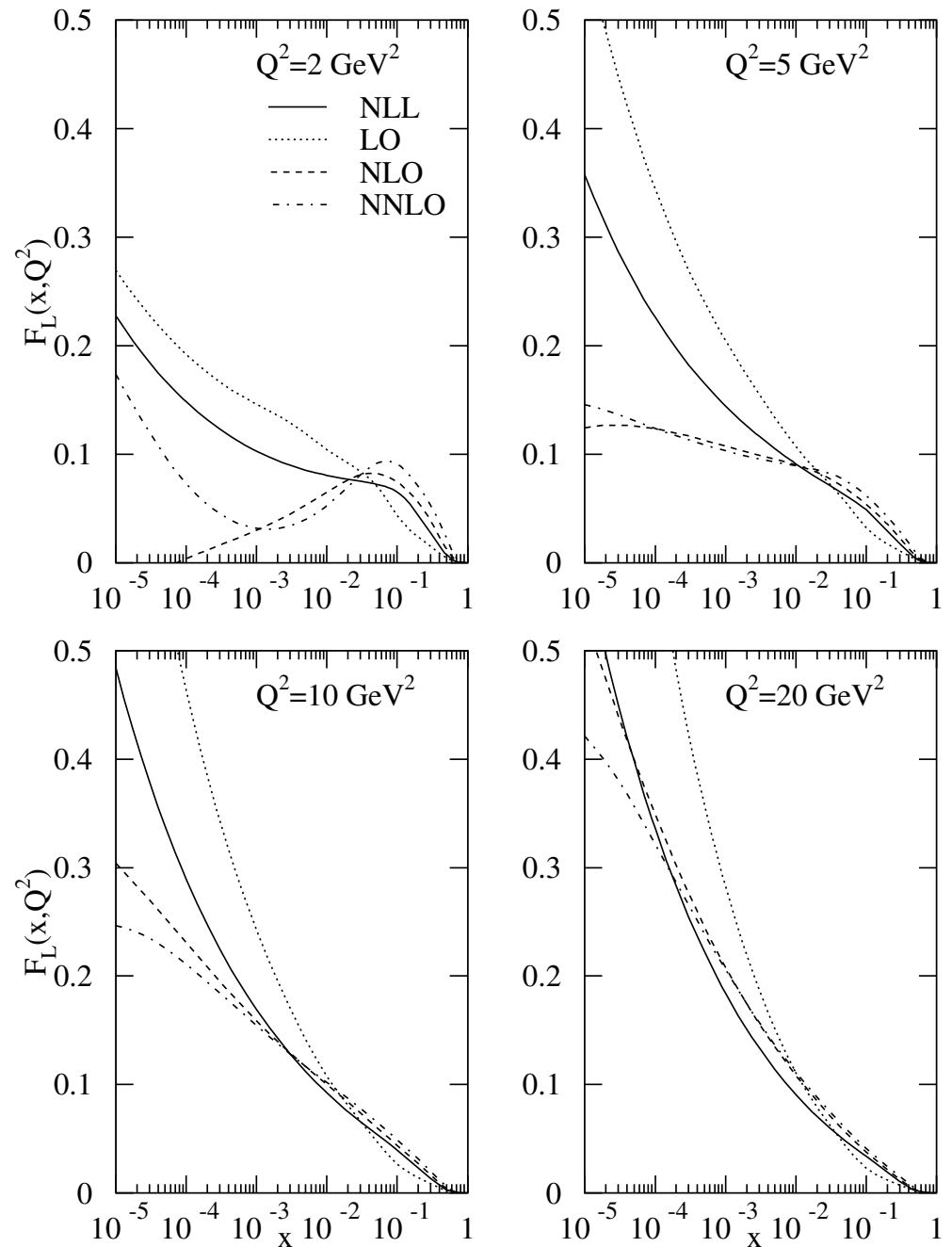
Similar problems possible for charm and/or bottom production, and low-mass **Drell-Yan** ( $\gamma$ ) production at the **LHC**.



Instability in physical, gluon dominated, quantity  $F_L(x, Q^2)$  going from LO  $\rightarrow$  NLO  $\rightarrow$  NNLO.

Improved by next-to-leading  $\ln(1/x)$  resummation in the global fit and prediction (White, RT).

HERA analysis of  $F_L(x, Q^2)$  will hopefully help us to determine best theoretical approach.



## Most recent Updates

Change in definition of  $\alpha_S$ . At **NLO** satisfies equation

$$\frac{\partial \alpha_S}{\partial \ln Q^2} = -\frac{\beta_0}{4\pi} \alpha_S^2 - \frac{\beta_1}{(4\pi)^2} \alpha_S^3,$$

where  $\beta_0 = 11 - 2/3 N_f$  and  $\beta_1 = 102 - 38/3 N_f$ .

Solve equation exactly. However, heavy flavour thresholds still allow for ambiguity. Previously **MRST** solved defining  $\Lambda_{QCD}$  via

$$\ln(Q^2/\Lambda_{QCD}^2) = \frac{4\pi}{\beta_0 \alpha_S} - \frac{\beta_1}{\beta_0^2} \ln \left[ \frac{4\pi}{\beta_0 \alpha_S} + \frac{\beta_1}{\beta_0^2} \right].$$

where  $\Lambda_{QCD}$  defined by case where  $N_f = 4$ . Extrapolate outside this range using

$$\frac{1}{\alpha_{S,5}(Q^2)} = \frac{1}{\alpha_{S,4}(Q^2, 5)} + \frac{1}{\alpha_{S,4}(m_b^2, 4)} - \frac{1}{\alpha_{S,4}(m_b^2, 5)}.$$

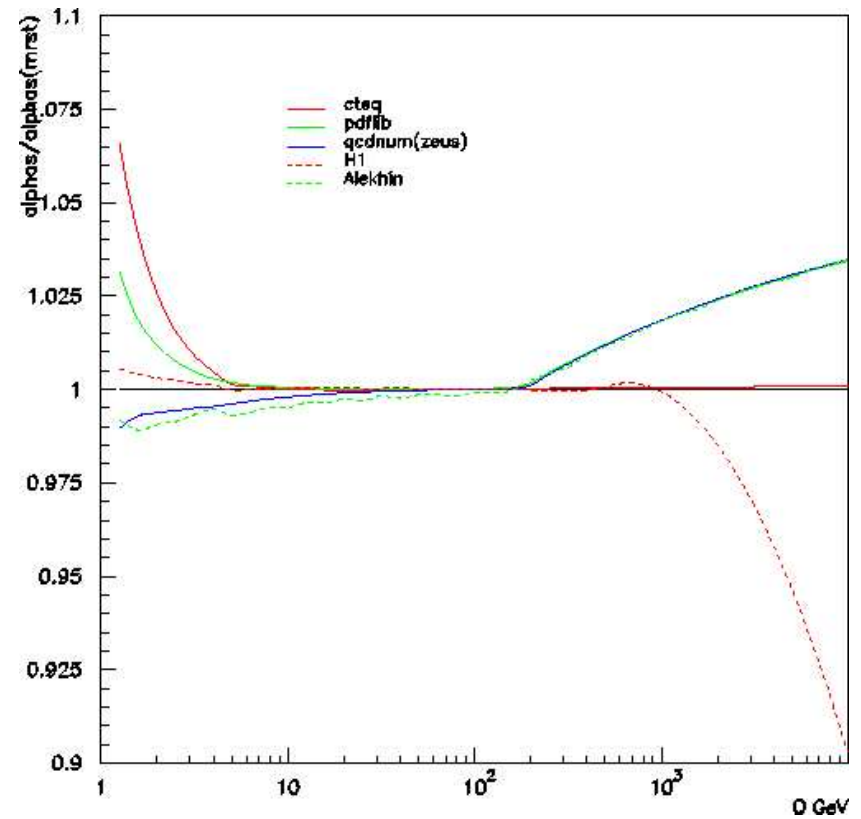
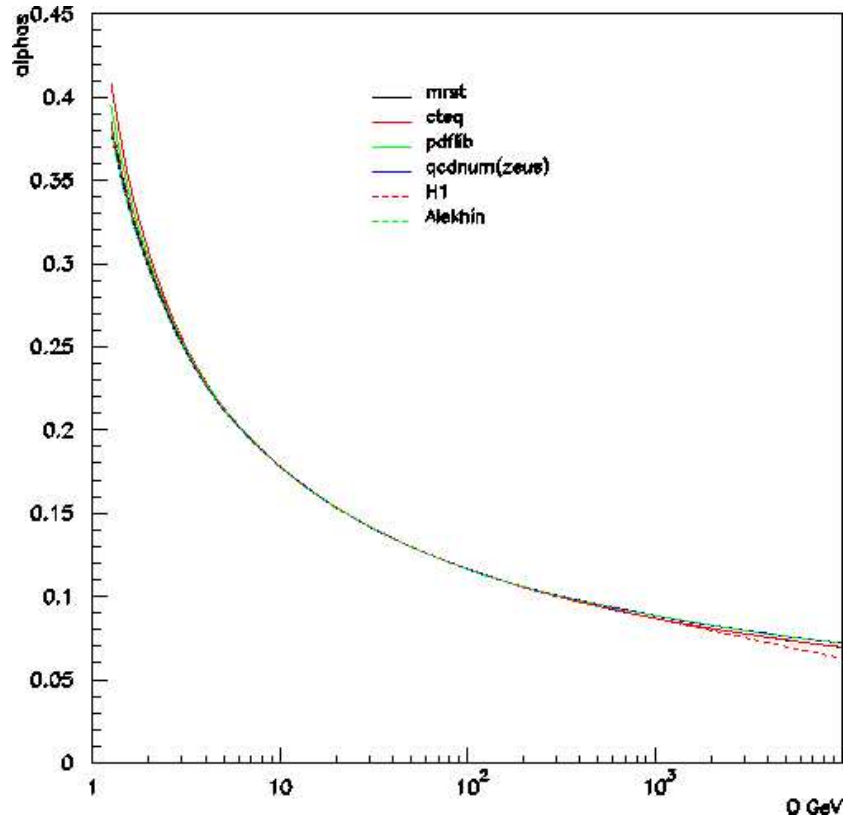
**QCDNUM** definition solves evolution equation using  $\alpha_S(M_Z^2)$  as boundary condition and changes  $N_f$  in equations at thresholds. Now adopt this definition.

Equivalent to higher orders but can differ by  $\sim 1\%$ .

Old **MRST** prescription not very wieldy for **NNLO**. Small errors (could be corrected) similar to size of ambiguity.

Variations in  $\alpha_S$  definitions shown at HERA-LHC 2005 Workshop by Whalley.

None wrong (except at very high  $Q^2$  maybe) just different choices.



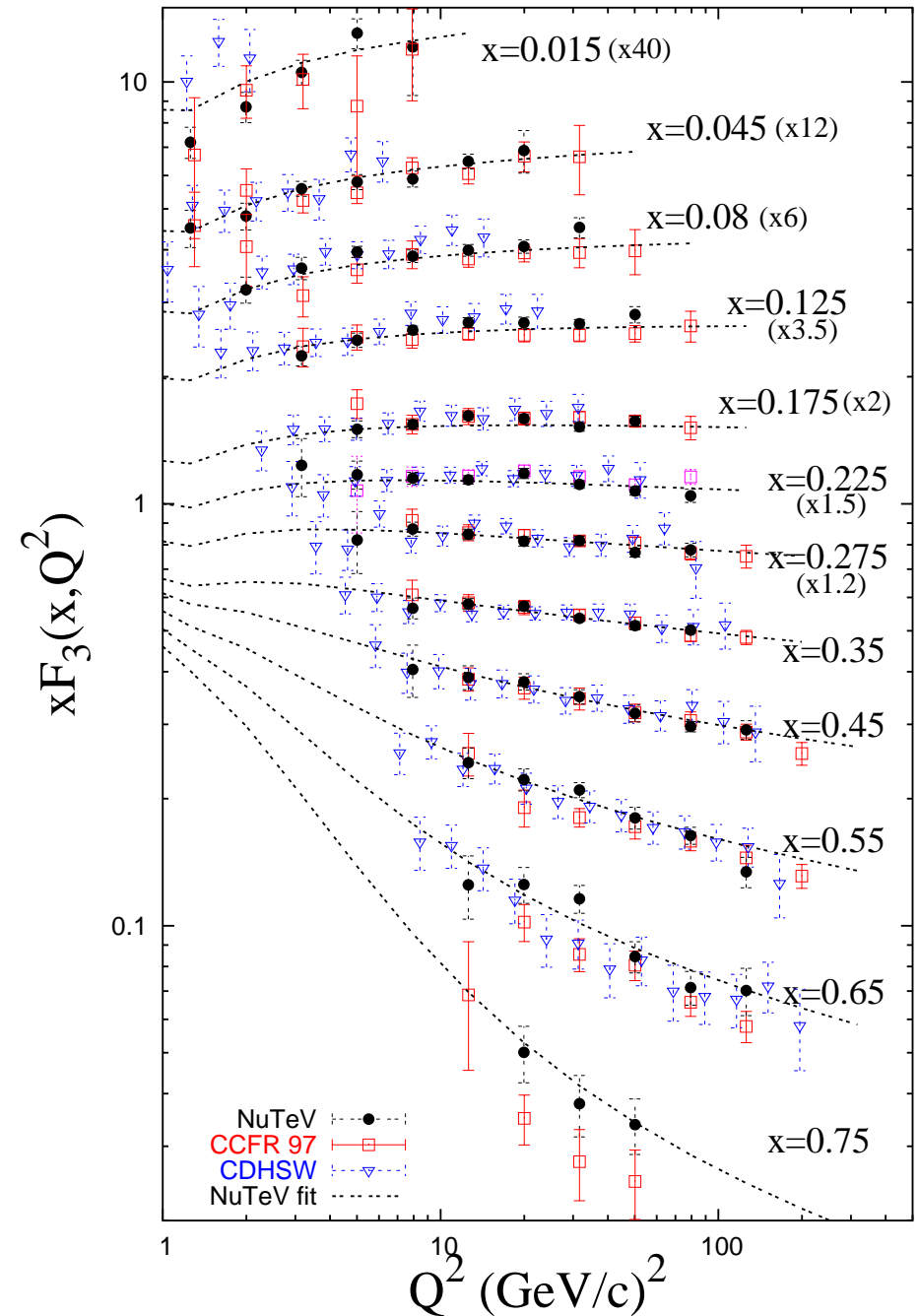
MSTW now use same definition as QCDNUM. Effectively input  $\alpha_S(Q_0^2)$  rather than  $\Lambda_{QCD}$ .

## New Data

New **NuTeV** data not completely compatible with the older **CCFR** data.

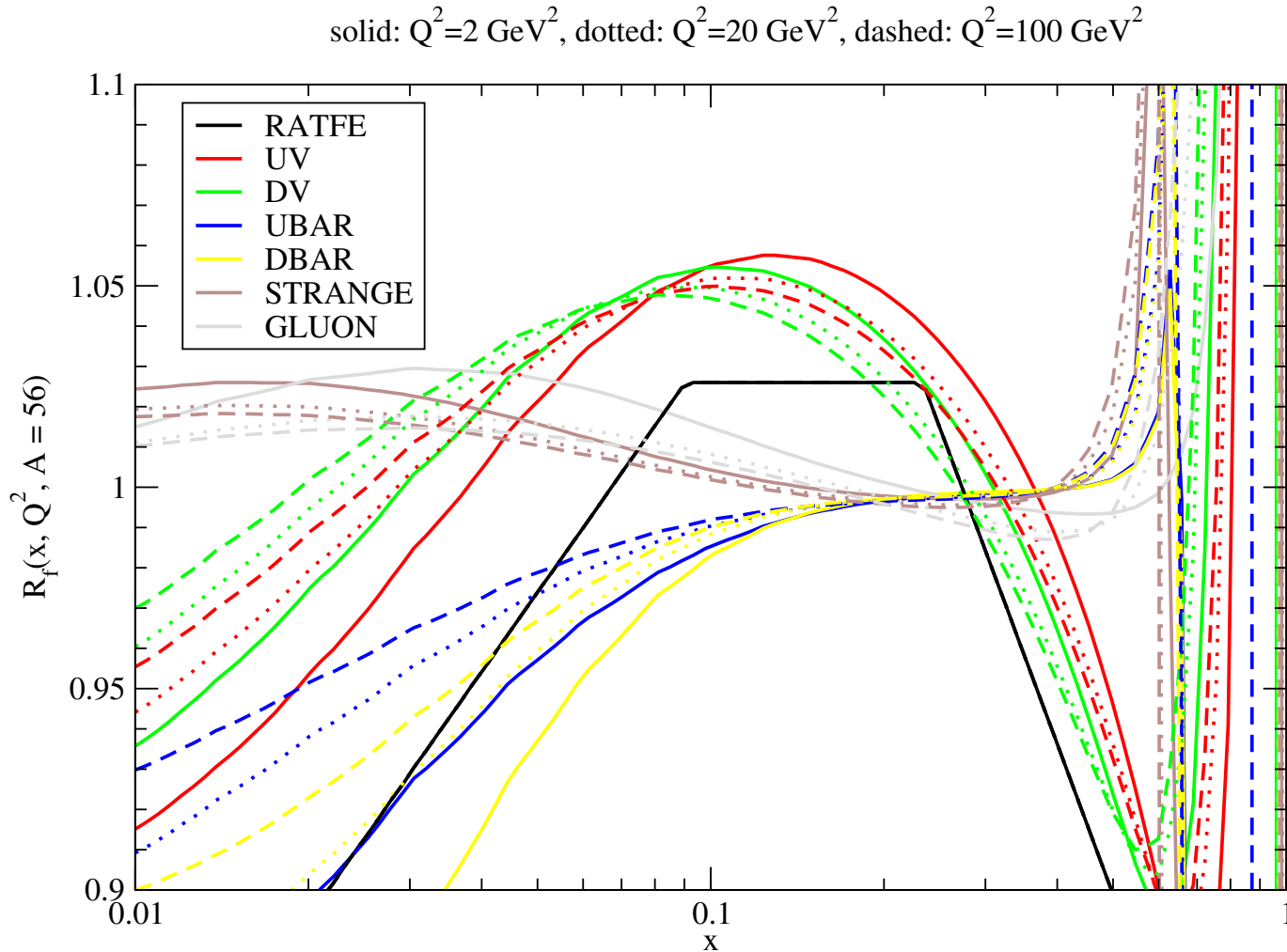
Main source of discrepancy is calibration of magnetic field map of muon spectrometer  $\rightarrow$  muon energy scale.

However, previous parton distribution fits were perfectly compatible with **CCFR** data using **EMC** inspired  $Q^2$  independent nuclear correction





Now implement far more sophisticated nuclear correction De Florian, Sassot. Extracted using **NLO** partons.



Same general shape as before. Allow  $\sim 3\%$  uncertainty on corrections. Cannot match high  $x$  NuTeV data.

CHORUS data also consistent with CCFR (lead not iron).

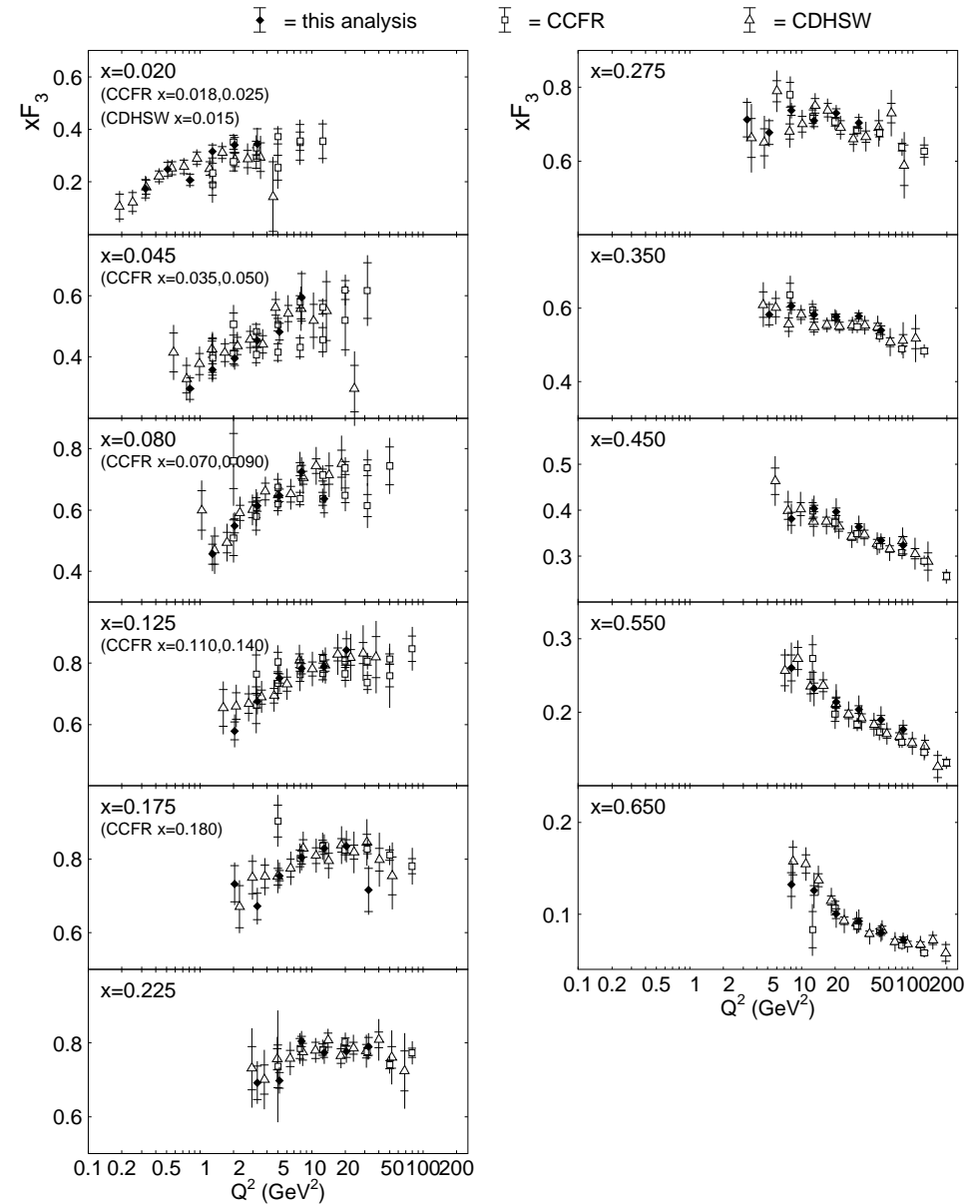
Inconsistencies at high  $x$ .

Partons in region of high  $x$  already well-determined from charged lepton structure functions.

Important information in the region  $x < 0.3$ , e.g. low  $x$  valence quarks - general consistency here.

Choose to cut neutrino structure function data for  $x \geq 0.5$ .

Also CHORUS data at lower  $W^2$ .  $F_3(x, Q^2)$  expected to have larger higher twist corrections than  $F_2(x, Q^2)$ , which we observe. Cut for  $W^2 \leq 20 \text{GeV}^2$ .



## CCFR/NuTeV dimuon cross-sections and strange quarks

$$\frac{d\sigma}{dx dy}(\nu_\mu(\bar{\nu}_\mu)N \rightarrow \mu^+\mu^-X) = B_c \mathcal{N} \mathcal{A} \frac{d\sigma}{dx dy}(\nu_\mu s(\bar{\nu}_\mu \bar{s}) \rightarrow c\mu^-(\bar{c}\mu^+)X),$$

$B_c$  = semileptonic branching fraction

$\mathcal{N}$  = nuclear correction

$\mathcal{A}$  = acceptance correction.

$\nu_\mu$  and  $\bar{\nu}_\mu$  cross-sections probe  $s$  and  $\bar{s}$  (small mixing with  $d$  and  $\bar{d}$ ).

Have previously indirectly used CCFR data to parameterise strange according to

$$s(x, Q_0^2) = \bar{s}(x, Q_0^2) = \frac{\kappa}{2}[\bar{u}(x, Q_0^2) + \bar{d}(x, Q_0^2)] \quad \kappa \approx 0.5$$

Now fit strange directly rather than assuming same shape as average of  $\bar{u} + \bar{d}$  at input and some **fixed** fraction.

Also allow possibility of  $s(x, Q_0^2) \neq \bar{s}(x, Q_0^2)$ .

Make definitions at input

$$s^+(x, Q_0^2) \equiv s(x, Q_0^2) + \bar{s}(x, Q_0^2) = A_+(1-x)^{\eta_+} S(x, Q_0^2)$$

$$s^-(x, Q_0^2) \equiv s(x, Q_0^2) - \bar{s}(x, Q_0^2) = A_-(1-x)^{\eta_-} x^{-1+\delta_-} (1-x/x_0)$$

where  $S(x, Q_0^2)$  is the total sea distribution and  $x_0$  is determined by zero strangeness of proton, i.e.

$$\int_0^1 dx s^-(x, Q_0^2) = 0.$$

Extra freedom in both  $s^+$  and  $s^-$  confirmed by fit.

Compared to  $s = \bar{s} = (\bar{u} + \bar{d})/4$  letting  $s^+$  free,  $s^- = 0 \rightarrow \Delta\chi^2 \sim -15$  with improvement mainly in dimuon data.

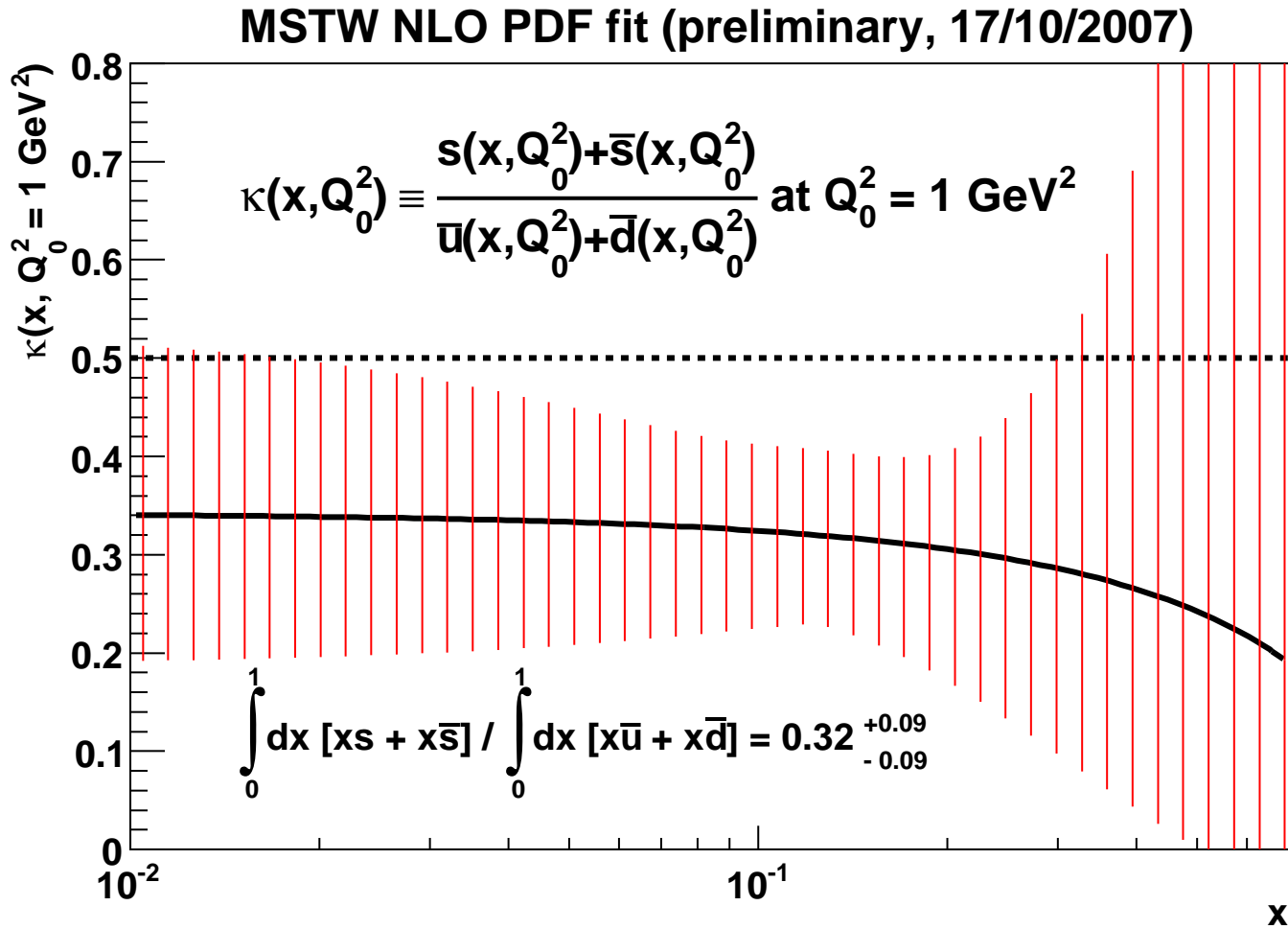
Letting both  $s^+$  free and  $s^-$  free  $\rightarrow \Delta\chi^2 \sim -30$  with improvement even more restricted to dimuon data.

No real improvement with further parameters.

Data generally prefer  $s^+$  free. Dimuon data only affected by  $s^-$ . Decoupled from other parameters to good approximation.  $\delta_- = 0.2$  fixed, i.e. valence-like value.

Find reduced ratio of strange to non-strange sea compared to previous default  $\kappa = 0.5$ .

Suppression at high  $x$ , i.e. low  $W^2$ . Effect of  $m_s$ ?

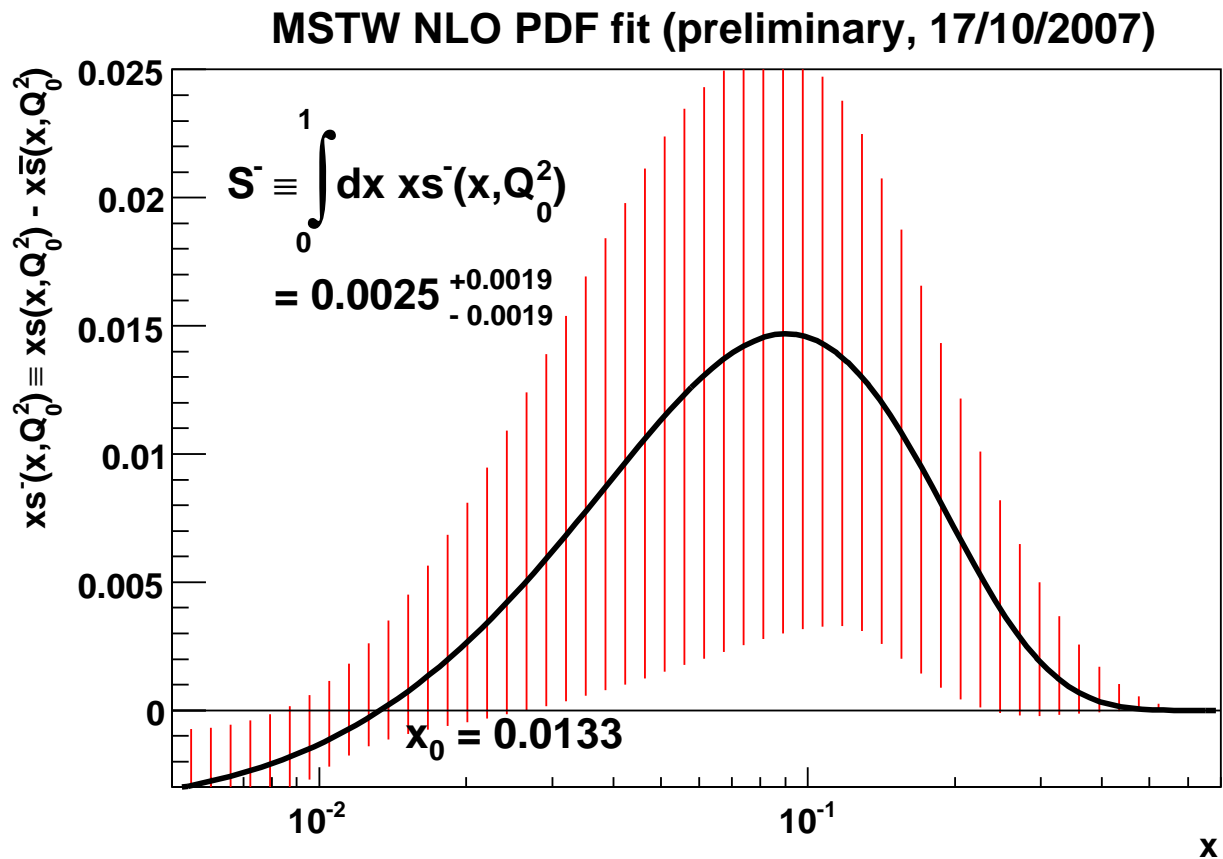


(Probably) similar at NNLO. Being finalised.

Strange sea asymmetry  $xs(x, Q_0^2) - x\bar{s}(x, Q_0^2)$  constrained by dimuon data for  $0.01 \geq x \geq 0.2$ .

Positive, with central value  $0.0025 \pm 0.0019$  (roughly  $1\sigma$  error). Nonzero value not much more than  $1\sigma$  significance. At  $Q^2 = 10\text{GeV}^2$  asymmetry of  $0.0019 \pm 0.0014$ .

Need  $S^- \sim 0.0068$  to bring NuTeV  $\sin^2 \theta_W$  in line with world average.



Fitting to strange from NuTeV dimuon data affects uncertainties on partons other than strange.

Previously for us (and everyone else) strange a fixed proportion of total sea in global fit.

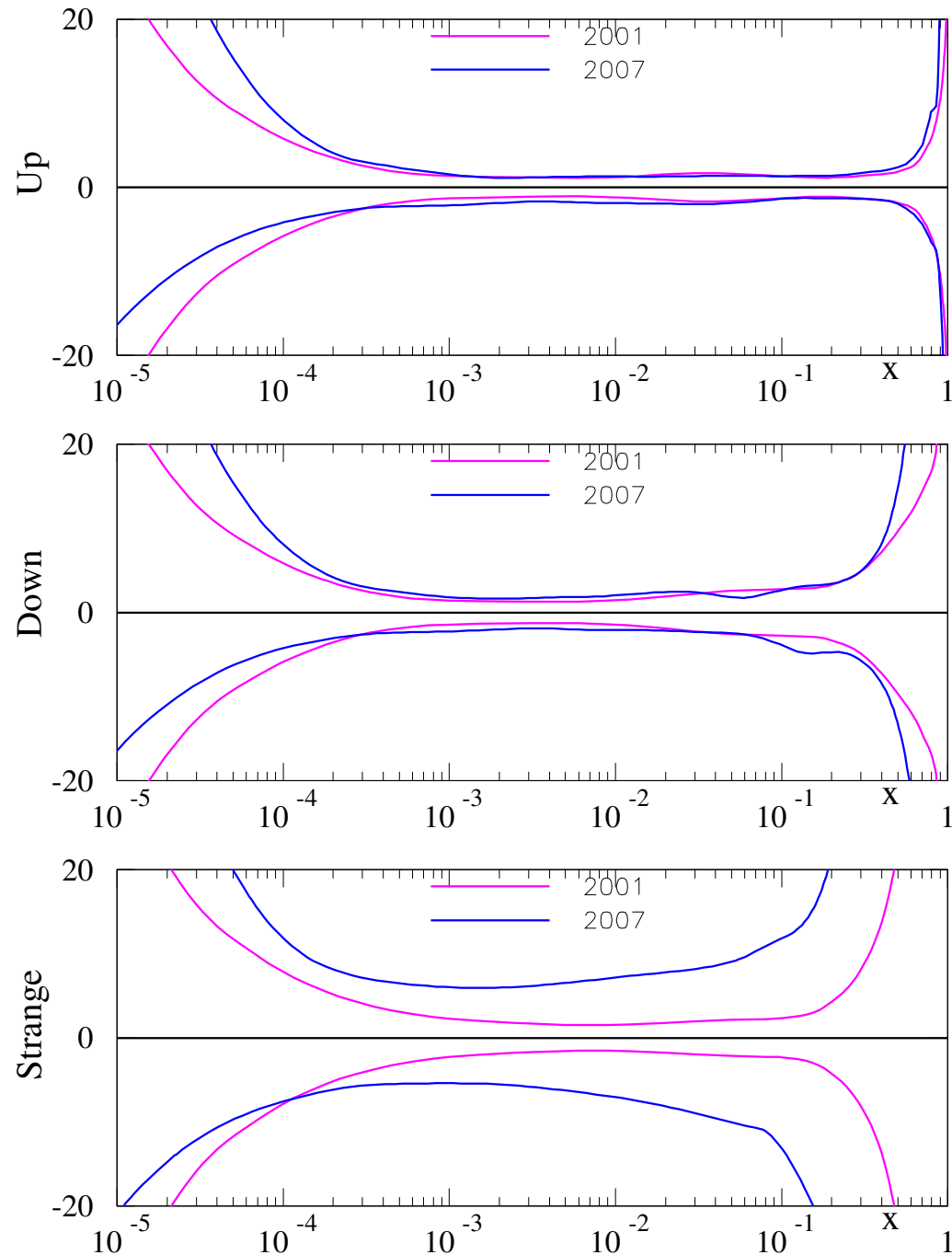
Genuine *larger* uncertainty on  $s(x)$ — feeds into that on  $\bar{u}$  and  $\bar{d}$  quarks.

Low  $x$  data on  $F_2(x, Q^2)$  constrains sum  $4/9(u + \bar{u}) + 1/9(d + \bar{d} + s + \bar{s})$ .

Changes in fraction of  $s + \bar{s}$  affects size of  $\bar{u}$  and  $\bar{d}$  at input.

The size of the uncertainty on the small  $x$  anti-quarks increases —  $\sim 1.5\% \rightarrow \sim 2 - 2.5\%$ , despite additional constraints on quarks in new fit.

percentage uncertainty at  $Q^2=100\text{GeV}^2$

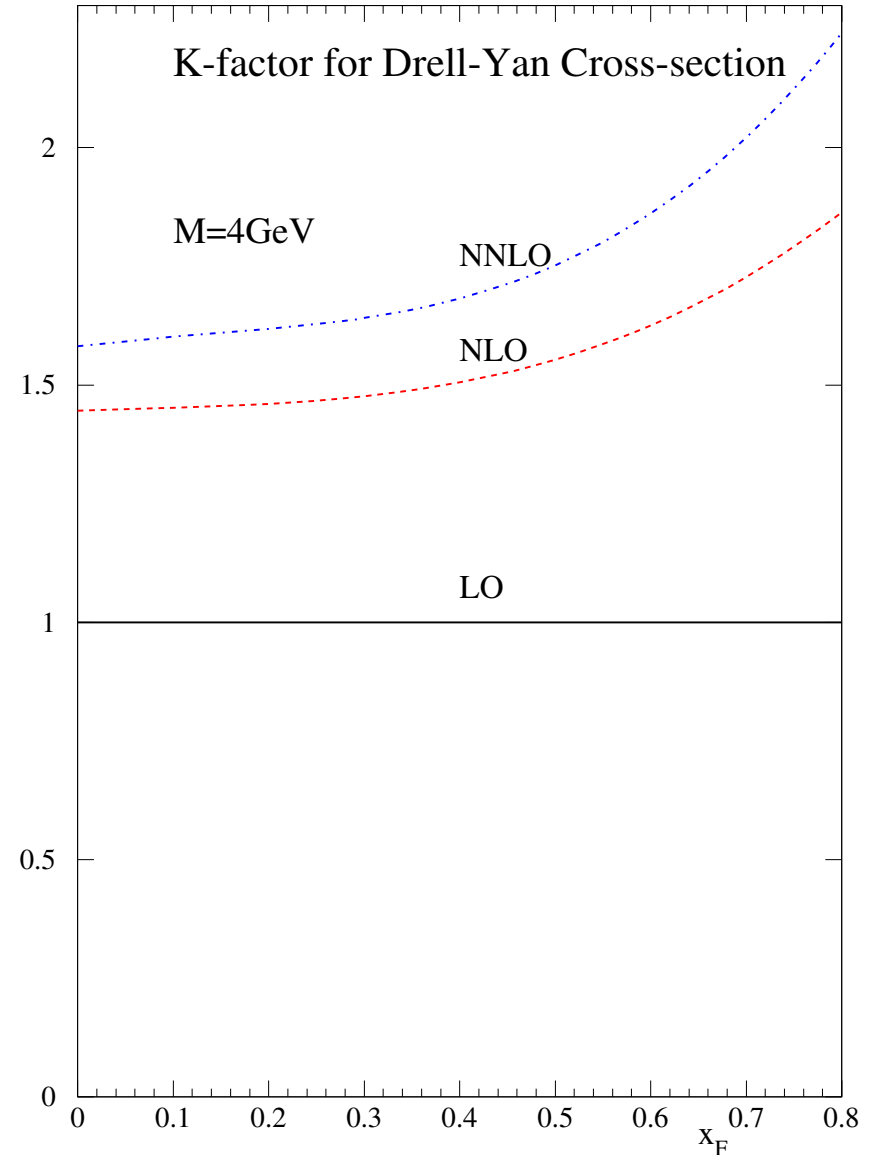


## Drell-Yan corrections

The  $K$ -factors for Drell-Yan production at E866 –  $\sqrt{s} = 38.8\text{GeV}$ .

Enhancement at higher  $x_F = x_1 - x_2$  due to logarithms. Similar to  $\ln(1-x)$  enhancement in structure functions.

NLO corrections large, NNLO corrections significant – 10% or more.



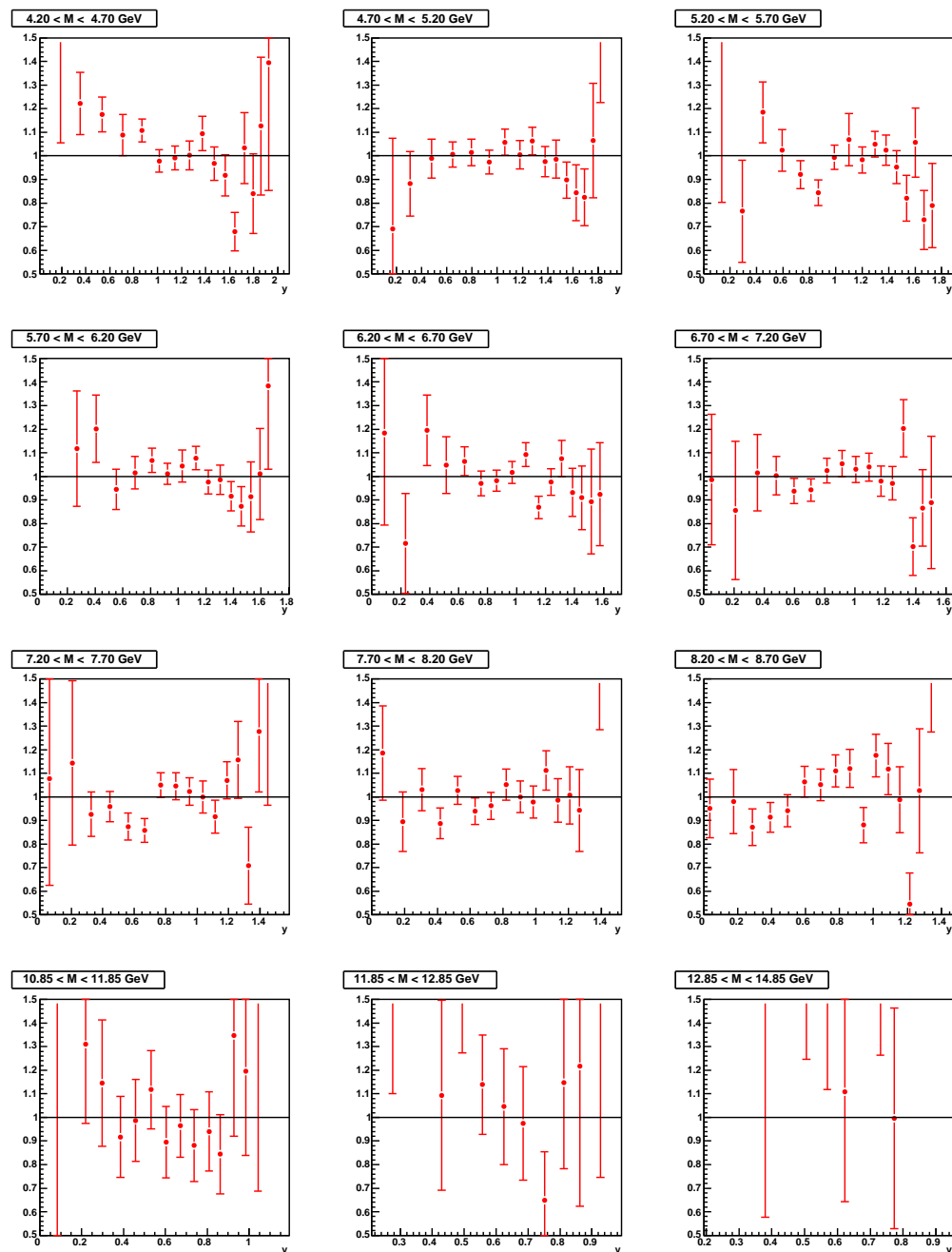


Quality of fit to E866 Drell-Yan production at E866 in proton-proton collisions – now with radiative corrections.

At NNLO requires normalization set to upper error band, i.e. 1.065.

Apart from some suggestion in lowest  $M$  bin no systematic problem with fit (contrary to other claims).

E866 pp DY data ( $\times 1.065$ ) / MSTW2007 NNLO (prel.) fit,  $\chi^2 = 231/184$  pts.



## W-asymmetry

The  $W$ -asymmetry at the Tevatron is defined by

$$A_W(y) = \frac{d\sigma(W^+)/dy - d\sigma(W^-)/dy}{d\sigma(W^+)/dy + d\sigma(W^-)/dy} \approx \frac{u(x_1)d(x_2) - d(x_1)u(x_2)}{u(x_1)d(x_2) + d(x_1)u(x_2)},$$

where  $x_{1,2} = x_0 \exp(\pm y)$ ,  $x_0 = \frac{M_W}{\sqrt{s}}$ .

In practice it is the final state leptons that are detected, so it is really the **lepton asymmetry**

$$A(y_l) = \frac{\sigma(l^+) - \sigma(l^-)}{\sigma(l^+) + \sigma(l^-)}$$

which is measured. Defining angle of lepton in  $W$  rest frame

$$\cos^2 \theta^* = 1 - 4E_T^2/M_W^2 \quad \rightarrow \quad y_{lep} = y_W \pm 1/2 \log((1 + \cos \theta^*)/(1 - \cos \theta^*))$$

In practice at highish  $y_{lep}$

$$\sigma(l^+) - \sigma(l^-) \propto u(x_1)d(x_2)(1 - \cos \theta^*)^2 - \bar{u}(x_1)\bar{d}(x_2)(1 + \cos \theta^*)^2 - u(x_2)d(x_1)(1 + \cos \theta^*)^2$$

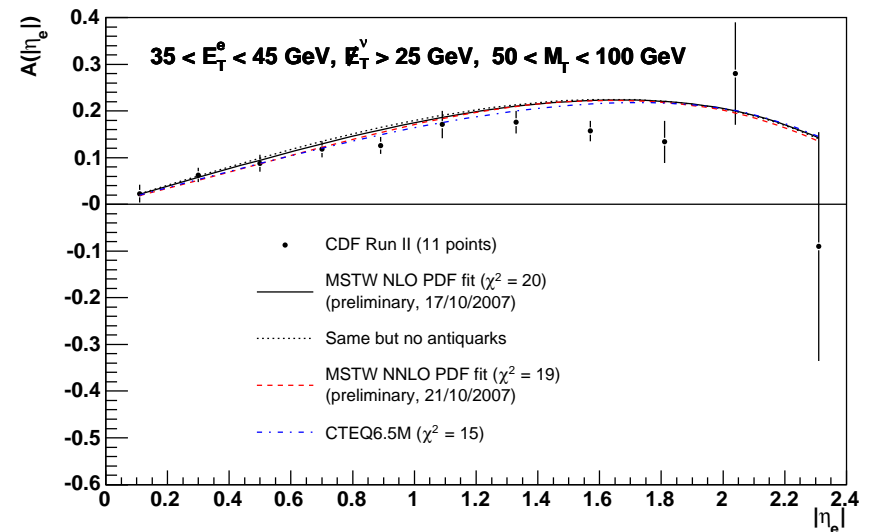
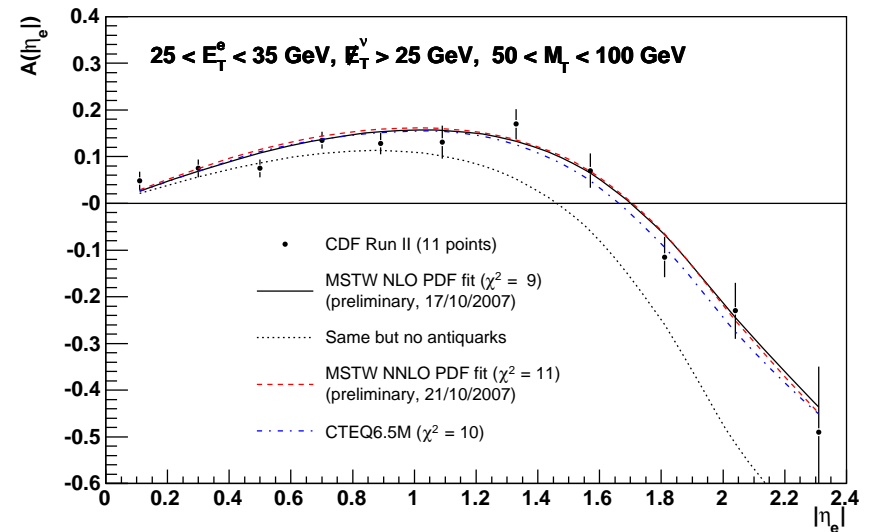
so fairly sensitive to anti-quarks at lower  $E_T$ .

Comparison of fits to CDF data with various partons. Some tension with other data sensitive to  $d(x, Q^2)$  and  $\bar{d}(x, Q^2)$ .

CTEQ seems to be slightly better shape for some reason.

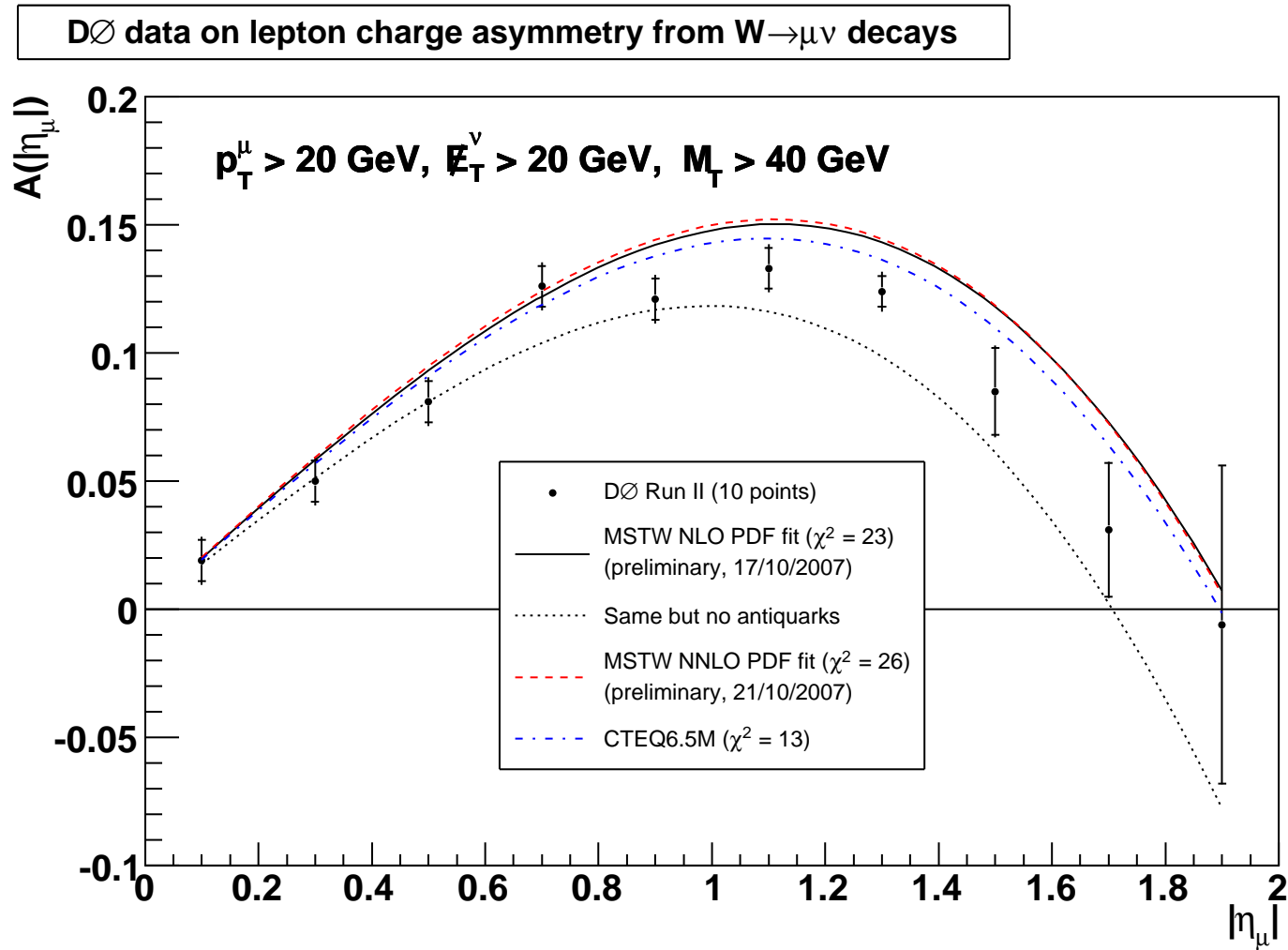
New CDF data does influence  $d(x, Q^2)$  in MSTW fit.

CDF data on lepton charge asymmetry from  $W \rightarrow e\nu$  decays



Same with **D0** data. Similar results. Would like larger  $d(x, Q^2)$  for  $x \sim 0.2$ .

More sensitivity to sea quarks due to lower  $p_T$  values.

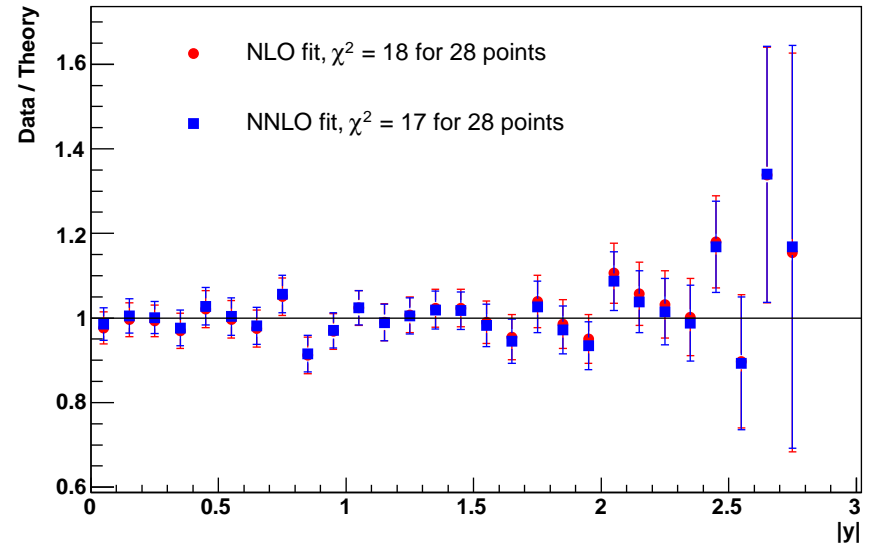
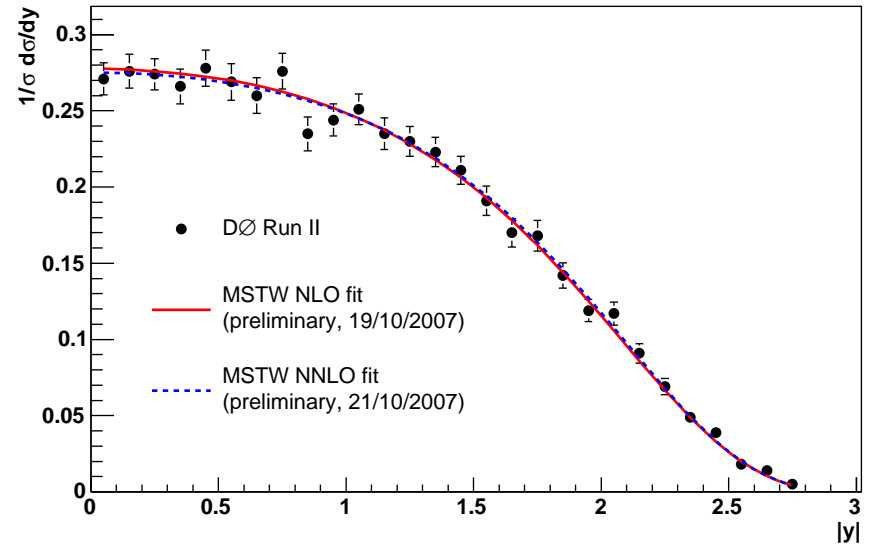


$$\frac{d\sigma(Z)}{dy} \propto 0.37u(x_1)\bar{u}(x_2)+0.54d(x_1)\bar{d}(x_2)$$

Sensitive to the down quark as well as the better constrained up quark.

D0 data with  $0.4fb^{-1}$  automatically fit well by MRST04 partons, easily accommodated in MSTW fit.

## Z/ $\gamma^*$ rapidity shape distribution from D0

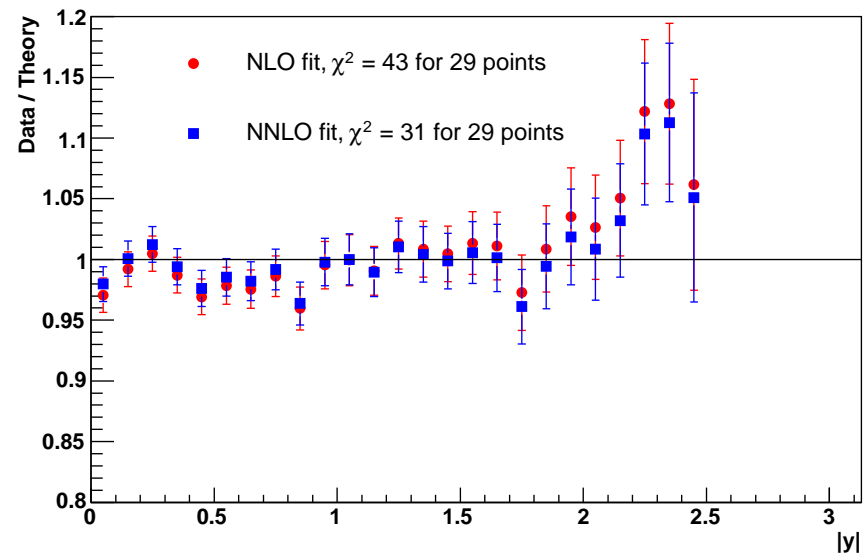
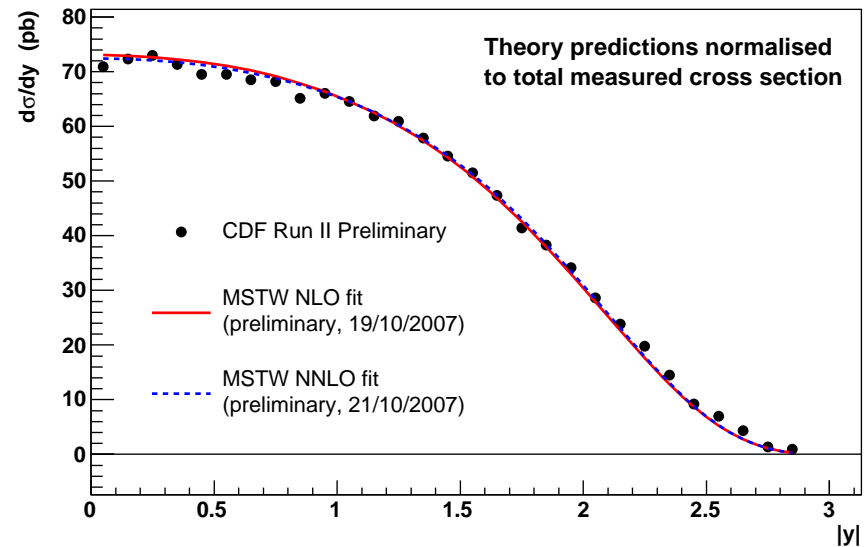


CDF data (preliminary) with  $1fb^{-1}$  more precise. Poor fit with existing MRST partons.

Improves in refit and constrains  $d(x, Q^2)$ . Pulls in opposite direction to  $W$ -asymmetry.

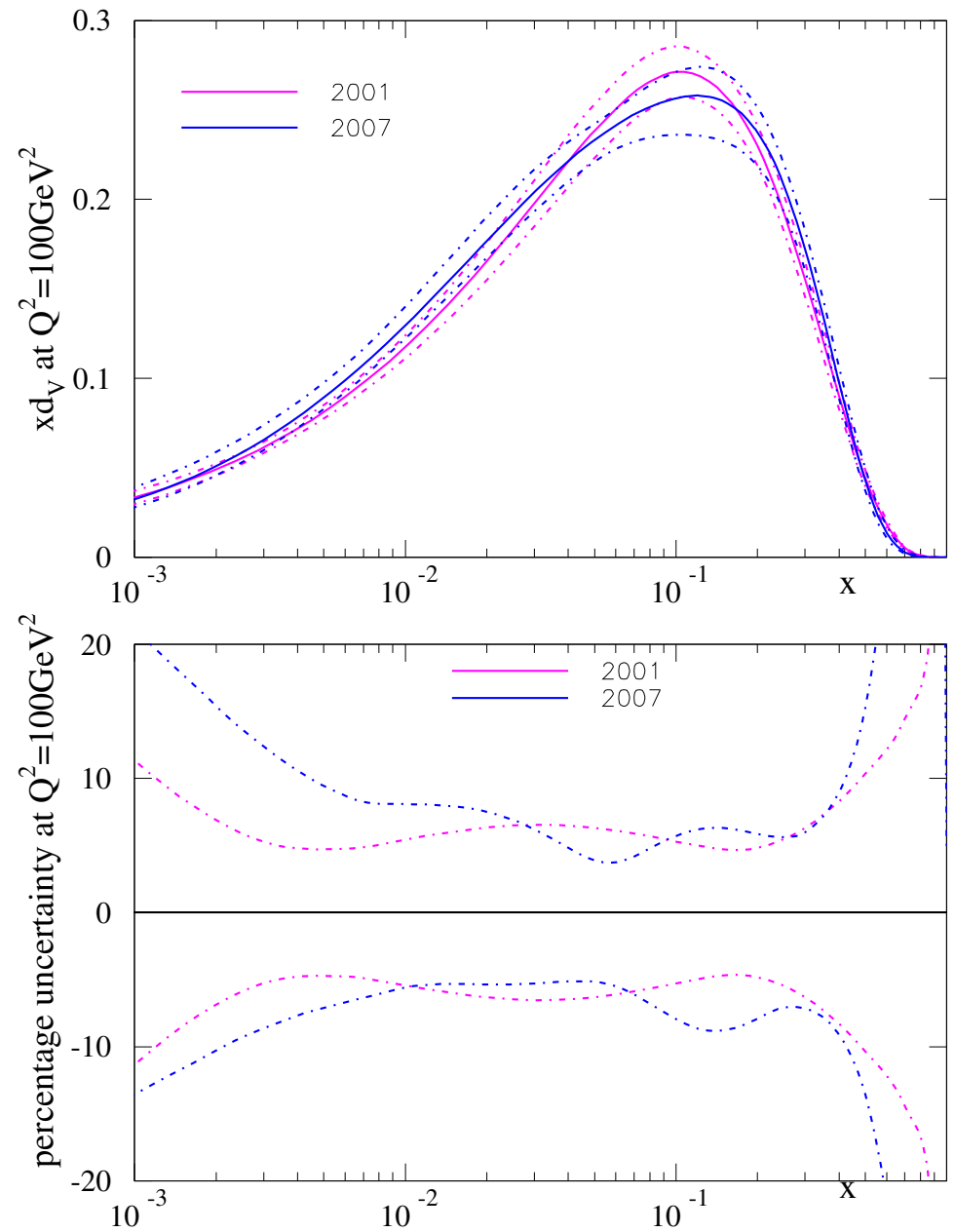
Automatically fit better at NNLO. Both cross-section and partons produce better shape.

## $Z/\gamma^*$ rapidity distribution from CDF



Overall  $d_V(x, Q^2)$  now chooses a different type of shape.

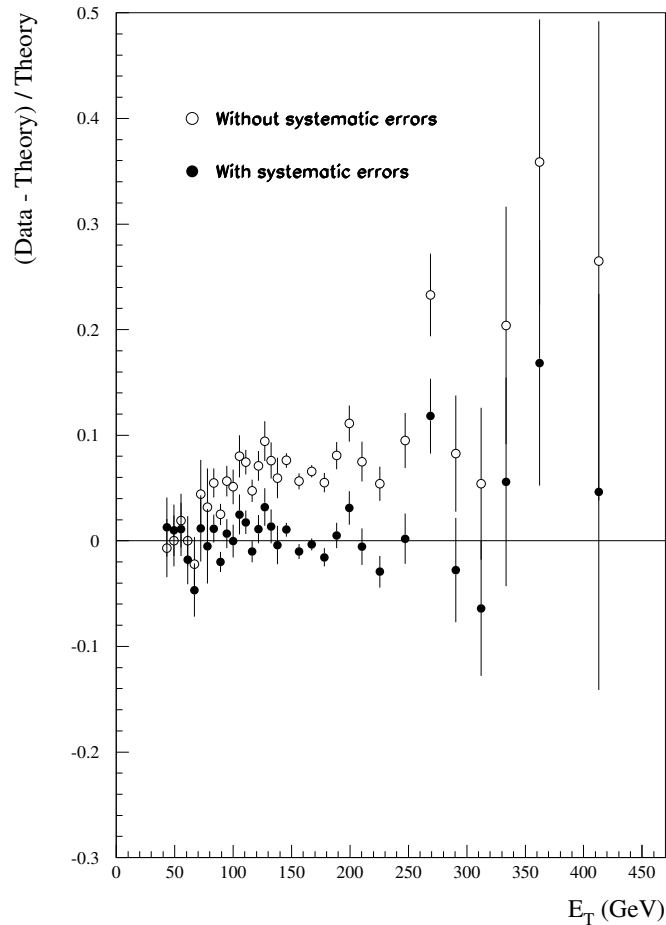
Uncertainty growing more quickly as  $x \rightarrow 0$  and  $x \rightarrow 1$  than before due to better parameterisation in determining uncertainty eigenvectors.



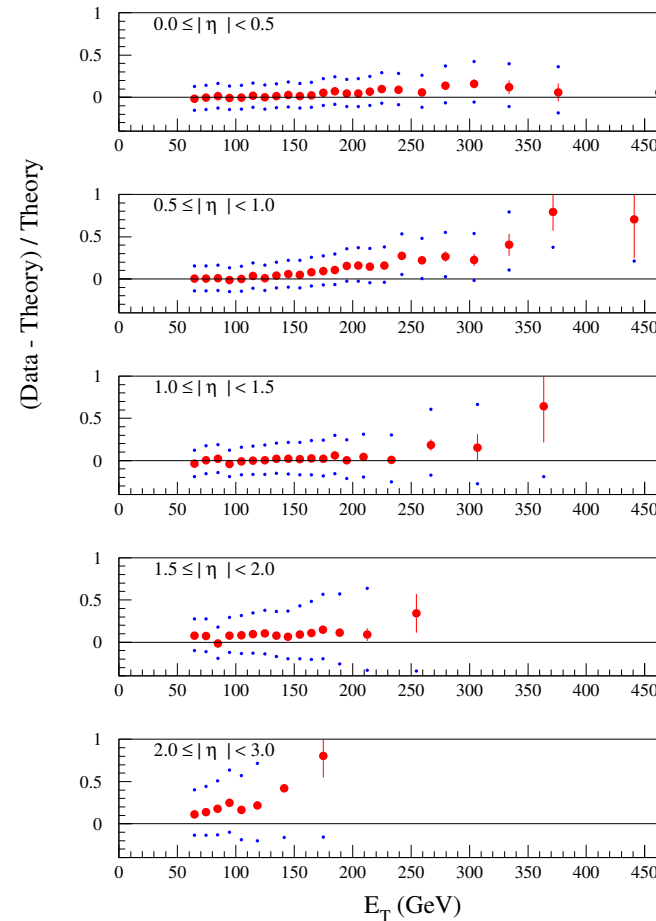
Now use **fastNLO** to implement **NLO** hard cross-section corrections to both **Tevatron** and **HERA** jets. Replaces previous “K-factors” and “pseudo-gluon data”.

No major effect on speed of fitting program. Slight influence on shape of gluon even using just **Tevatron** Run I data. (Hadronization corrections now included).

CDF Run I inclusive jet data,  $\chi^2 = 50/33$  pts.



DØ Run I inclusive jet data,  $\chi^2 = 58/90$  pts.





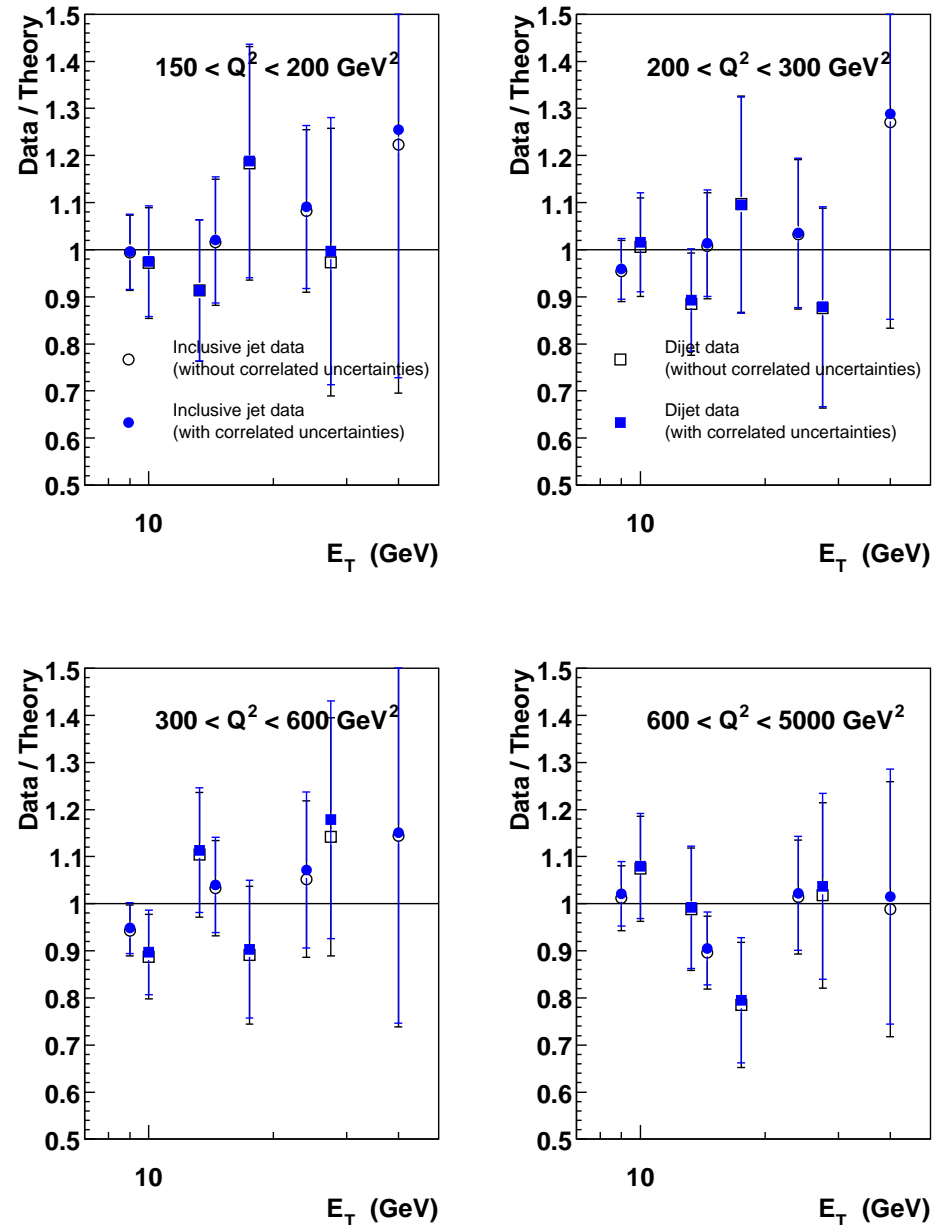
Also now include HERA inclusive and dijet DIS data using fastNLO.

Fit generally excellent. Correlated systematic uncertainties have little effect in this case.

At NNLO do not know cross-section. Leave out of NNLO fit.

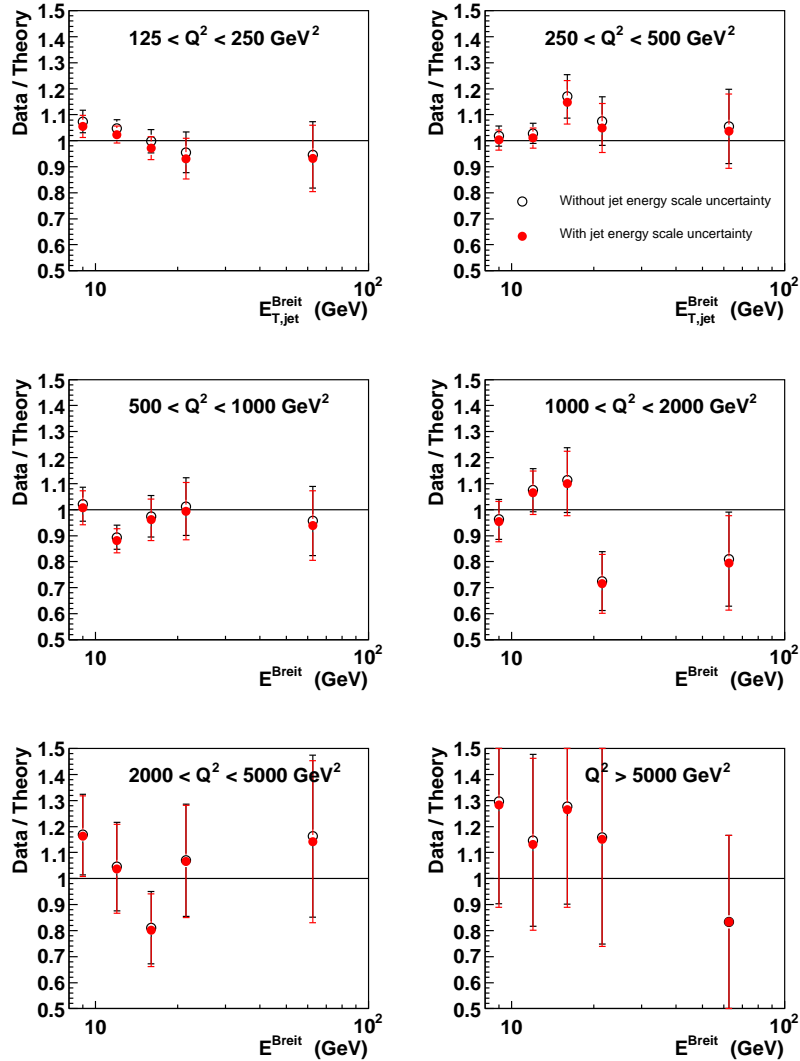
Comparison to data using NNLO partons and NLO cross-sections very good.

## H1 95-97 incl. jet and dijet data, $\chi^2 = 13/32$ pts. MSTW NLO PDF fit (preliminary, 17/10/2007)



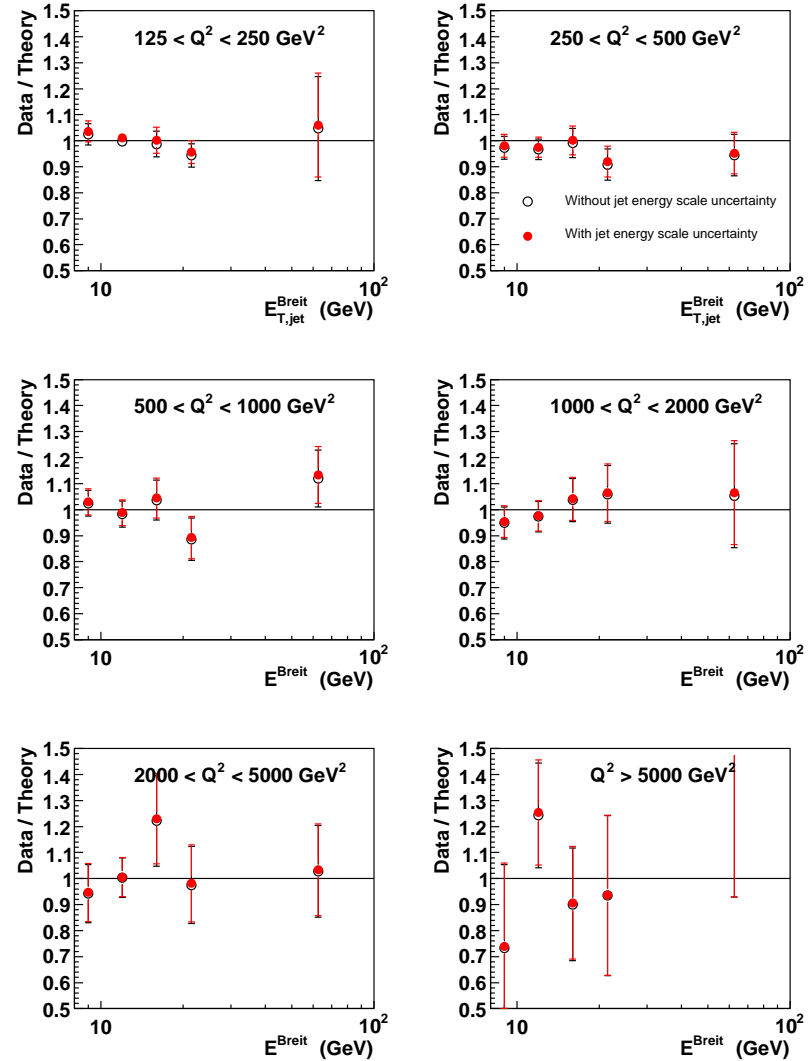
## ZEUS 96-97 inclusive jet data, $\chi^2 = 29/30$ pts.

MSTW NLO PDF fit (preliminary, 17/10/2007)



## ZEUS 98-00 inclusive jet data, $\chi^2 = 16/30$ pts.

MSTW NLO PDF fit (preliminary, 17/10/2007)



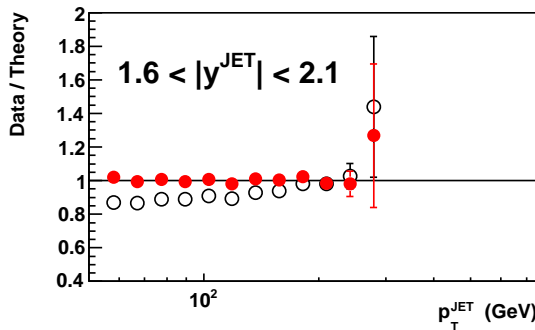
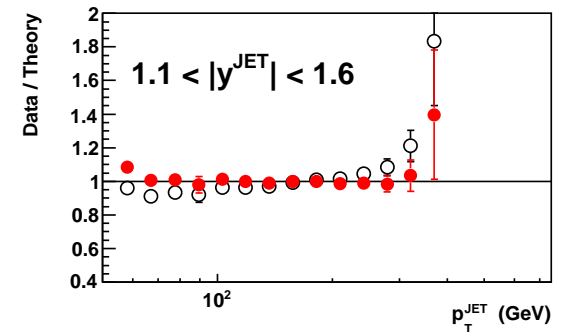
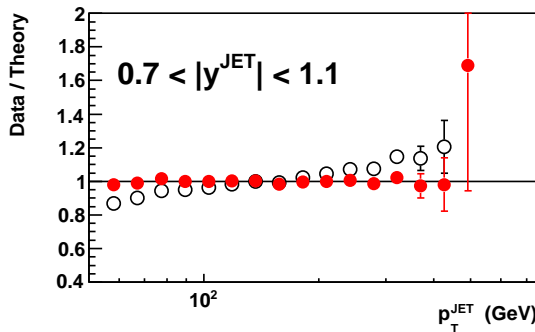
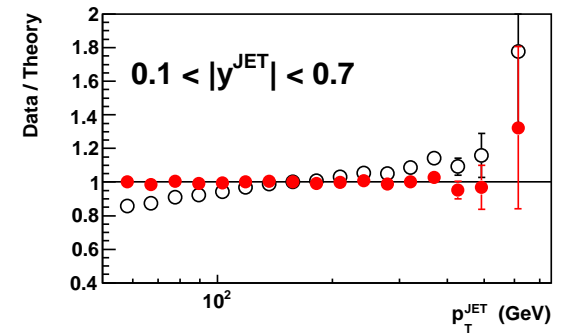
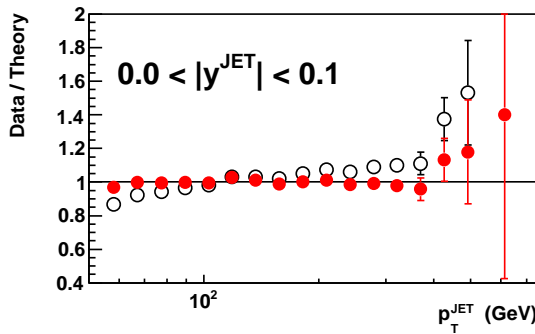
Perhaps more constraint from photo-production data, but requires (rather uncertain) photon distributions.

Now also include CDF Run II inclusive jet data in different rapidity bins using  $k_T$  jet algorithm (mid-point cone algorithm data seems very similar, but numbers not yet available).

Very good fit –  $\chi^2 = 58/76$ .

Full use of correlated systematic errors required for any sensible result.

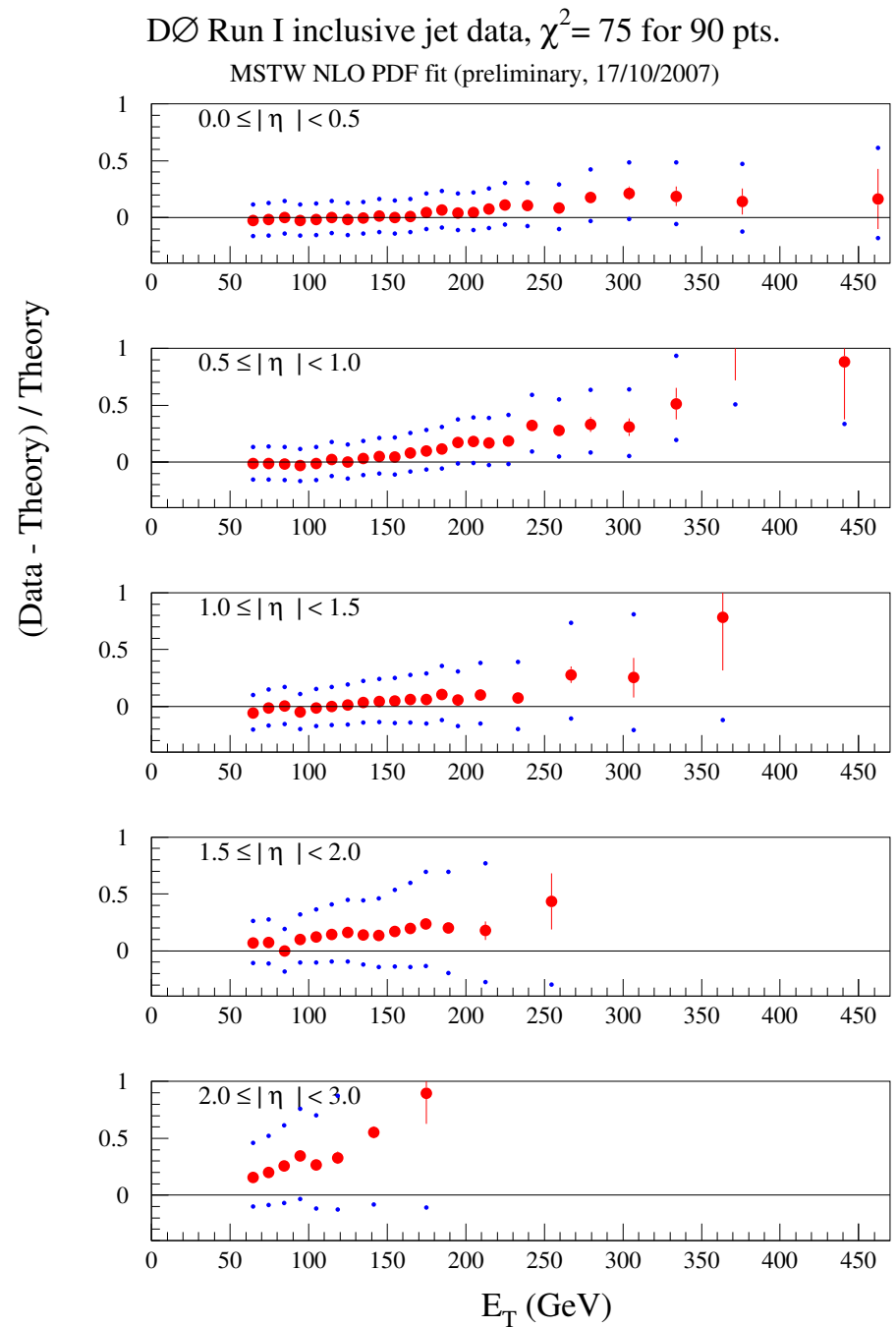
## CDF Run II inclusive jet data, $\chi^2 = 58$ for 76 pts.



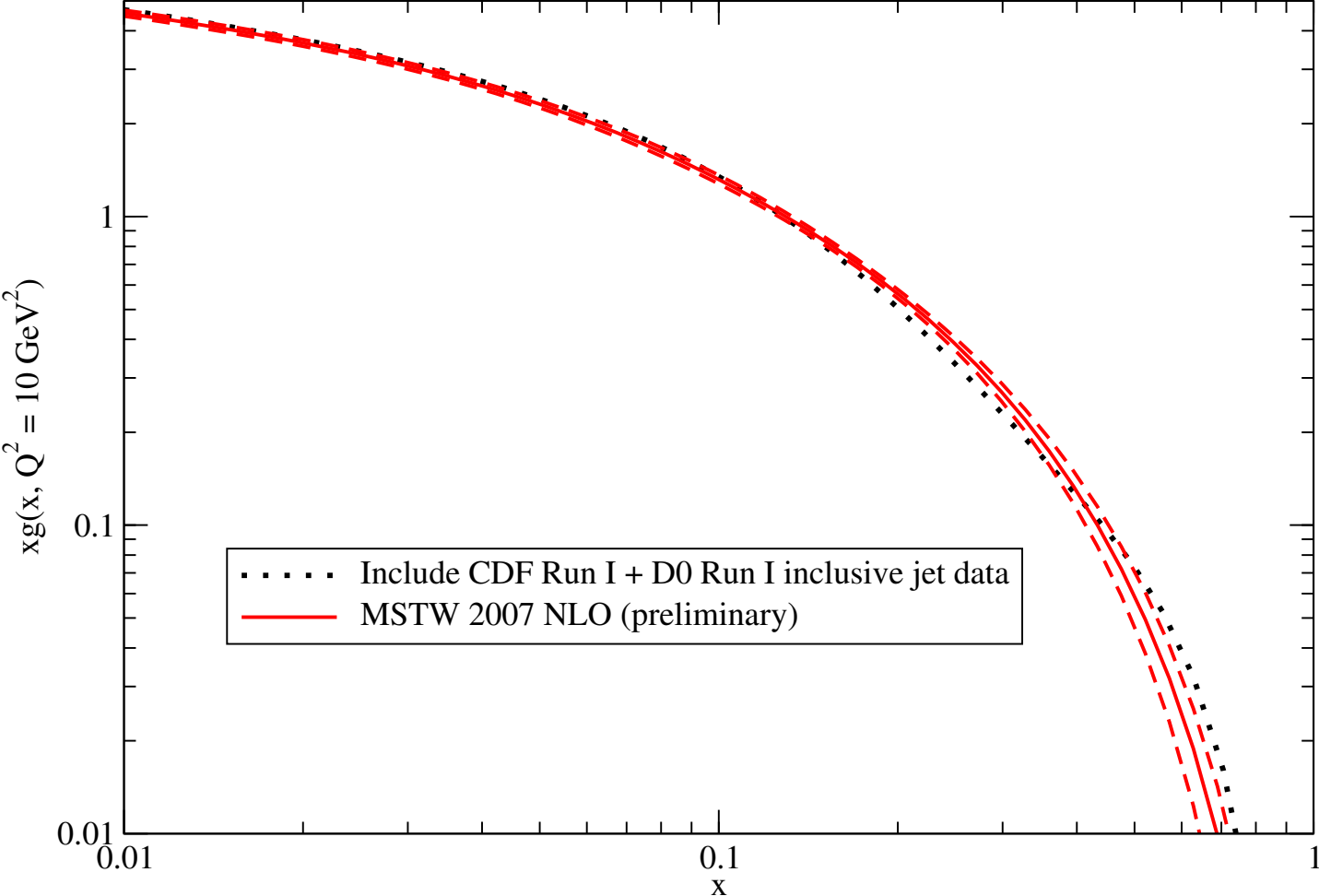
$k_T$  algorithm with  $D = 0.7$   
MSTW NLO PDF fit  
(preliminary, 17/10/2007)

- Without systematic uncertainties
- With systematic uncertainties

Slight deterioration in fit to **D0** run I data in different rapidity bins compared to using **CDF** run I data.



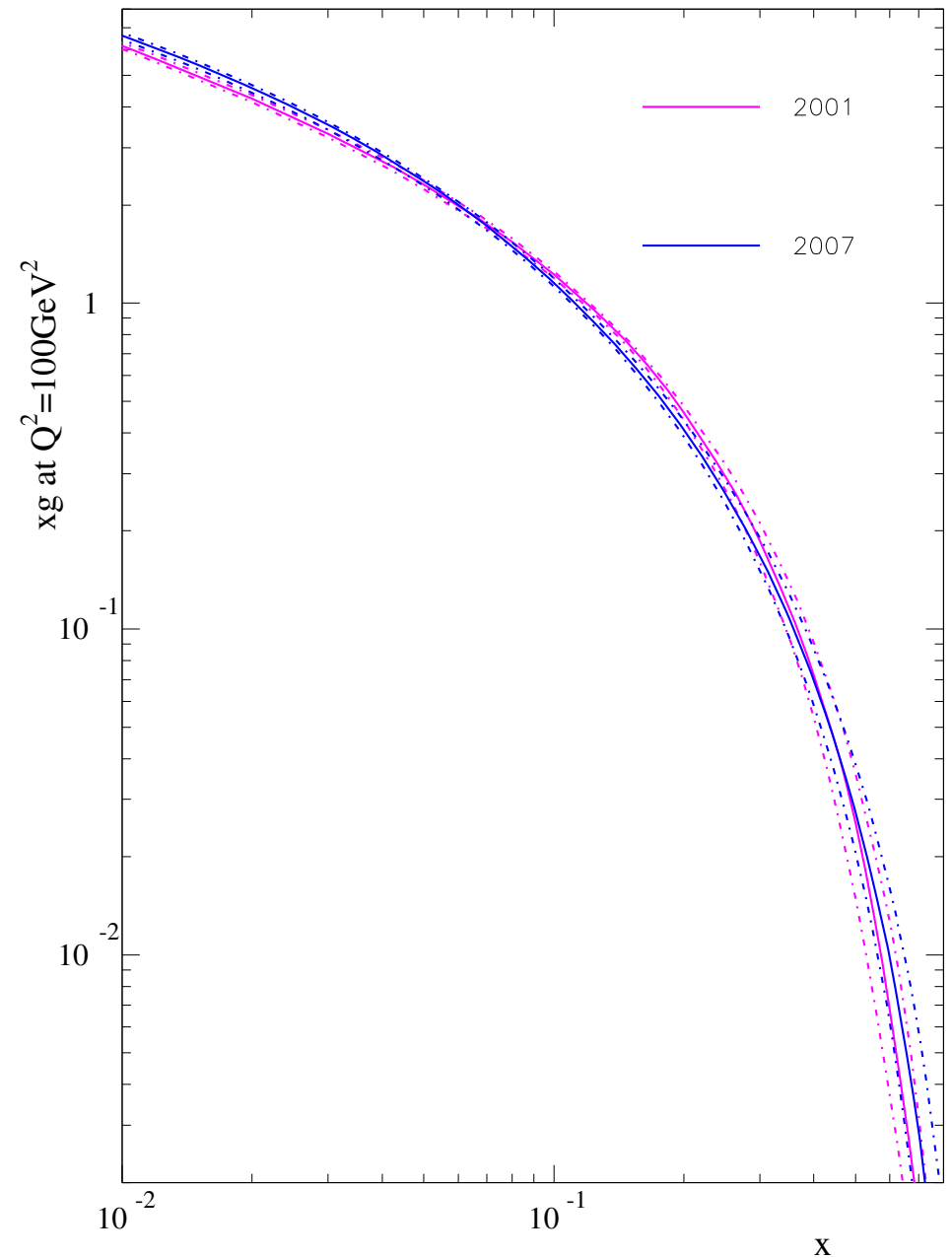
CDF run II data prefers a smaller very high  $x$  gluon distribution compared to run I data. Just outside uncertainties at our  $1\sigma$  level.



Uncertainties at high  $x$  are now a little smaller than those for MRST2001.

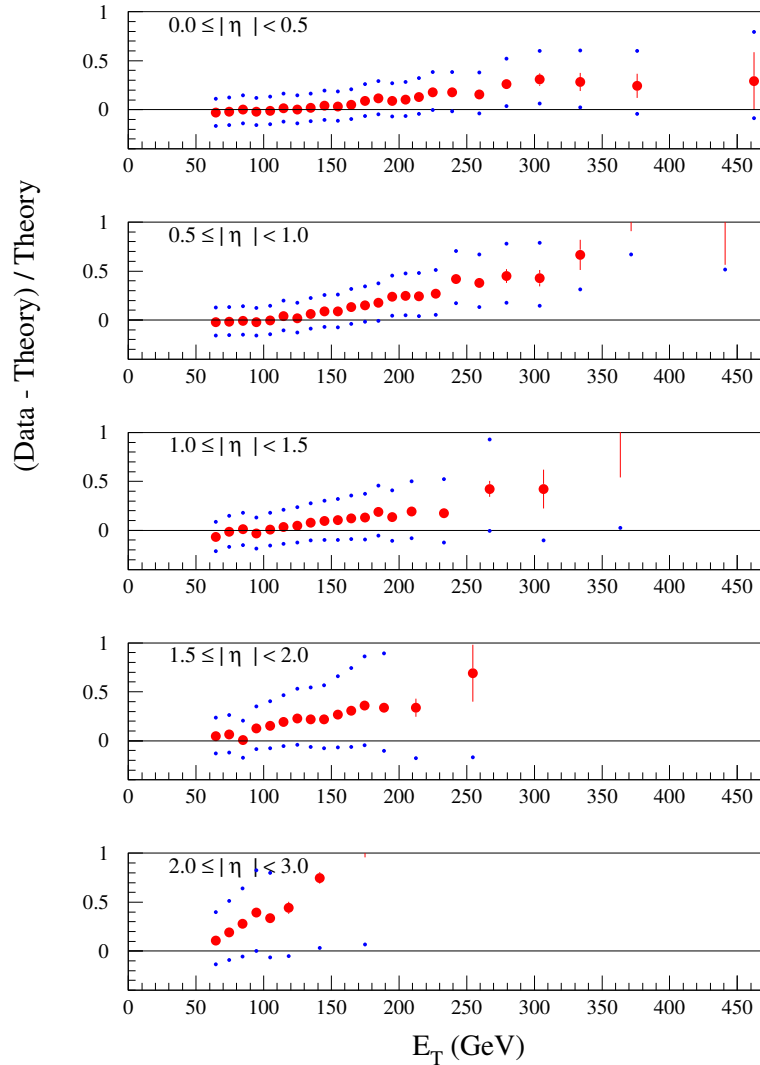
At NNLO only know threshold corrections to cross-section. Few % and flat in  $E_T$ .

Total NLO corrections only  $\sim 10\%$  and smooth with  $E_T \rightarrow$  unlikely NNLO corrections larger than systematic uncertainties.

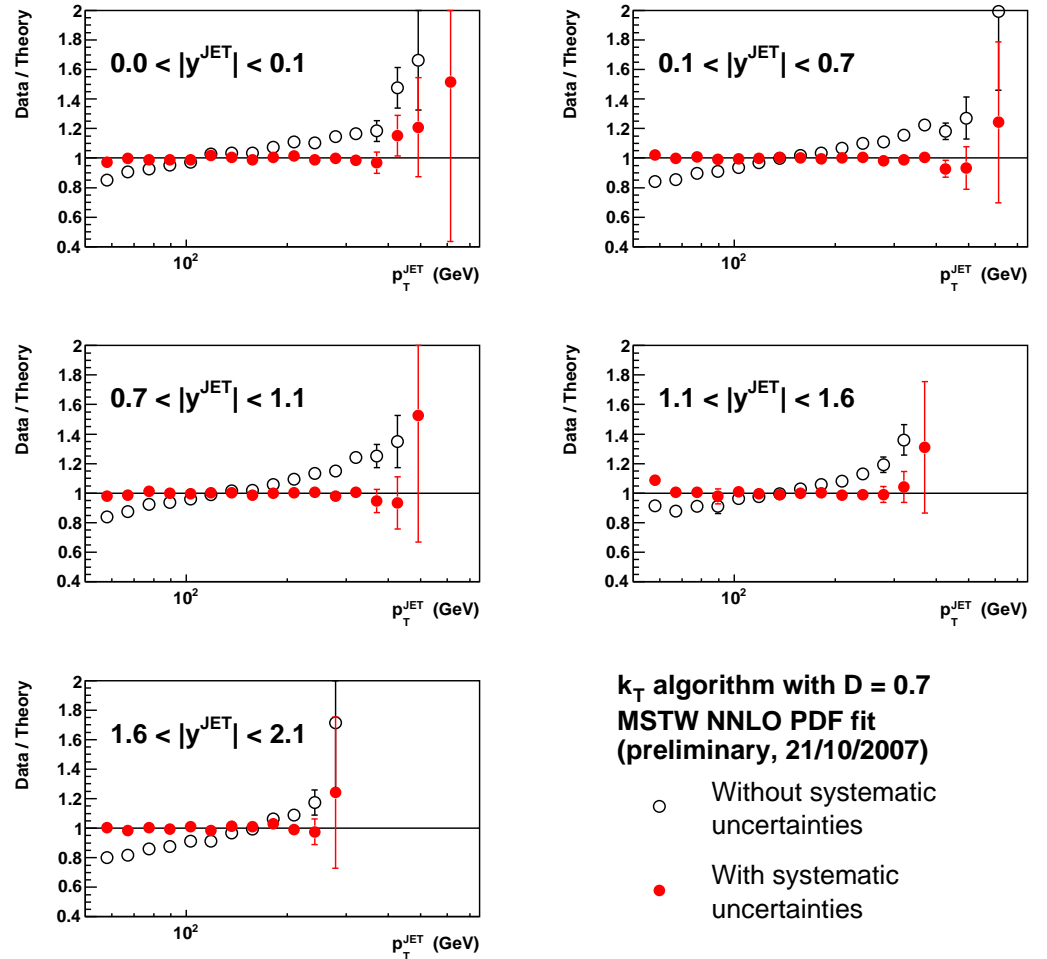


Fit to Tevatron jet data little worse at NNLO since high- $x$  quarks automatically smaller.

DØ Run I inclusive jet data,  $\chi^2 = 93$  for 90 pts.  
MSTW NNLO PDF fit (preliminary, 21/10/2007)



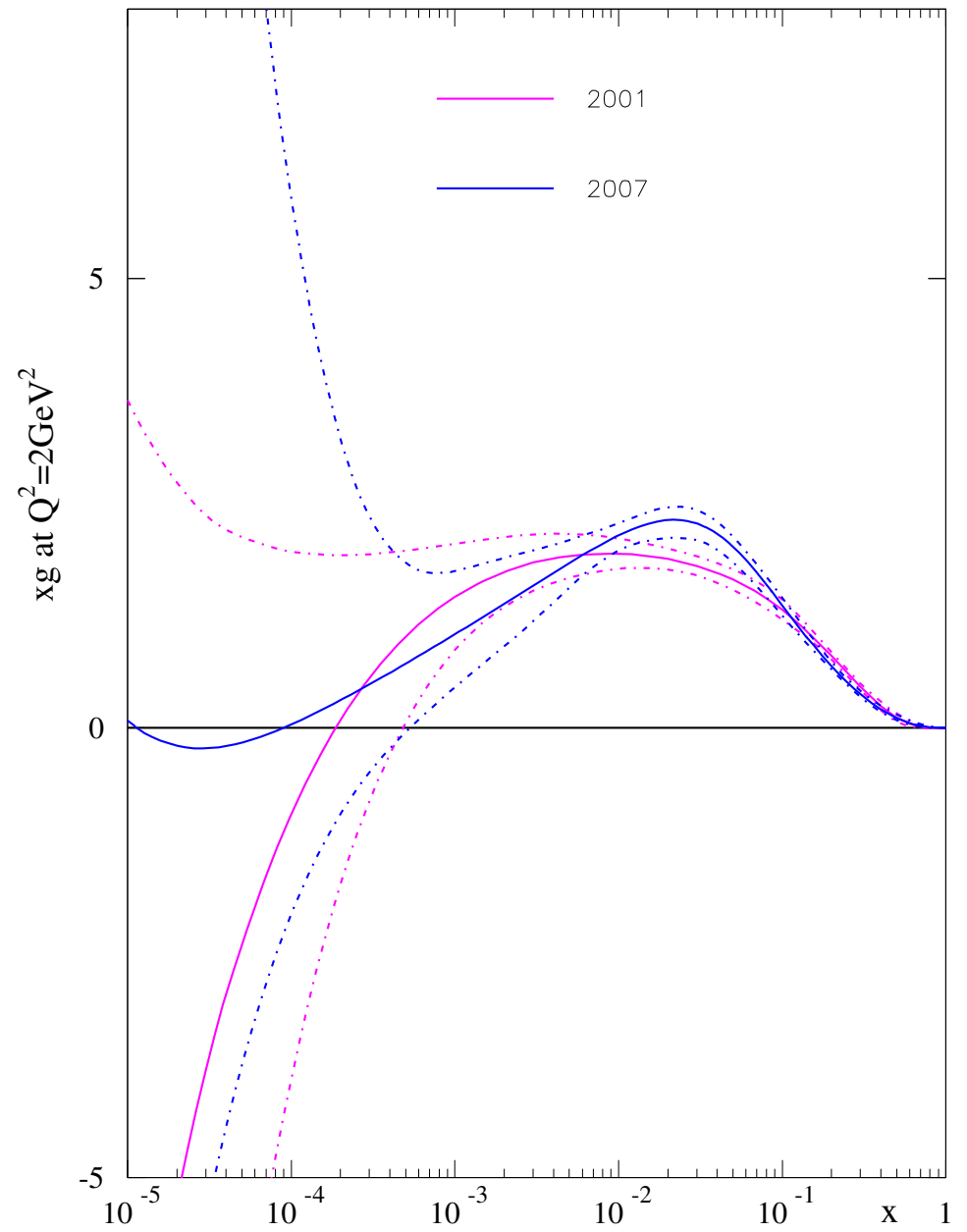
CDF Run II inclusive jet data,  $\chi^2 = 65$  for 76 pts.



$k_T$  algorithm with  $D = 0.7$   
MSTW NNLO PDF fit  
(preliminary, 21/10/2007)

- Without systematic uncertainties
- With systematic uncertainties

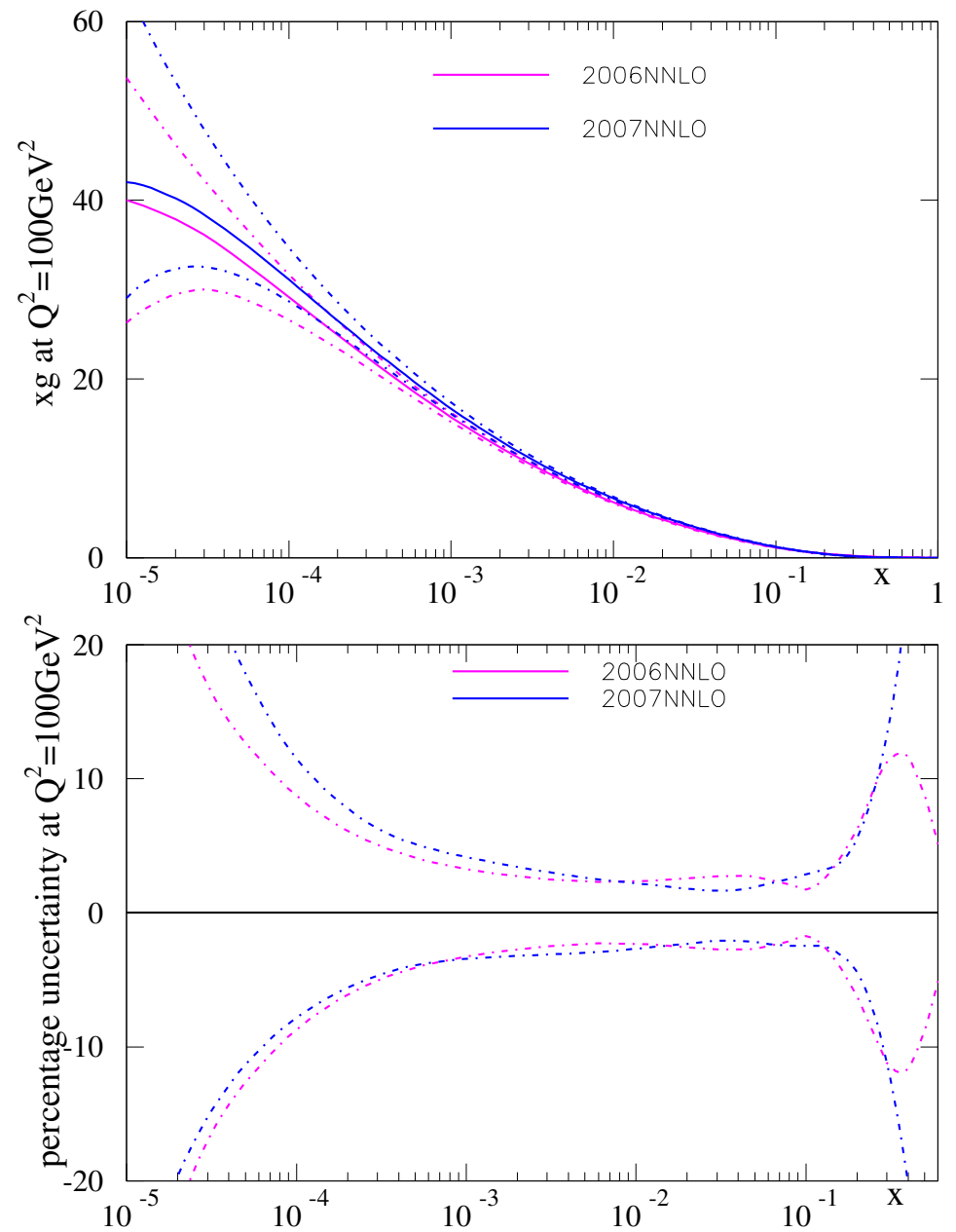
Overall input gluon of same general shape to previously. Still dips negative at low  $x$ , not quite so much.





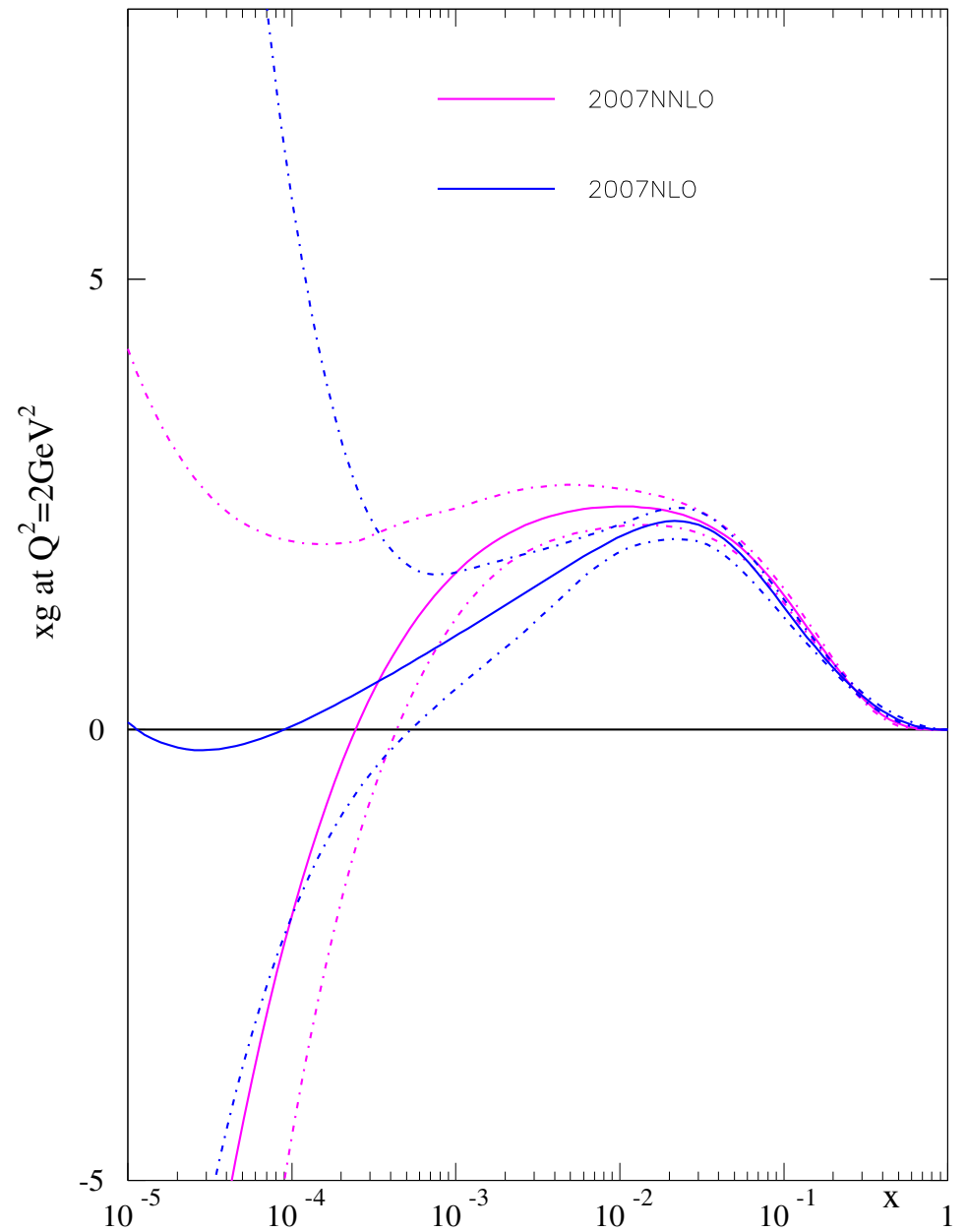
Comparison of most up-to-date gluon distributions at NNLO and MRST06 at  $Q^2 = 100\text{GeV}^2$ .

MSTW2007 has smaller high- $x$  distribution with better uncertainty determination. Slightly bigger at low  $x$ .



Comparison of most up-to-date gluon distributions at **NLO** and **NNLO**. General result that **NNLO** becomes more negative at very low  $x$ , still true.

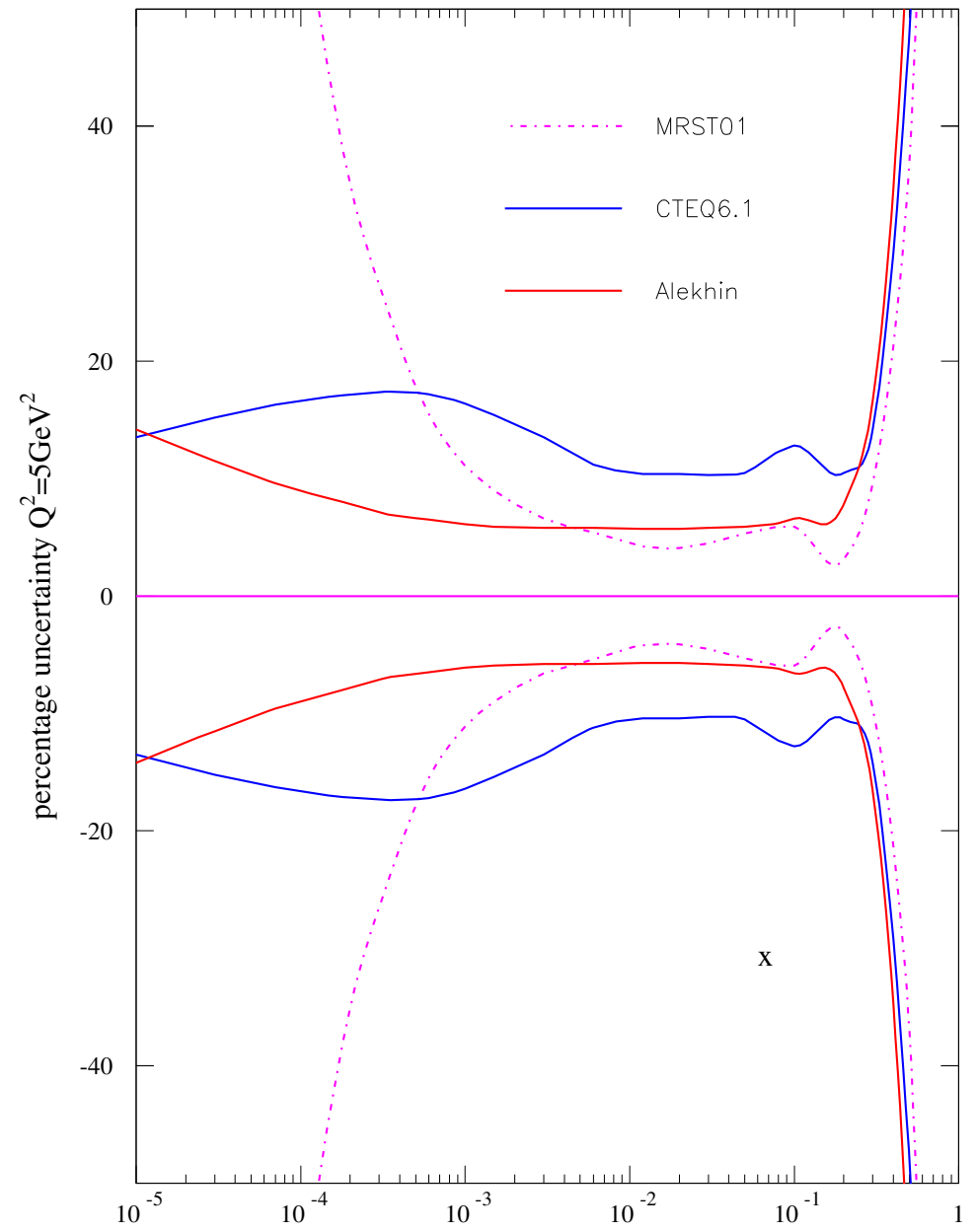
Uncertainty on gluon also extremely large at  $x \sim 10^{-5}$  at **NNLO**.



MRST uncertainty blows up for very small  $x$ , whereas Alekhin (and ZEUS and H1) gets slowly bigger, and CTEQ saturates (or even decreases).

Related to input forms and scales.

(*Neck* in MRST gluon cured in MSTW).



MRST (MSTW) parameterise at  $Q_0^2 = 1\text{GeV}^2$  but allow negative and positive small  $x$  contributions. Very flexible. Represent true uncertainty at low  $x$ ?

Alekhin and ZEUS gluons input at higher scale – behave like  $x^{-\lambda}$  at small  $x$ . Uncertainty due to uncertainty in one parameter.

CTEQ gluons input at  $Q_0^2 = 1.69\text{GeV}^2$ . Behave like  $x^\lambda$  at small  $x$  where  $\lambda$  large and positive. Input gluon valence-like.

Requires fine tuning. Evolving backwards from steep gluon at higher scale valence-like gluon only exists for very narrow range of  $Q^2$  (if at all).

Small  $x$  input gluon tiny – very small absolute error. At higher  $Q^2$  all uncertainty due to evolution driven by higher  $x$ , well-determined gluon. Very small  $x$  gluon no more uncertain than at  $x = 0.01 - 0.001$ .

## Dependence on $m_c$

Vary  $m_c$  in steps of  $0.1\text{GeV}$  (DIS07 - expect each  $\alpha_s(M_Z^2)$  about  $0.001$  lower).

$m_c$ (GeV)	$\chi_{global}^2$ 2659 pts	$\chi_{F_2^c}^2$ 78 pts	$\alpha_s(M_Z^2)$
1.2	2541	179	0.1183
1.3	2485	129	0.1191
1.4	2472	100	0.1206
1.5	2479	95	0.1213
1.6	2518	101	0.1223
1.7	2576	123	0.1221

Clear correlation between  $m_c$  and  $\alpha_s(M_Z^2)$ .

For low  $m_c$  overshoot low  $Q^2$  medium  $x$  data badly.

Preference for  $m_c = 1.4\text{GeV}$ . Towards lower end of pole mass determinations. Uncertainty from fit  $\sim 0.1 - 0.15\text{GeV}$ . At NNLO best fit gives  $m_c = 1.3\text{GeV}$ .

Also now choose  $m_b = 4.75\text{GeV}$ , i.e. reasonable pole mass value. Not determined well by fit.

## Summary of Updates.

Implemented all new data at both **NLO** and **NNLO**. Fit very good in both cases though **NLO** better for some data sets.

Obtain  $\alpha_S(M_Z^2) = 0.1197$  at **NLO** and  $\alpha_S(M_Z^2) = 0.116$  at **NNLO** – new data and change in definition lead to slightly lower value. At **NNLO** lower  $m_c \rightarrow 0.0015$  of change.

Two new parameters for  $s^+(x, Q^2)$  and two for  $s^-(x, Q^2)$ . Additional one for gluon compared to previous sets whilst maintaining stability for eigenvectors, and better choice of parameters for quarks  $\rightarrow$  more realistic uncertainties, particularly at small  $x$ .

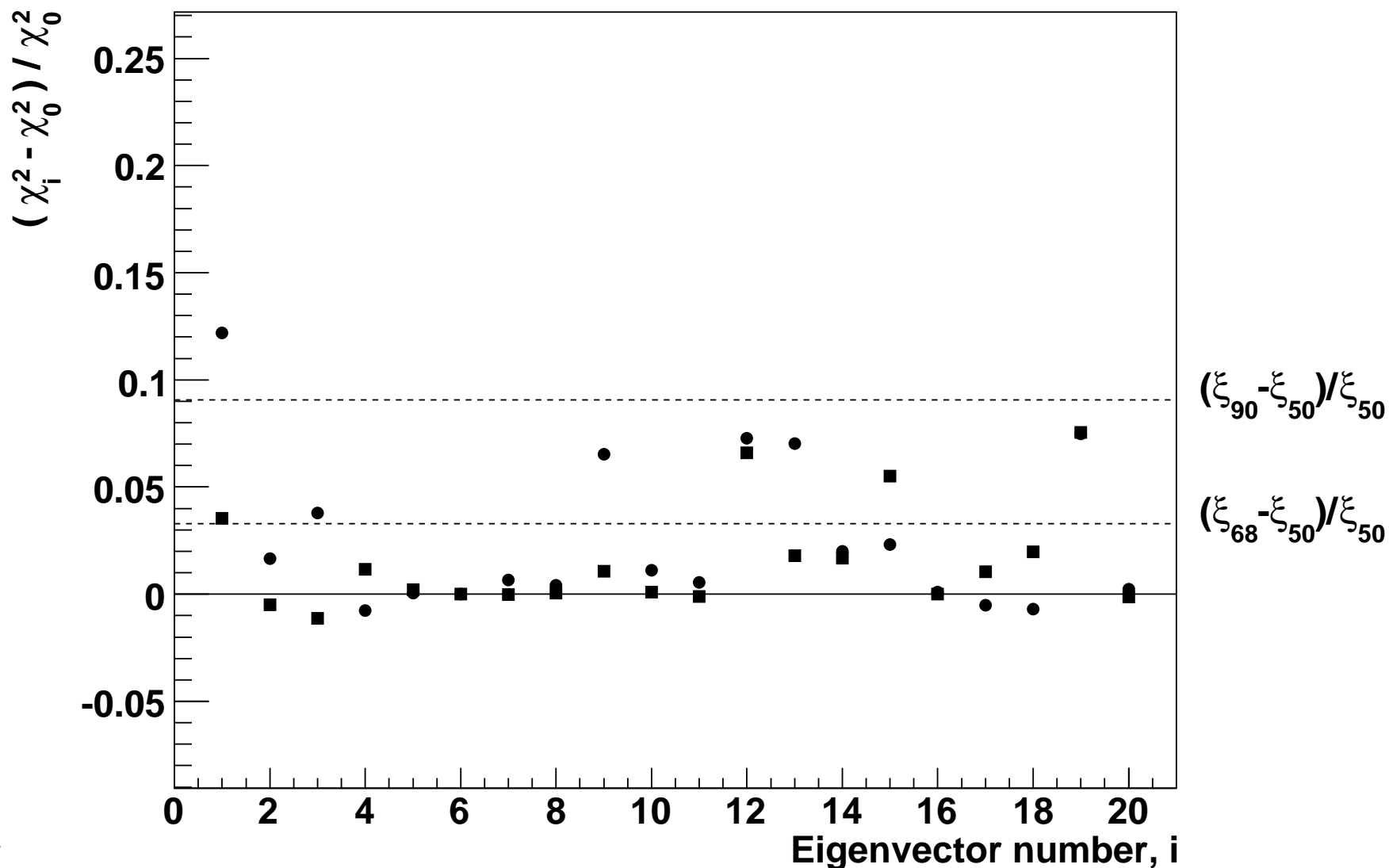
$\rightarrow$  now **20** eigenvector sets. Provisionally still using  $\Delta\chi^2 = 50$  as general rule for uncertainty, except for  $s^-(x, Q^2)$ , which only small subset of data is sensitive to.

However, all parameters, or parameters eigenvectors sensitive to only some data sets. Detailed examination of this sensitivity underway to improve definition of uncertainties.

Can quickly see main features of which data sets are constraining which parameters, and how much.

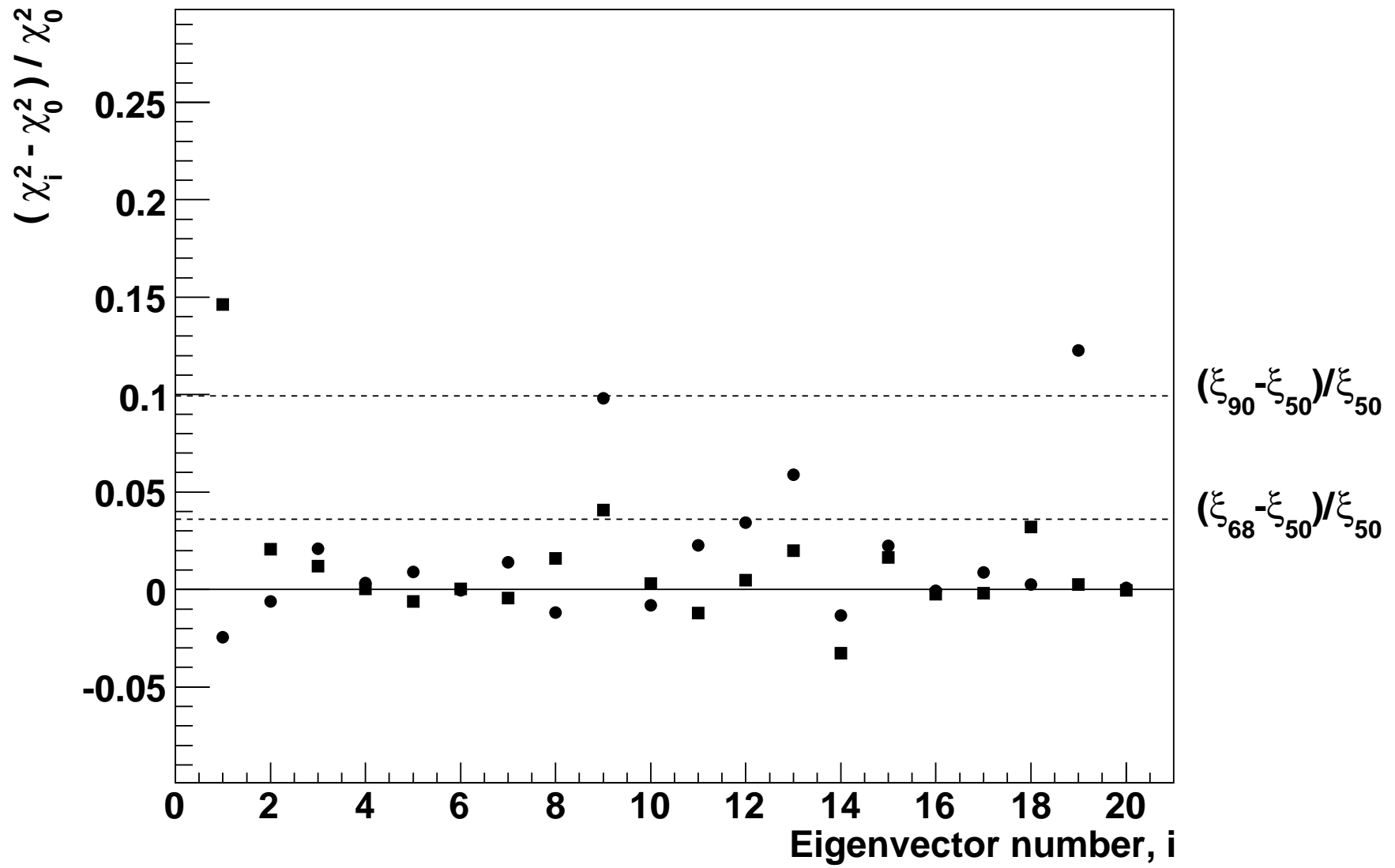
H1 data on  $F_2(x, Q^2)$  constrains many parameters. Mainly small- $x$  gluon (vector 1 and 9) medium and high- $x$  gluon (19) and quark/gluon interplay (12).  $\Delta\chi^2 = 50$  increase in some eigenvector directions takes fit to about 90% confidence limit.

H1



ZEUS data on  $F_2(x, Q^2)$  has (unsurprisingly) very similar features.

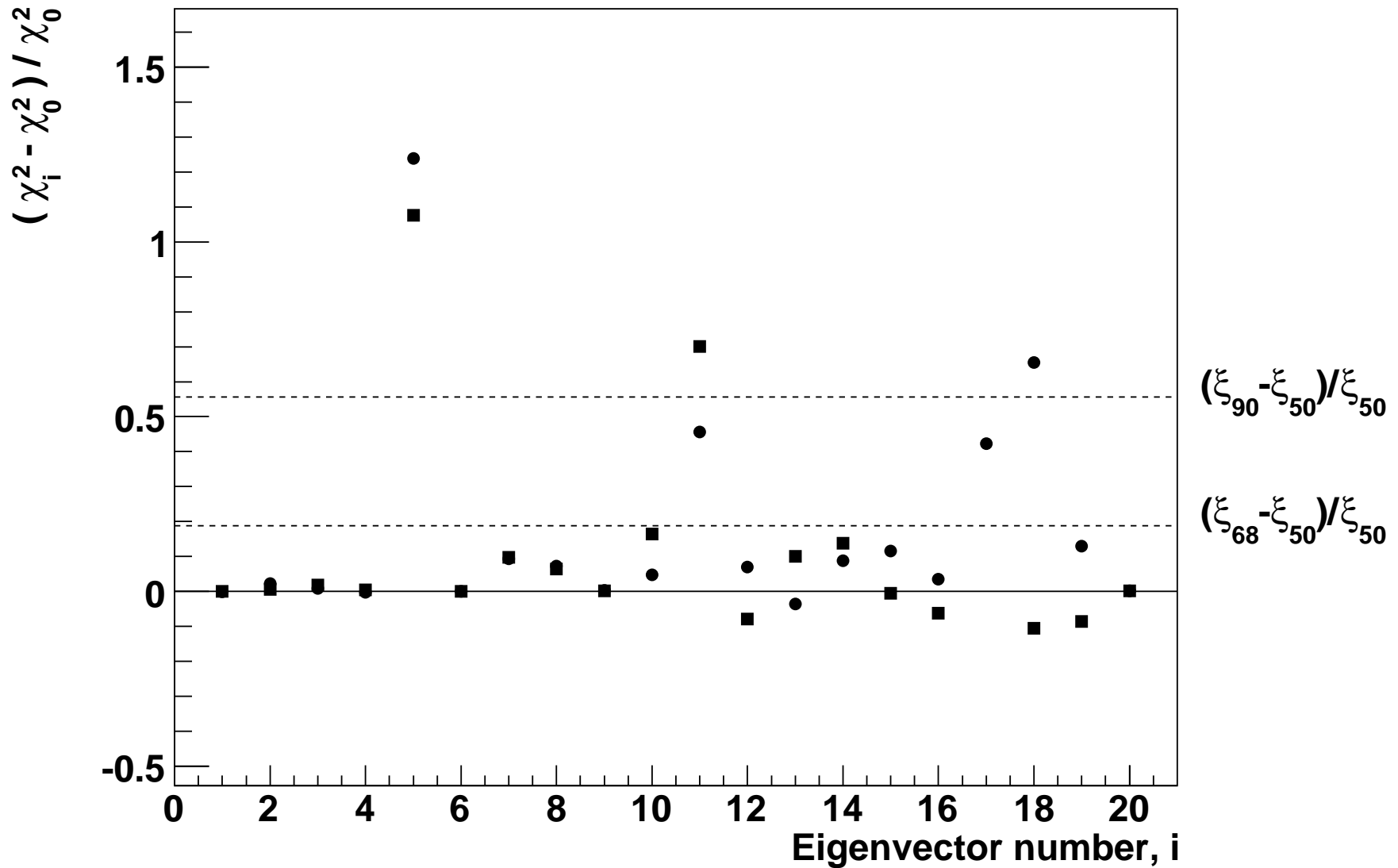
**ZEUS**





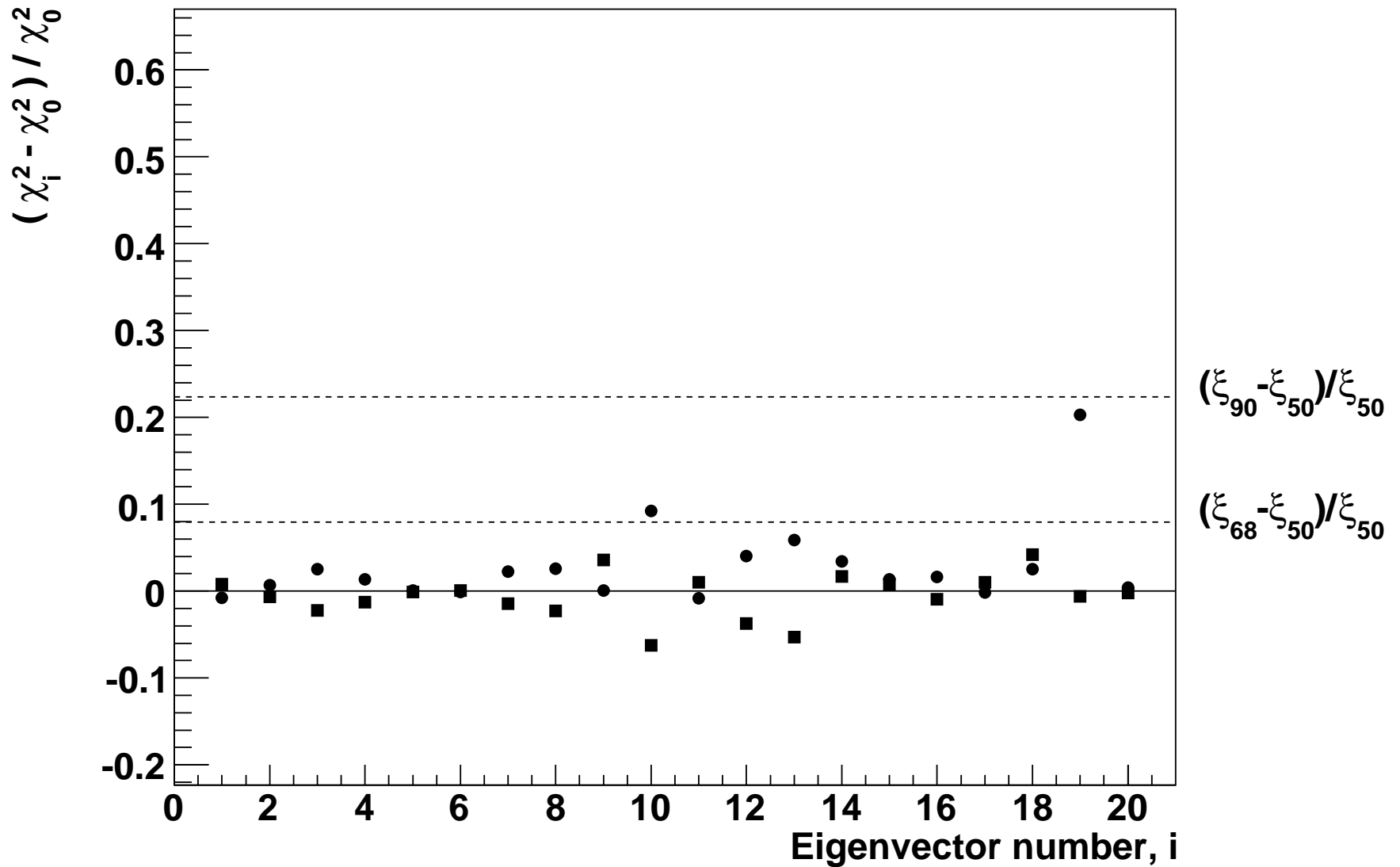
E866 Drell-Yan ratio data only really sensitive to 3 parameters defining  $\bar{d}(x, Q^2) - \bar{u}(x, Q^2)$ . Eigenvector 5 (normalization) over-constrained?

**DY RATIO**



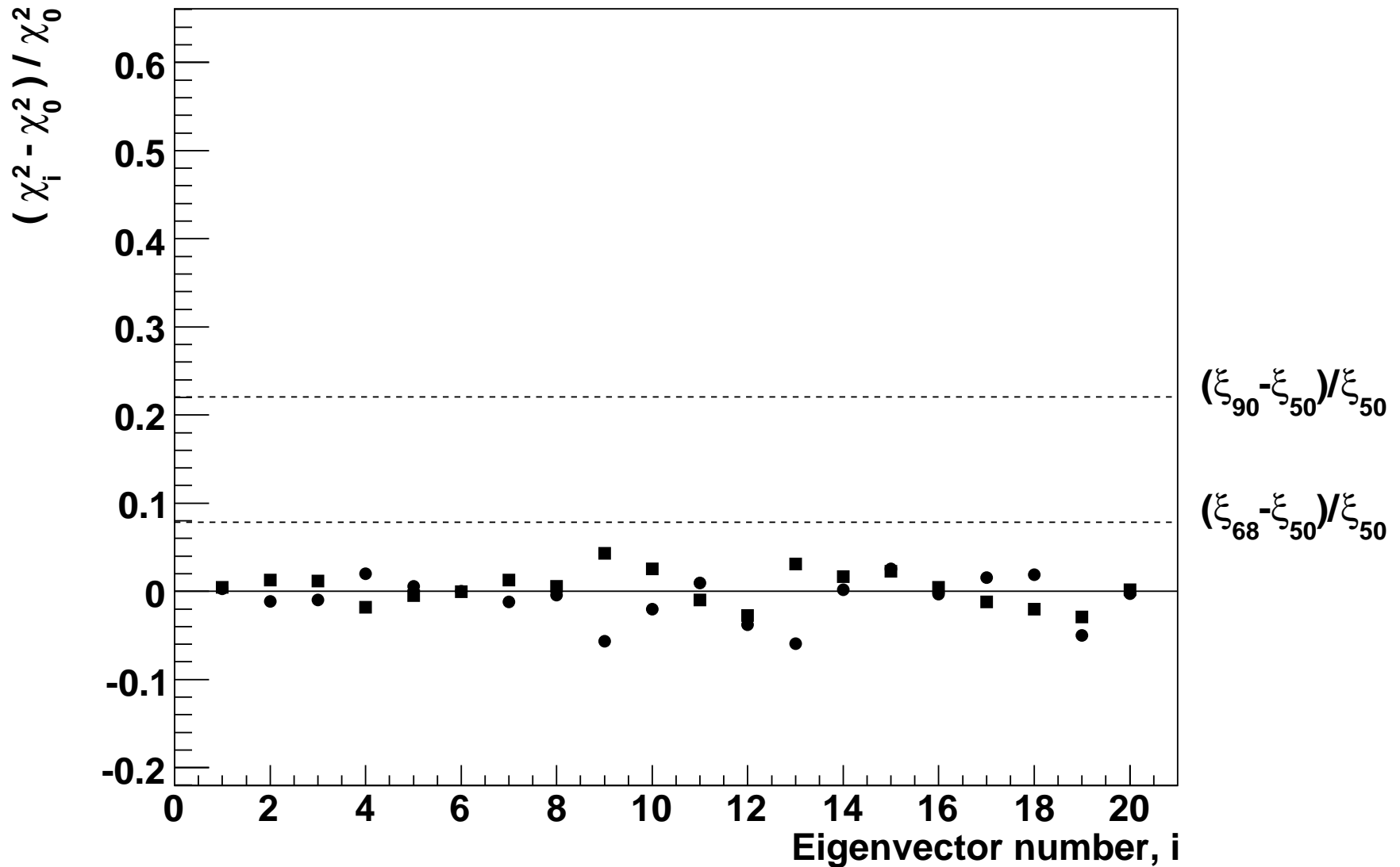
CDF run II high- $E_T$  jet data not sensitive to many parameters, but main constraint on medium and high- $x$  gluon (19). D0 high- $E_T$  jet data similar.

### CDFjet2



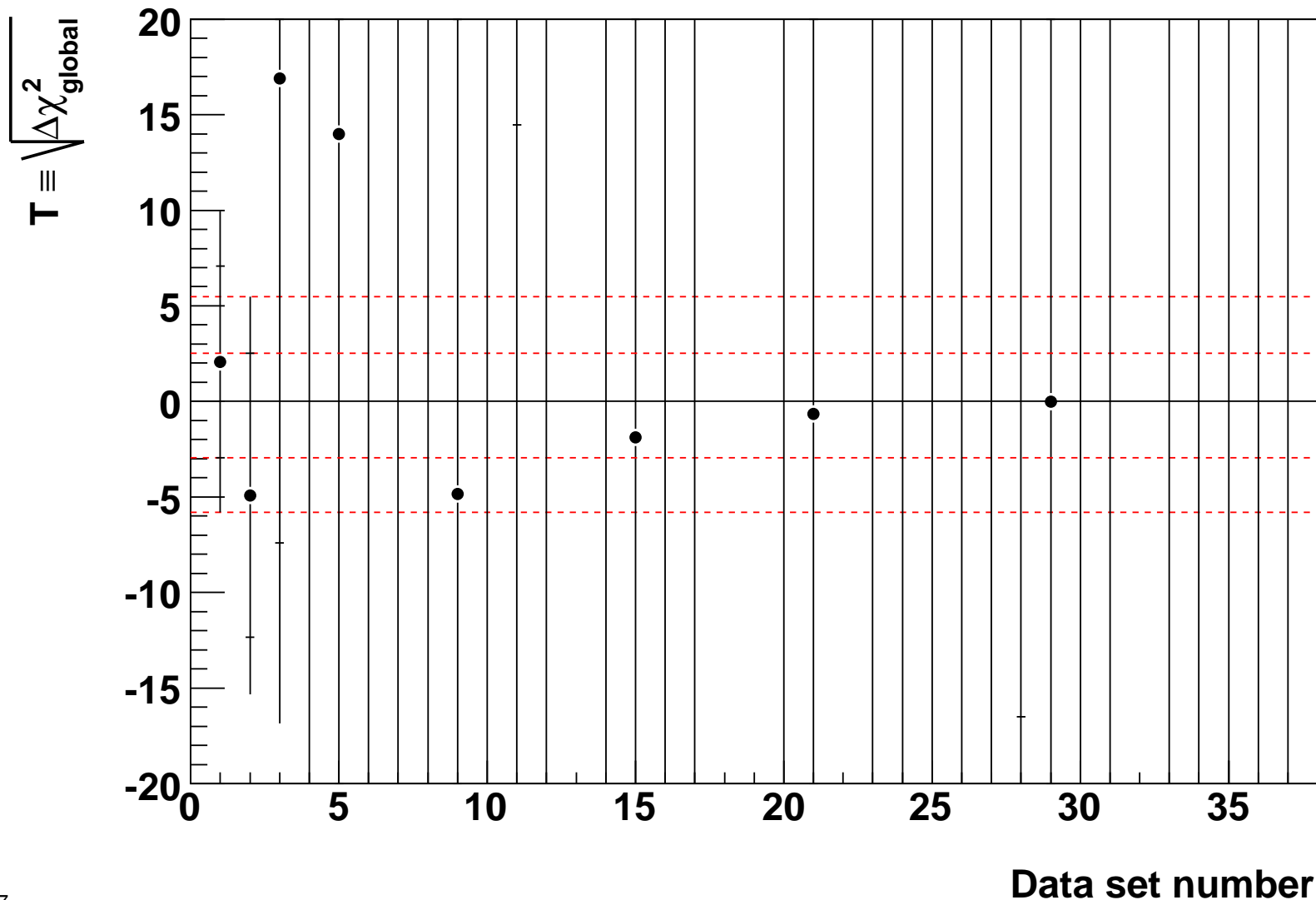
HERA  $F_2^c(x, Q^2)$  has no very strong parton parameter constraint (half a dozen data sets similar). Constrains  $m_c$  to  $\pm 0.15$ , and nontrivially consistent with rest of fit.

**f2 charm**



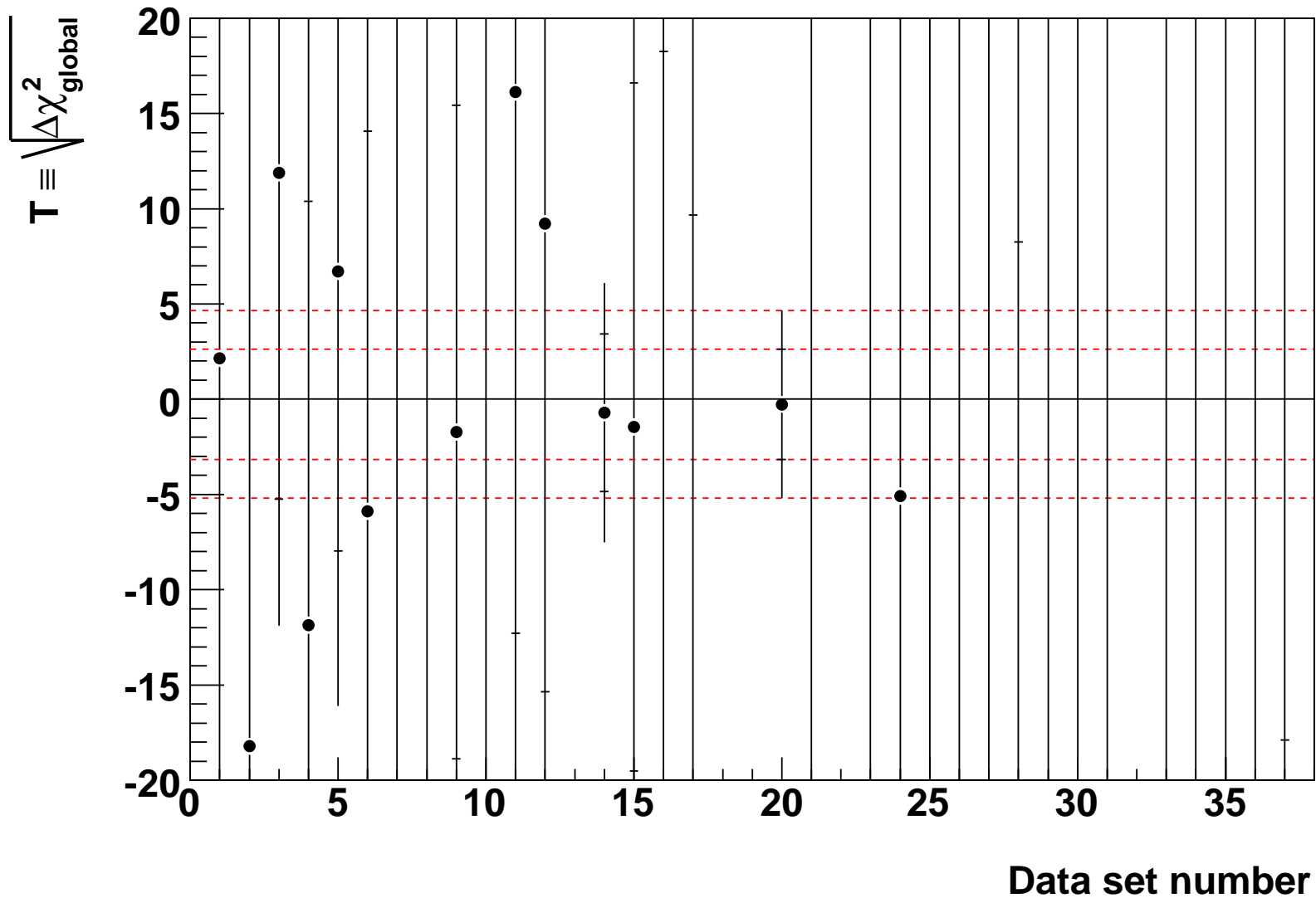
Can also look at variation in  $\chi^2$  for each data set for an eigenvector. Number **1**, related to small- $x$  gluon constrained almost entirely by H1 (1) and ZEUS (2) data on  $F_2(x, Q^2)$ .

### Eigenvector number 1



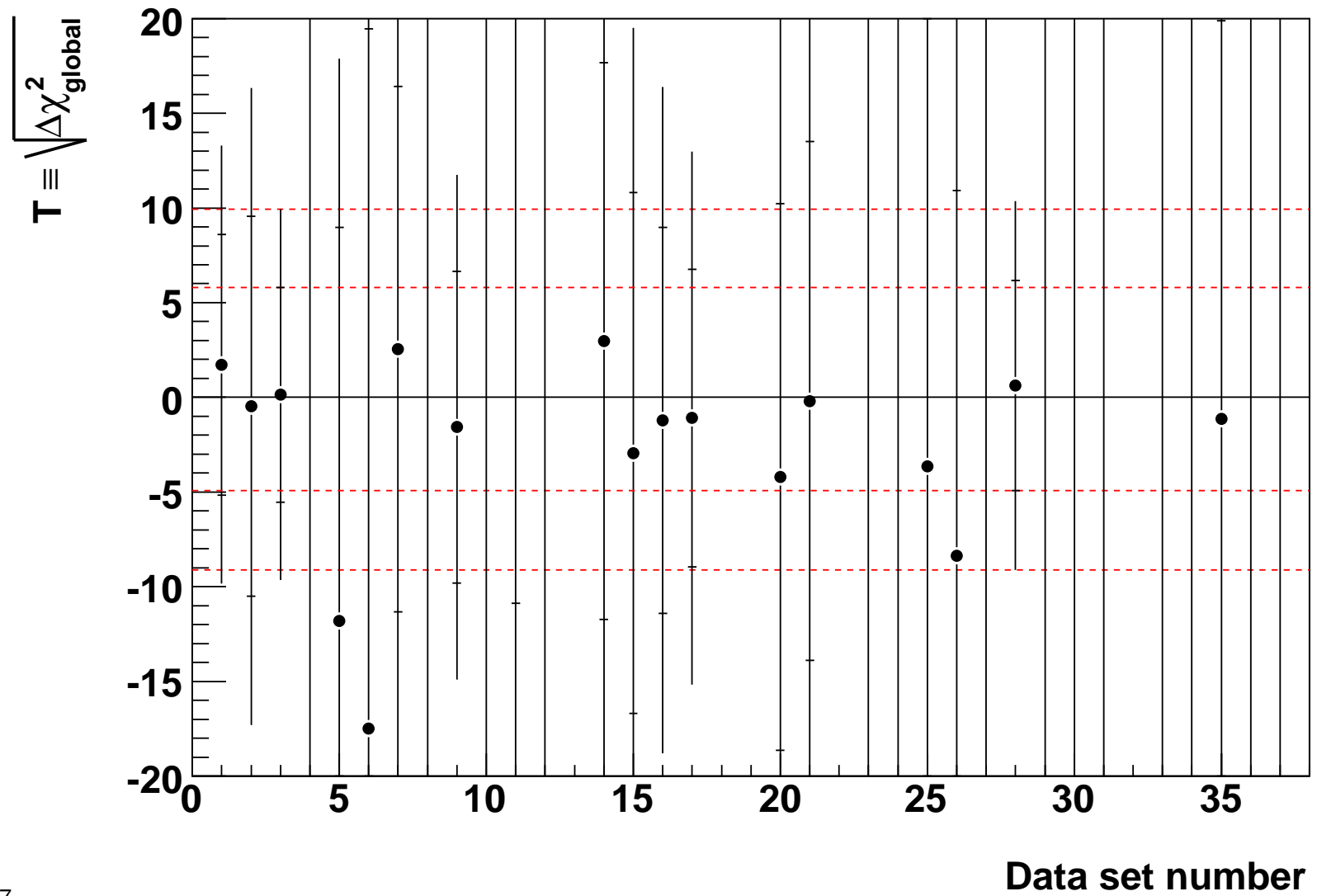
Number 5, related to  $\bar{d} - \bar{u}$  normalization constrained most by E866 Drell-Yan asymmetry (20) but also, and consistently by NMC data (14) on  $F_2^n(x, Q^2)/F_2^p(x, Q^2)$ .

### Eigenvector number 5



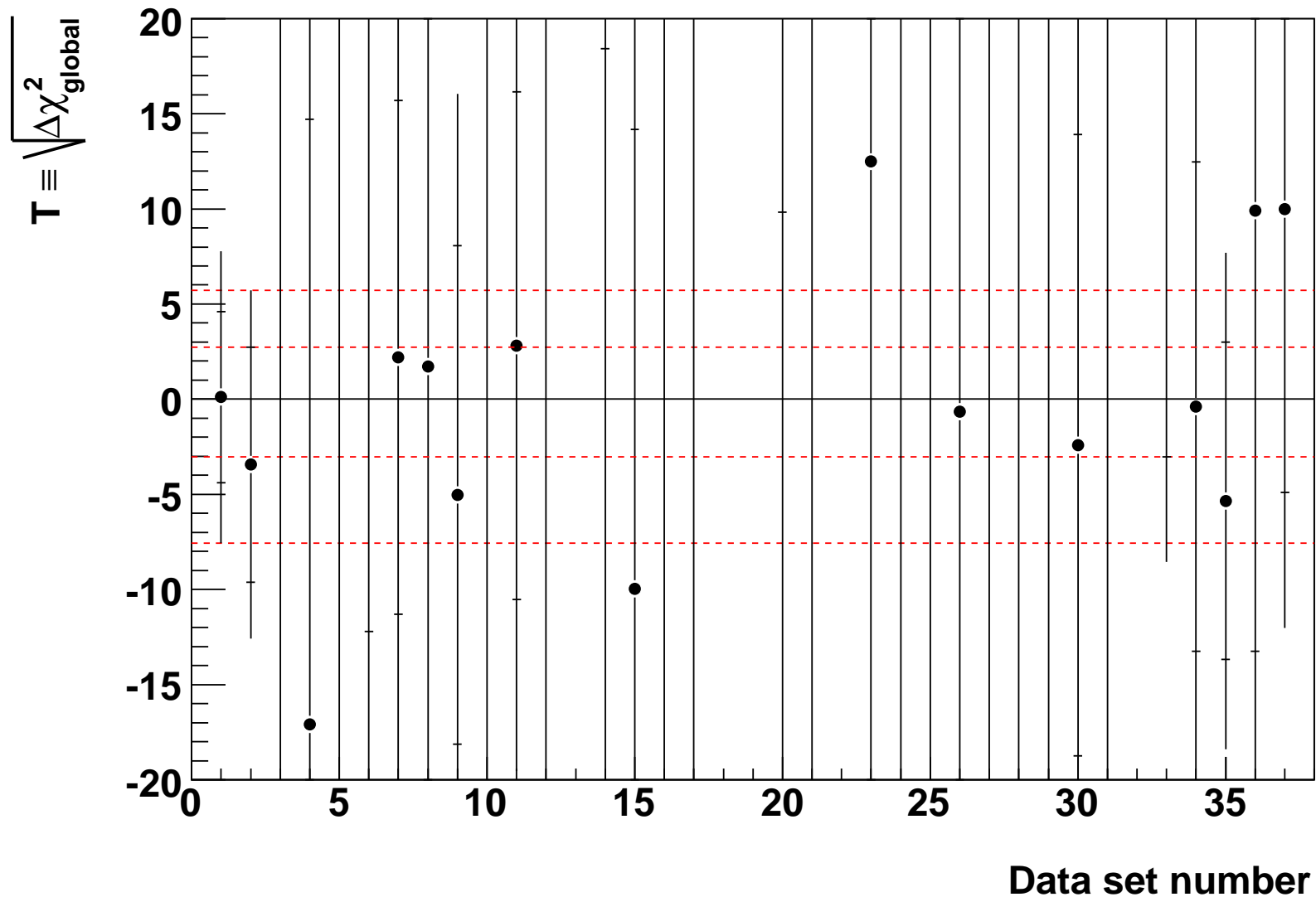
Number **15**, related to medium- $x$  sea quarks constrained by **H1** (1) and **ZEUS** data (2) on  $F_2(x, Q^2)$  as well as various fixed target data (**BCDMS**  $F_2^p(x, Q^2)$  (3), and **CHORUS** (28) and **NuTeV**  $F_2(x, Q^2)$  (9)) and  $W$ -asymmetry data (16,17).

**Eigenvector number 15**



Number 19, related to medium and high- $x$  gluon constrained almost mainly by H1 (1) and ZEUS data (2) on  $F_2(x, Q^2)$ , but also Tevatron high- $E_T$  jet data (33,35).

### Eigenvector number 19



# Predictions/tests at the LHC

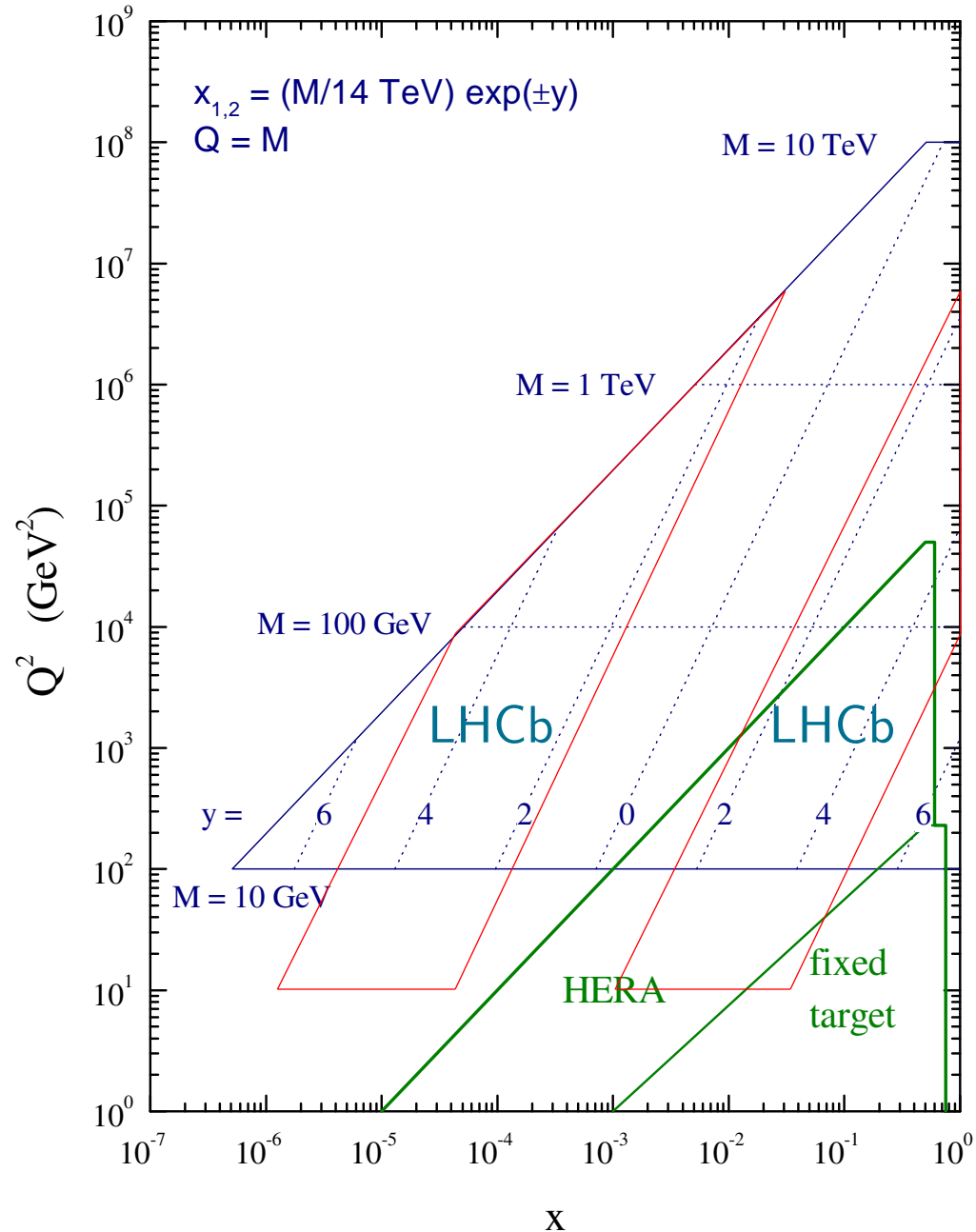
The kinematic range for particle production at the LHC is shown.

Smallish  $x \sim 0.001 - 0.01$  parton distributions therefore vital for understanding the standard production processes at the LHC.

However, even smaller (and higher)  $x$  required when one moves away from zero rapidity, e.g. when calculating total cross-sections.

Already seen different predictions from different groups or prescriptions, e.g.  $\sigma_{tot}(W)$ .

## LHC parton kinematics



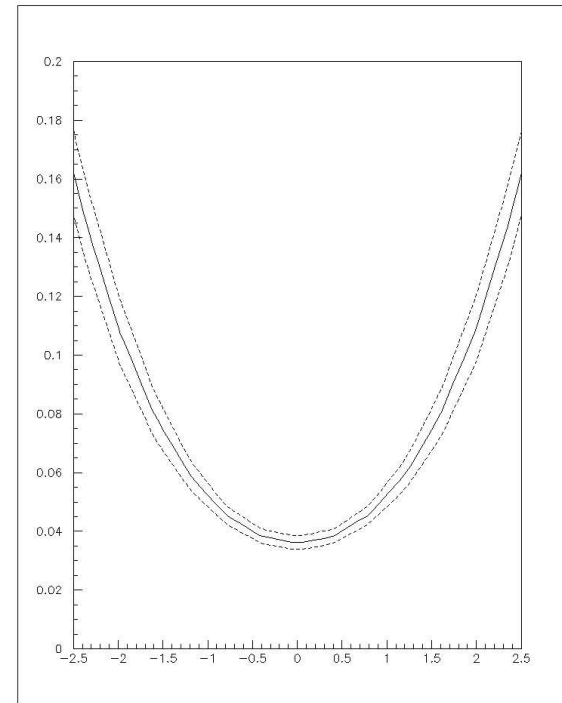
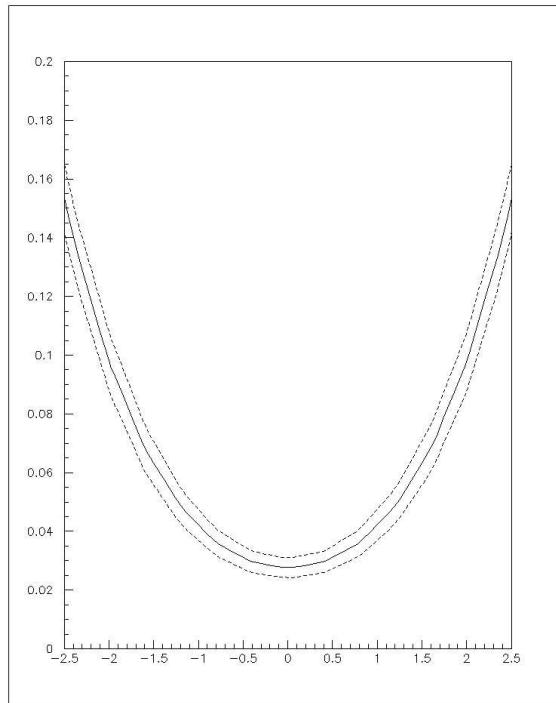


“Safe” predictions from different groups differ by more than their quoted uncertainties, e.g. study by ZEUS/ATLAS parton analysis group (Cooper-Sarkar *et al*) of

$$\frac{(\sigma(W^+) - \sigma(W^-))}{(\sigma(W^+) + \sigma(W^-))}$$

Left – MRST

Right – CTEQ



At  $y = 0$  MRST give  $0.026 \pm 0.005$  while CTEQ give  $0.036 \pm 0.004$ .

Different ideas about quark decomposition at lowish  $x$  , i.e.  $y = 0$  corresponds to  $x = 0.006$  – i.e. separation of valence and sea quarks.

$$\frac{(\sigma(W^+) - \sigma(W^-))}{(\sigma(W^+) + \sigma(W^-))} \approx \frac{u(x)\bar{d}(x) - d(x)\bar{u}(x)}{u(x)\bar{d}(x) + d(x)\bar{u}(x)}$$

At this  $x$  to a good approximation  $\bar{u}(x) = \bar{d}(x)$  so

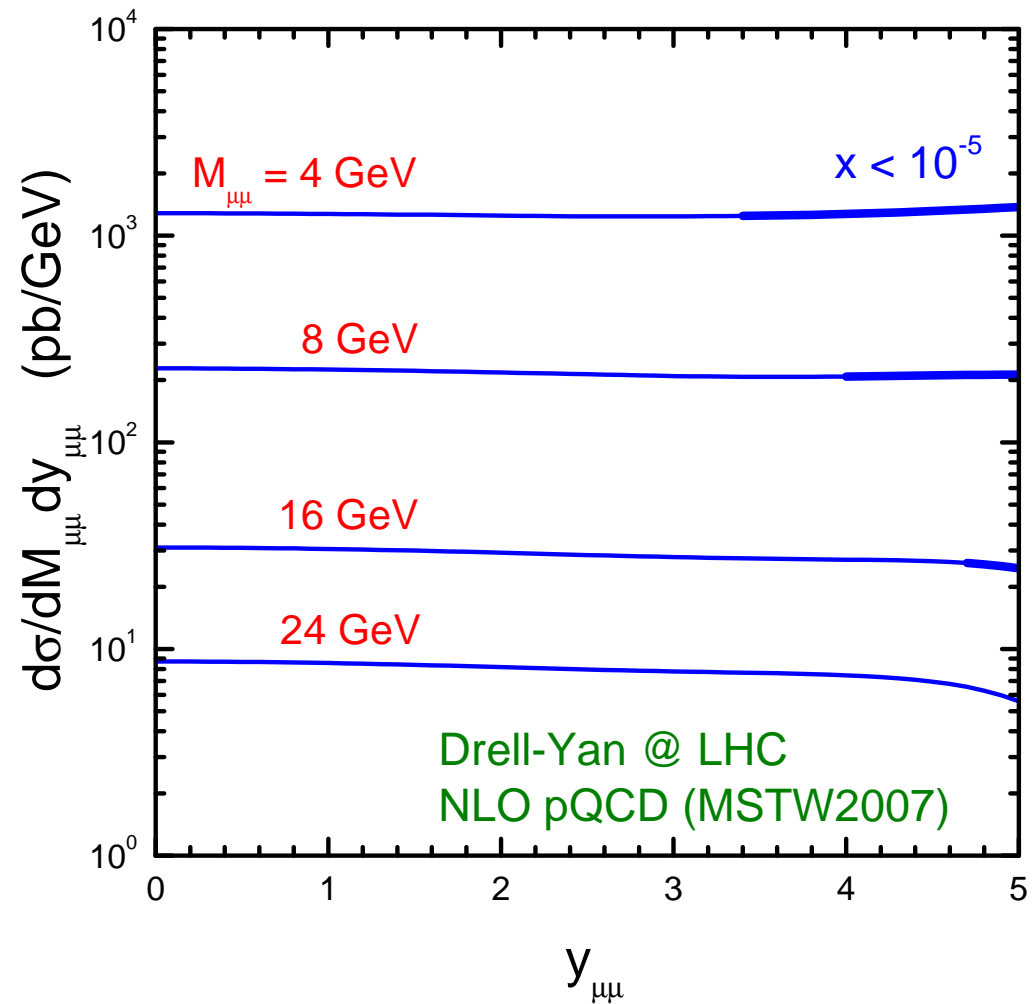
$$\frac{(\sigma(W^+) - \sigma(W^-))}{(\sigma(W^+) + \sigma(W^-))} \approx \frac{u(x) - d(x) - (\bar{u}(x) - \bar{d}(x))}{u(x) + d(x)} = \frac{u_V(x) - d_V(x)}{u(x) + d(x)}$$

Total quark distributions well-constrained but valence quarks obtained only by extrapolation into this region (and number sum rule). Can be probed by [ATLAS](#) and [CMS](#).

Best prediction actually for  $x_1 > 0.01$ , i.e for rapidity  $y \approx 1.5 - 2.5$ , not at centre. Something for [LHCb](#) to check.

Possible to get to very low values of  $x$  at the LHC, particularly LHCb.

Can probe below  $x = 10^{-5}$  - beyond range tested at HERA.



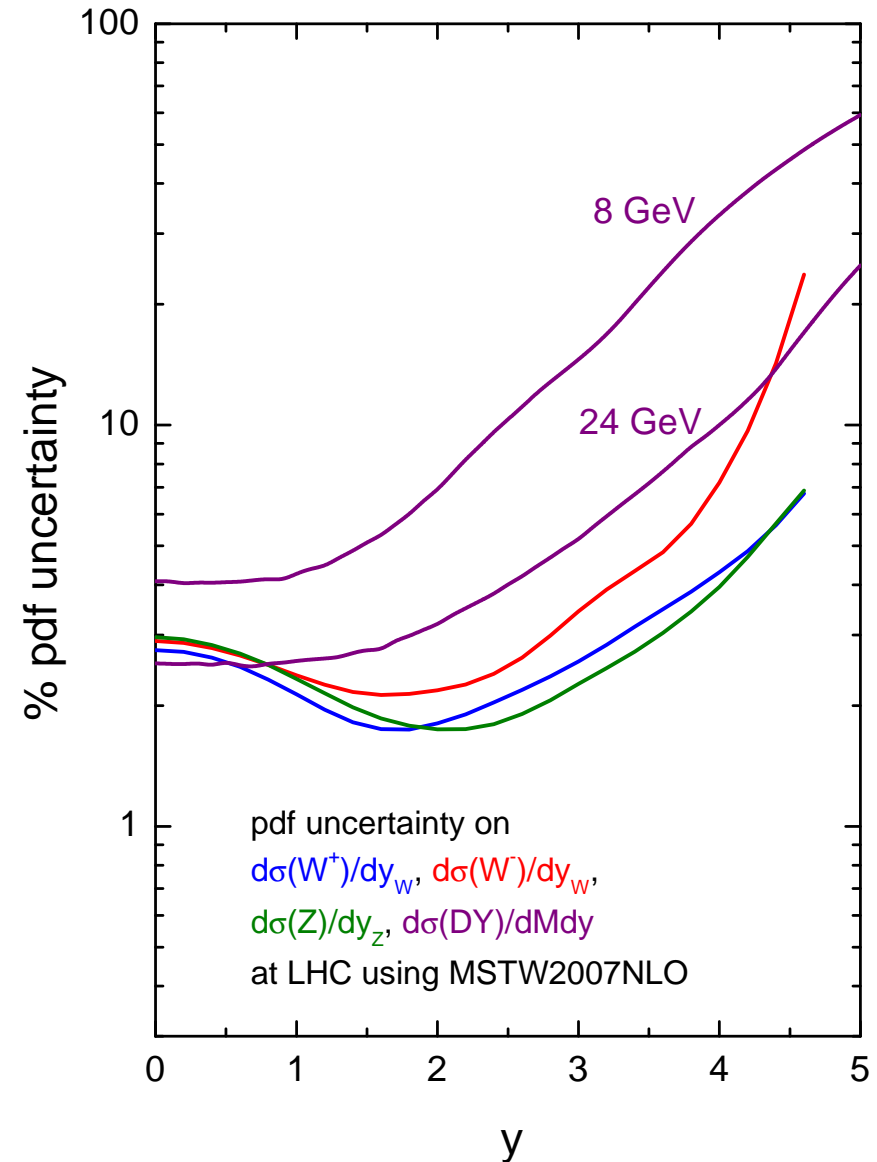
Uncertainty on all cross-sections grows at high rapidity.

Uncertainty on  $\sigma(Z)$  and  $\sigma(W^+)$  converges – both dominated by  $u(x_1)\bar{u}(x_2)$  at very high  $y$ .

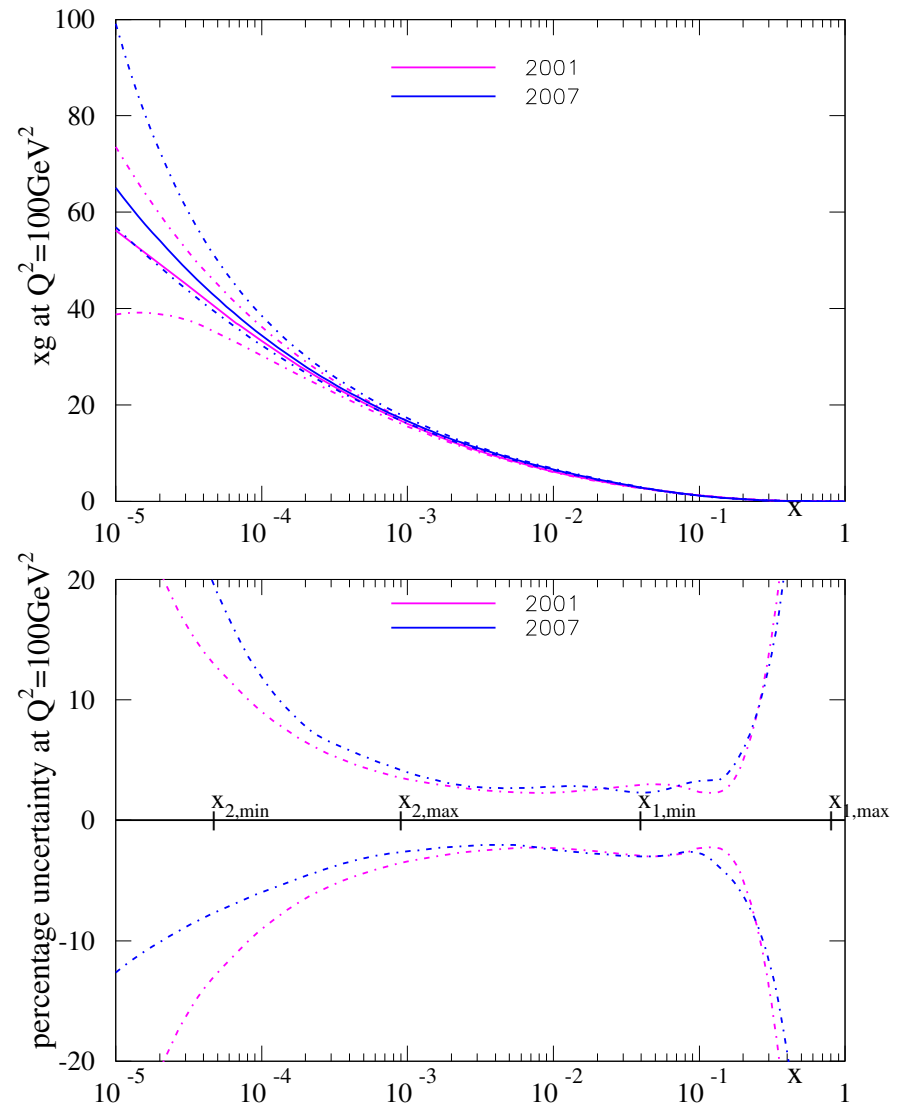
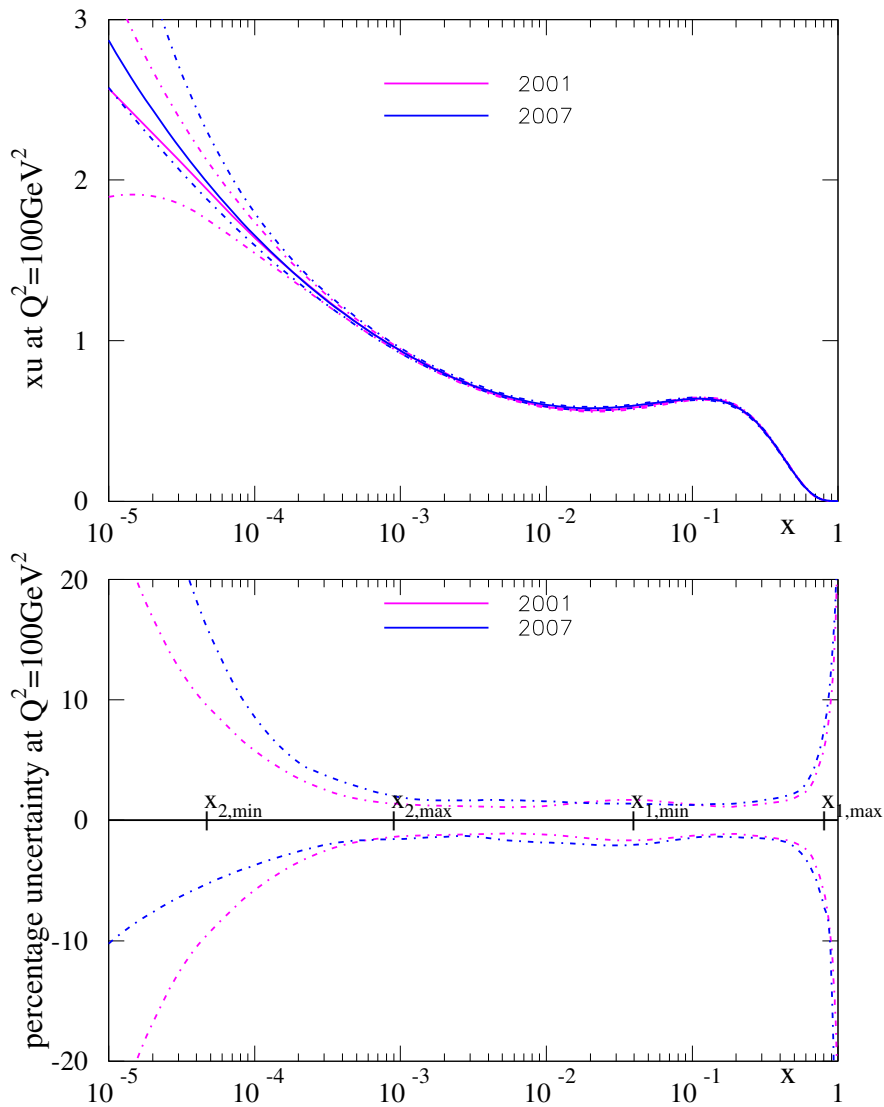
Uncertainty on  $\sigma(W^-)$  grows more quickly at very high  $y$ .

Uncertainty on  $\sigma(\gamma^*)$  is greatest as  $y$  increases.

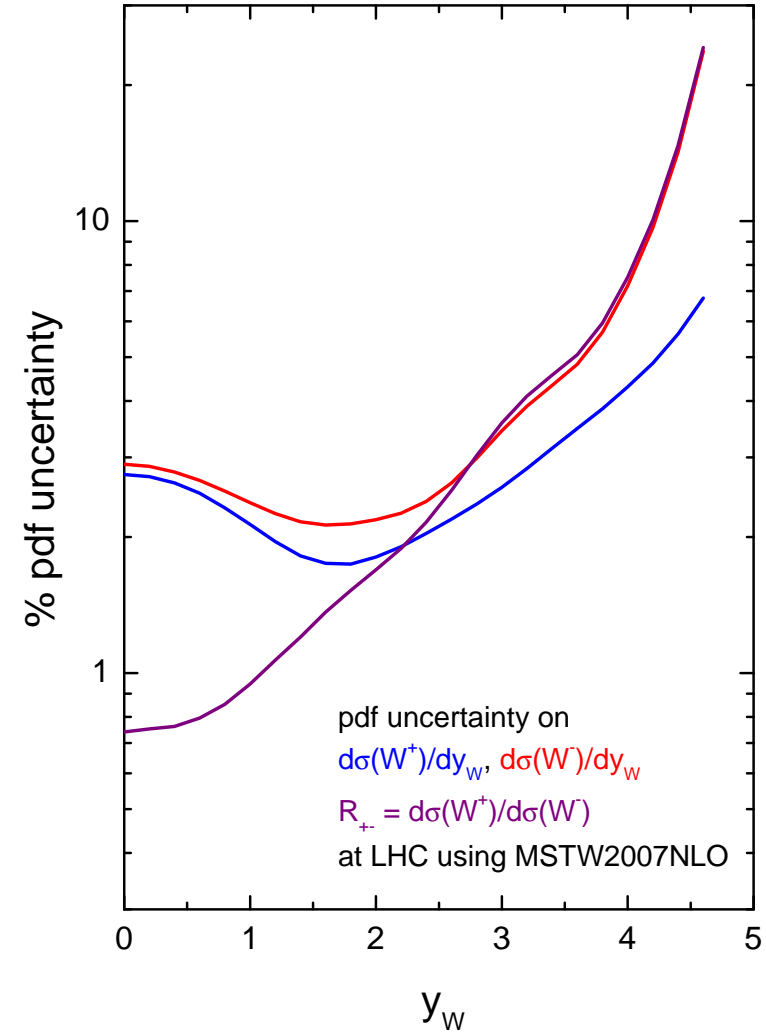
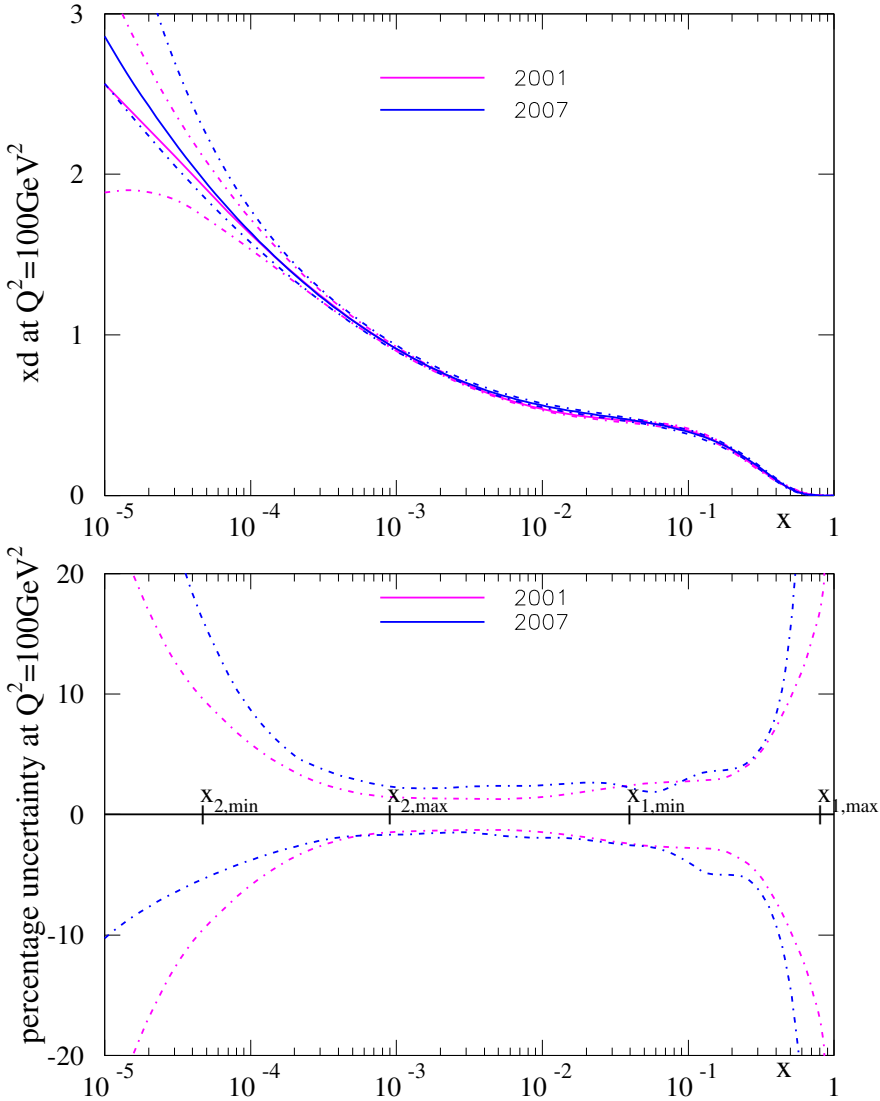
All but low mass  $\gamma^*$  very precise at  $y \leq 2$ . Consistency tests for ATLAS and CMS, or added constraints with very precise data.



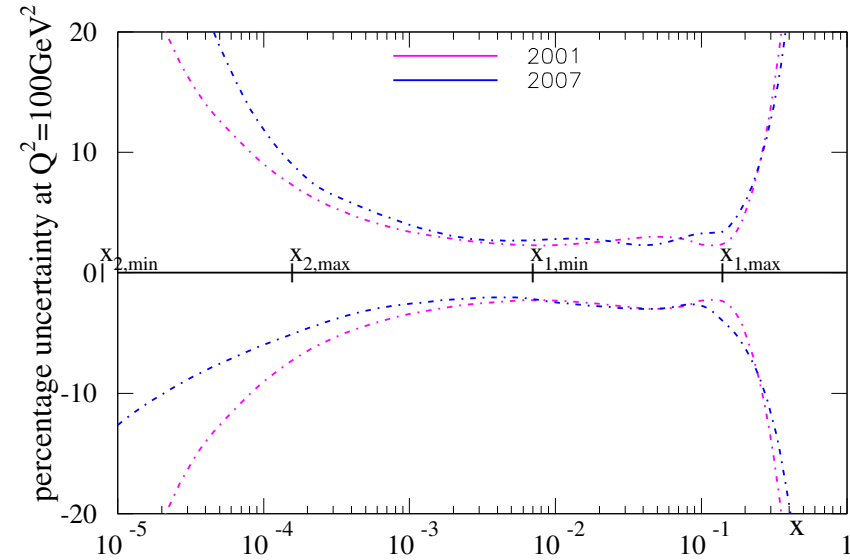
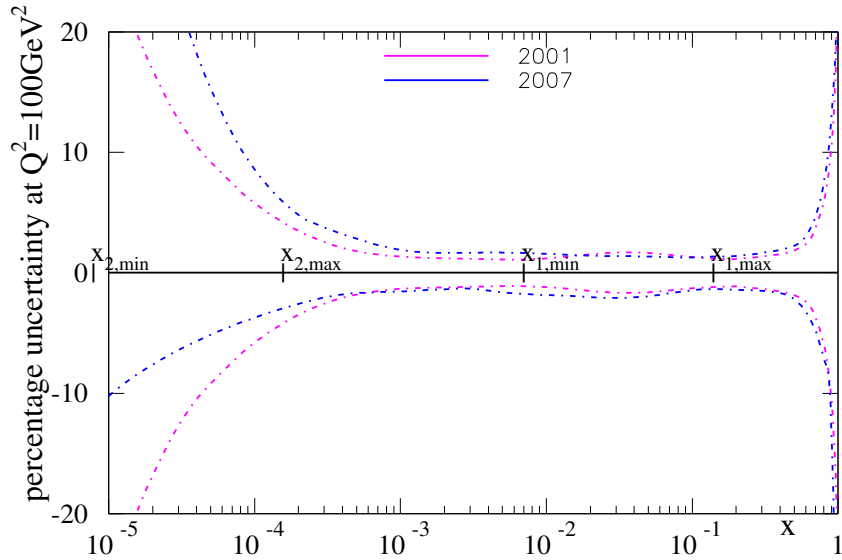
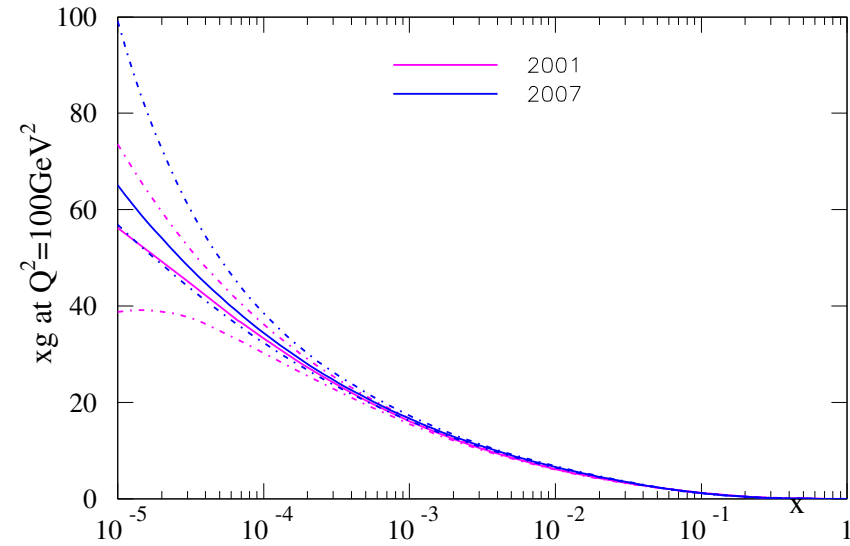
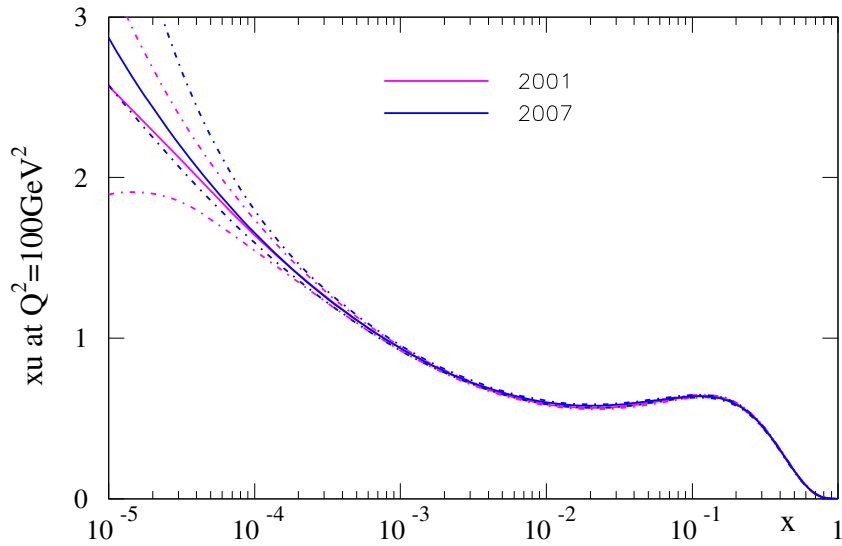
Uncertainty on  $\sigma(Z)$  and  $\sigma(W^+)$  dominated at high  $y$  by sea quark small- $x$  uncertainty rather than high- $x$   $u_V(x)$ . Related to evolution and gluon distribution.



Uncertainty on  $\sigma(W^-)$  dominated at very high  $y$  by high- $x$   $d_V(x)$ . Cleaner probe in ratio.



Uncertainty on  $\sigma(\gamma^*)$  driven by very small- $x$  parton distributions not very well determined by HERA. Dominated by evolution, gluon distribution and small- $x$  physics. Consider  $M_{\gamma^*} = 14\text{GeV}$  as example.



## Potential Results from LHCb

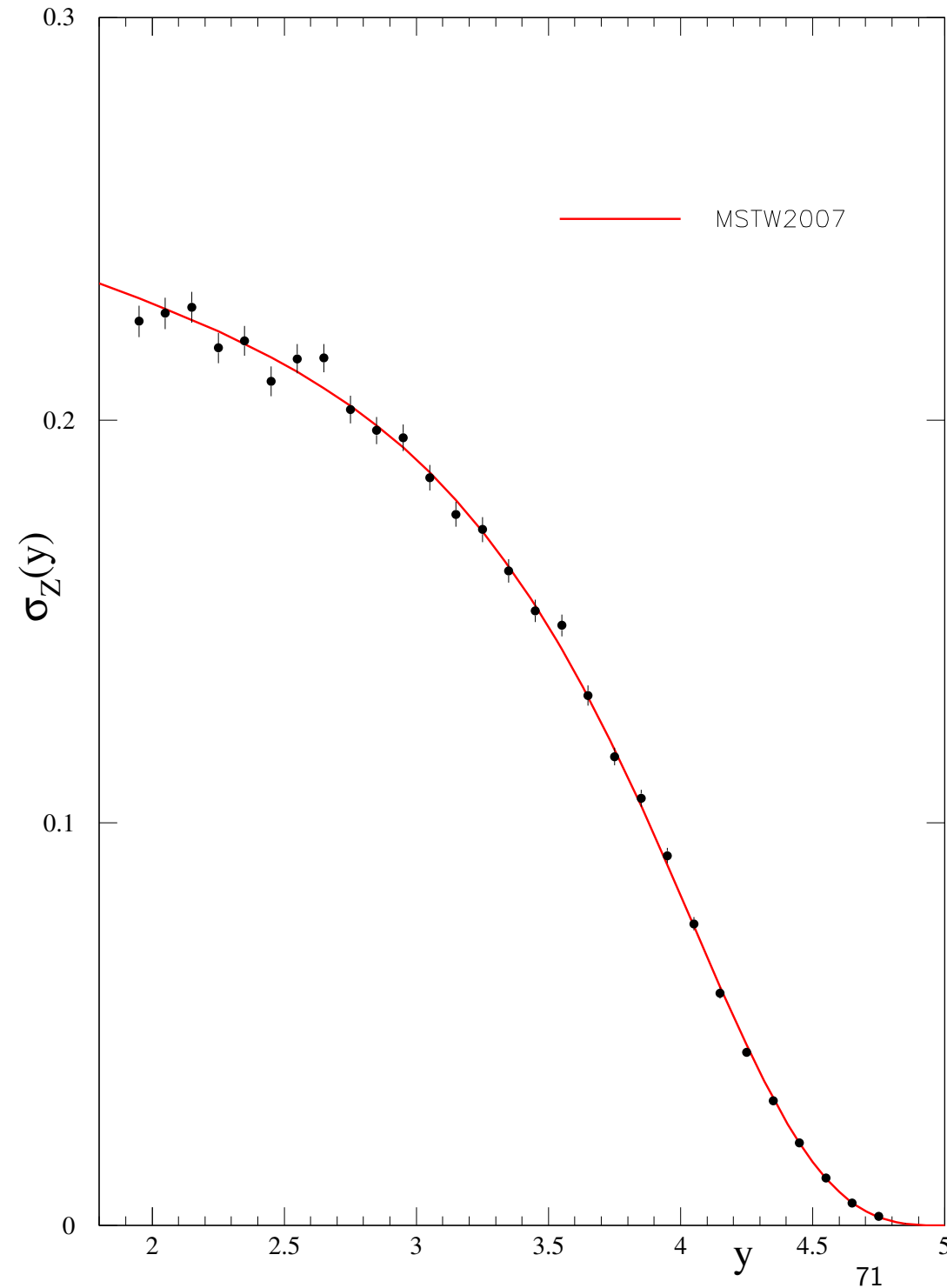
With  $1fb^{-1}$  of data LHCb expects to obtain 212100 events for  $Z \rightarrow \mu^+\mu^-$  for  $1.9 < y < 4.9$ .

Can correspond to 30 equal rapidity bins with  $\sim 1\%$  statistical error at lowest rapidity becoming higher as data falls off at high  $y$ .

Systematic uncertainties also  $\sim 1\%$  with fairly high correlation.

Luminosity uncertainty similarly projected at  $\sim 1\%$ . Since this is a common factor less important in parton determination/QCD test since no impact on shape.

Possible data if completely consistent with current prediction shown opposite.





However, main discriminating power in this type of data if result is not exactly what is expected.

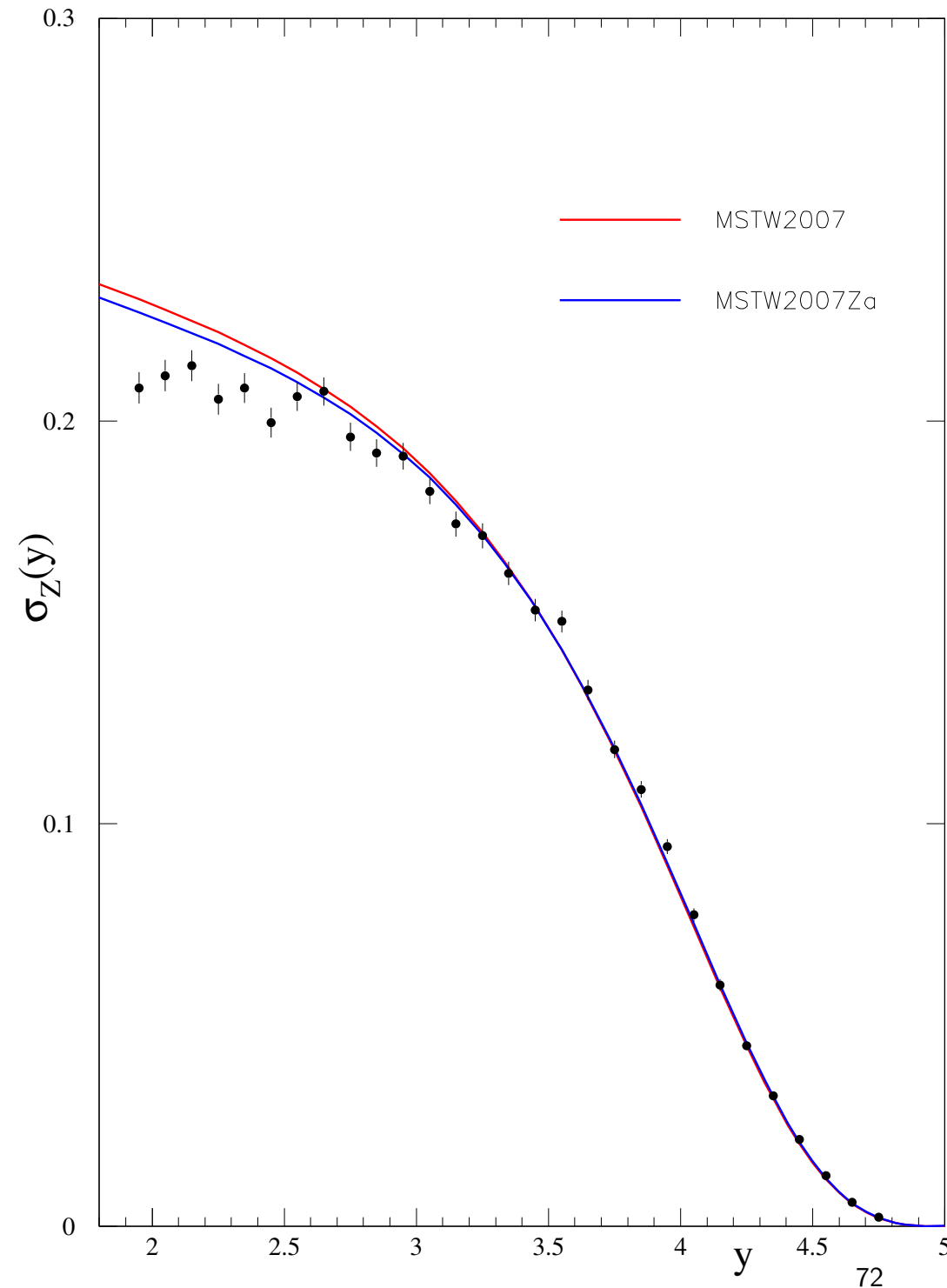
Illustrated opposite is data shifted compared to current prediction where data shifted by factor  $0.05(y - 3.4)$ . Relatively small shift.

Comparing to prediction  $\chi^2 = 153/30$ .

Blue line shows result of new fit. Not possible to obtain good agreement  $\chi^2 = 103/30$ .

HERA data and Tevatron high- $E_T$  jet data do not allow enough movement for good fit.

Discrepancy with theory discovered.



Also look at influence of data from LHCb on  $\sigma(W^-)/\sigma(W^+)$ .

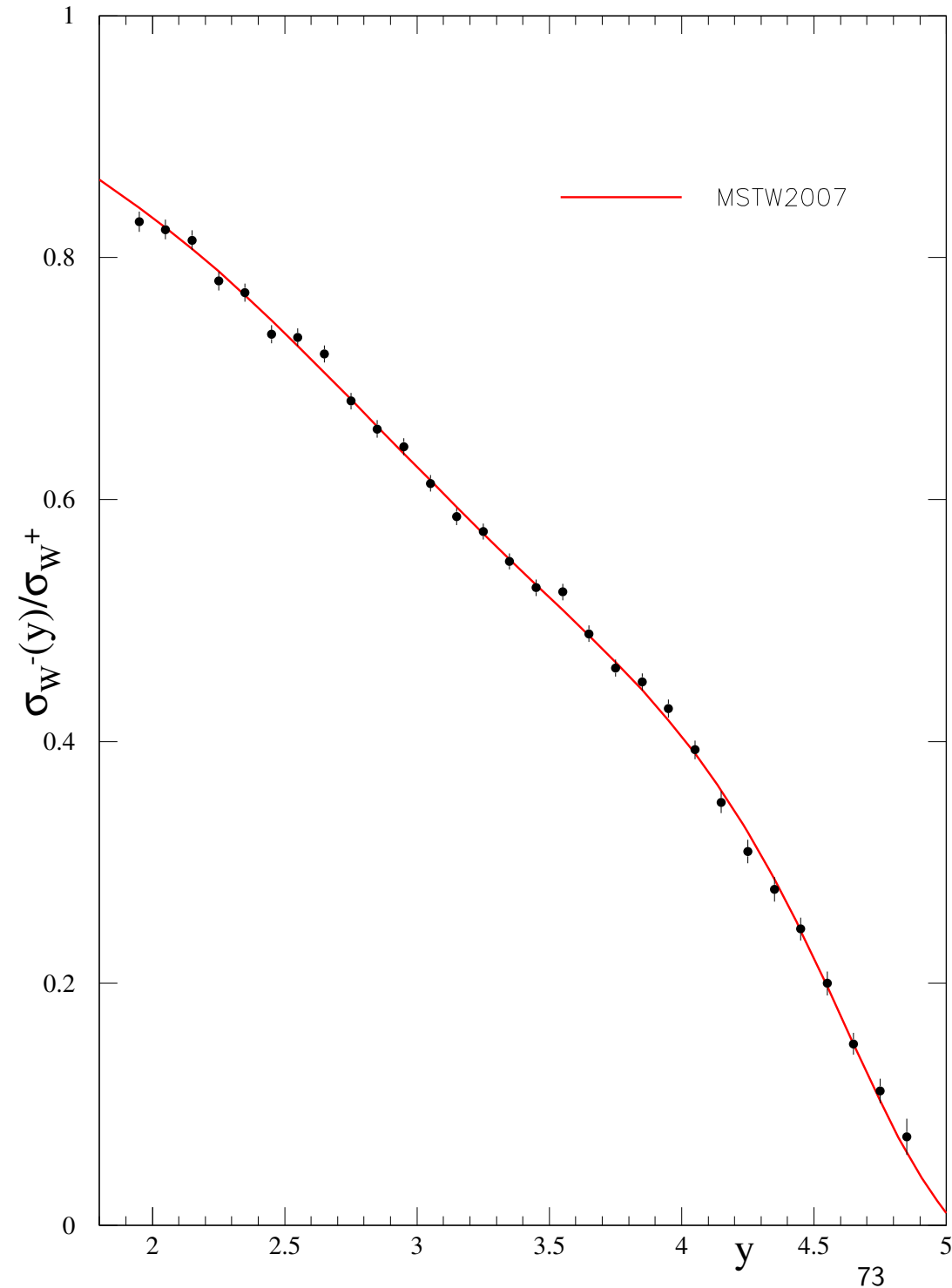
Cross-section for  $W \rightarrow \mu\nu_\mu$  ten times  $Z \rightarrow \mu^+\mu^-$ , but more difficult and more systematics.

In particular measure lepton rapidity not  $W$ . Ignore this here. (CDF now work back to  $W$ ).

Systematics also cancel in ratio.

Assume that for  $1fb^{-1}$  error  $\sim 1\%$  at lowest  $y$  with similar decrease to before at high  $y$ .

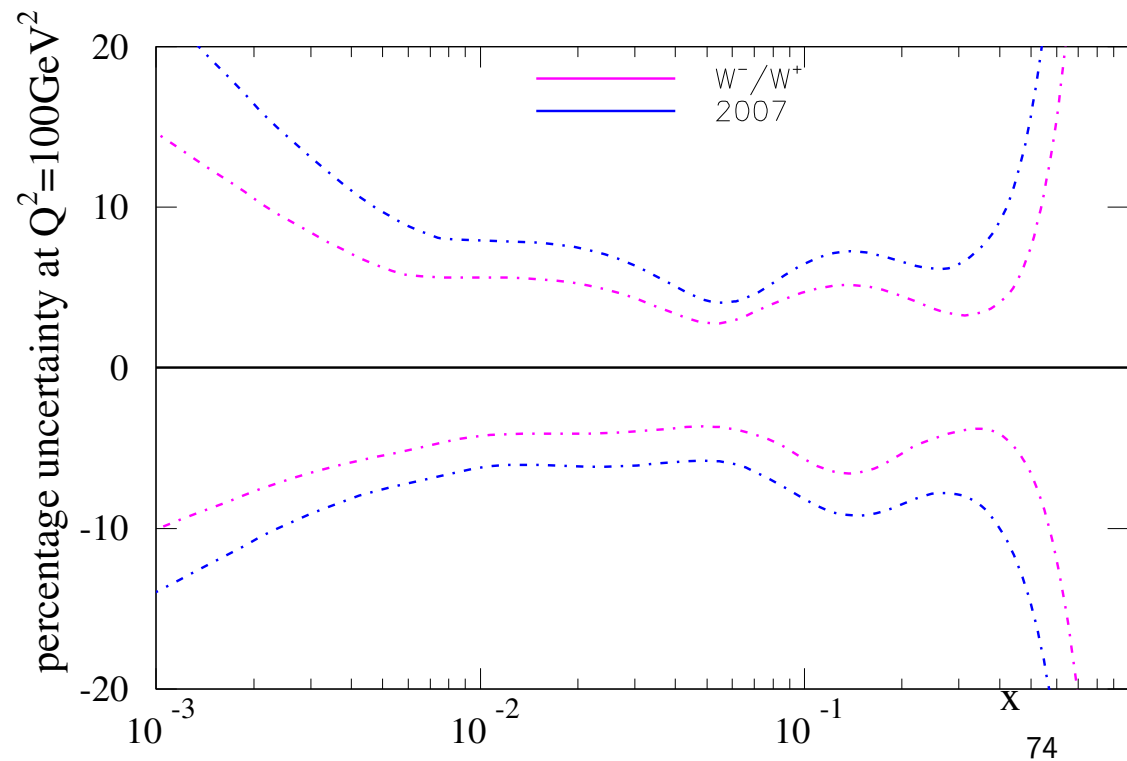
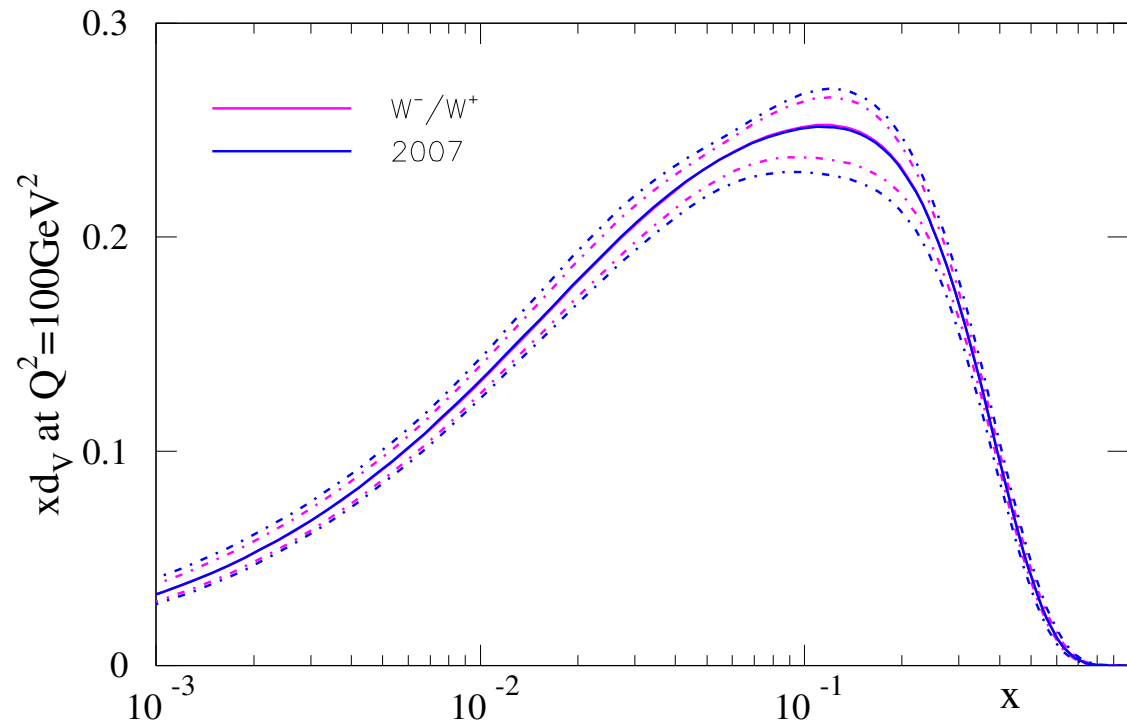
Data compared with prediction shown.



This time data most sensitive to high- $x$  down distribution, i.e.  $d_V(x, Q^2)$ .

Significant reduction in this at all  $x$  (helped by sum rule).

Immediately just about main constraint on this parton.

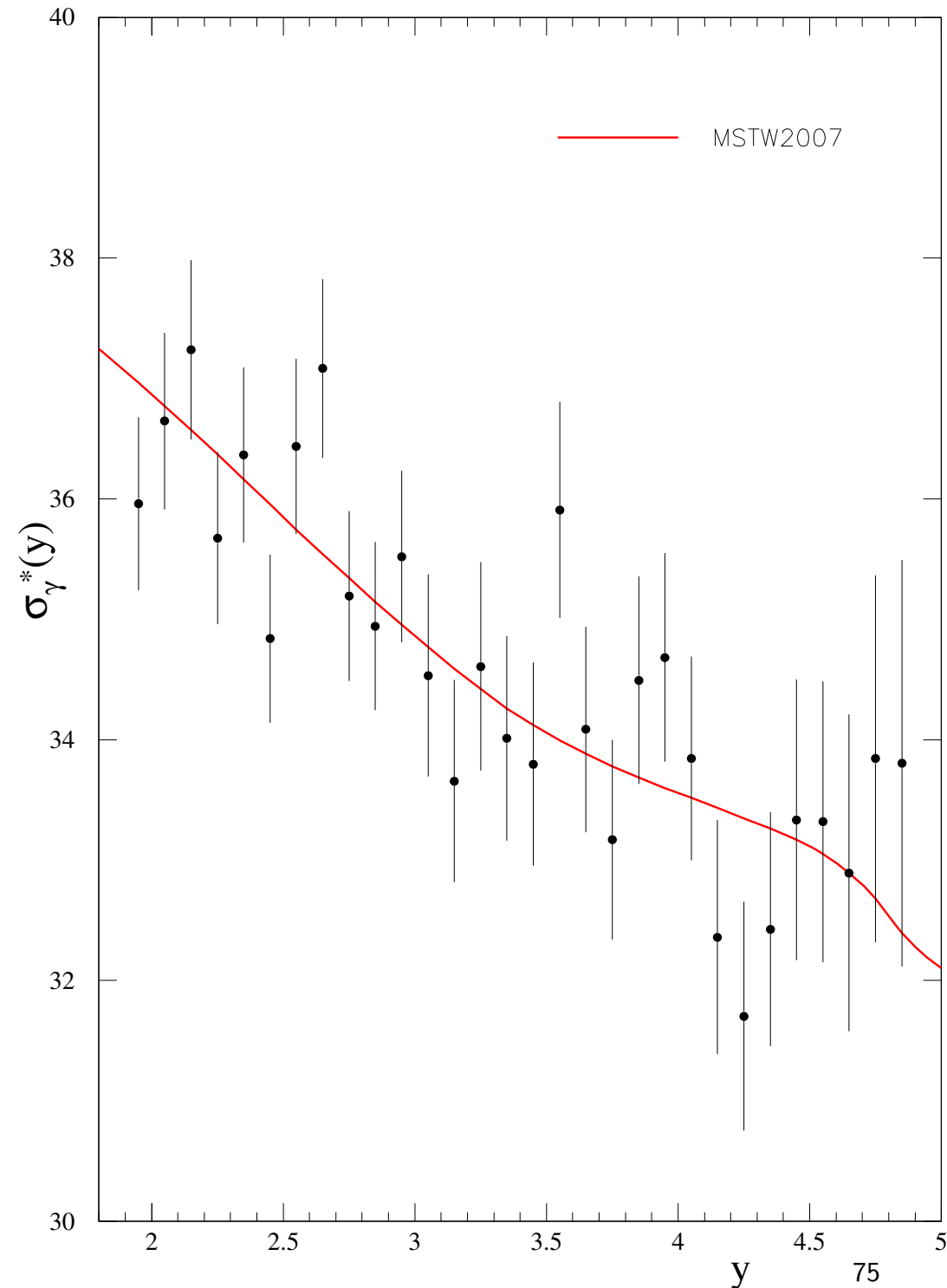


Finally look at influence of data from LHCb on  $\sigma(\gamma^*)$  for  $M_{\gamma^*} = 14\text{GeV}$ .

$d\sigma/dMdy$  for  $\gamma^*$  for this virtuality similar to that for  $Z \rightarrow \mu^+\mu^-$ , at the  $Z$  peak.

Assume that for  $1fb^{-1}$  error a bit bigger than for  $Z \rightarrow \mu^+\mu^-$  at lowest  $y$  but much less decrease at high  $y$  since cross-section is not falling off – not reaching valence quark fall off.

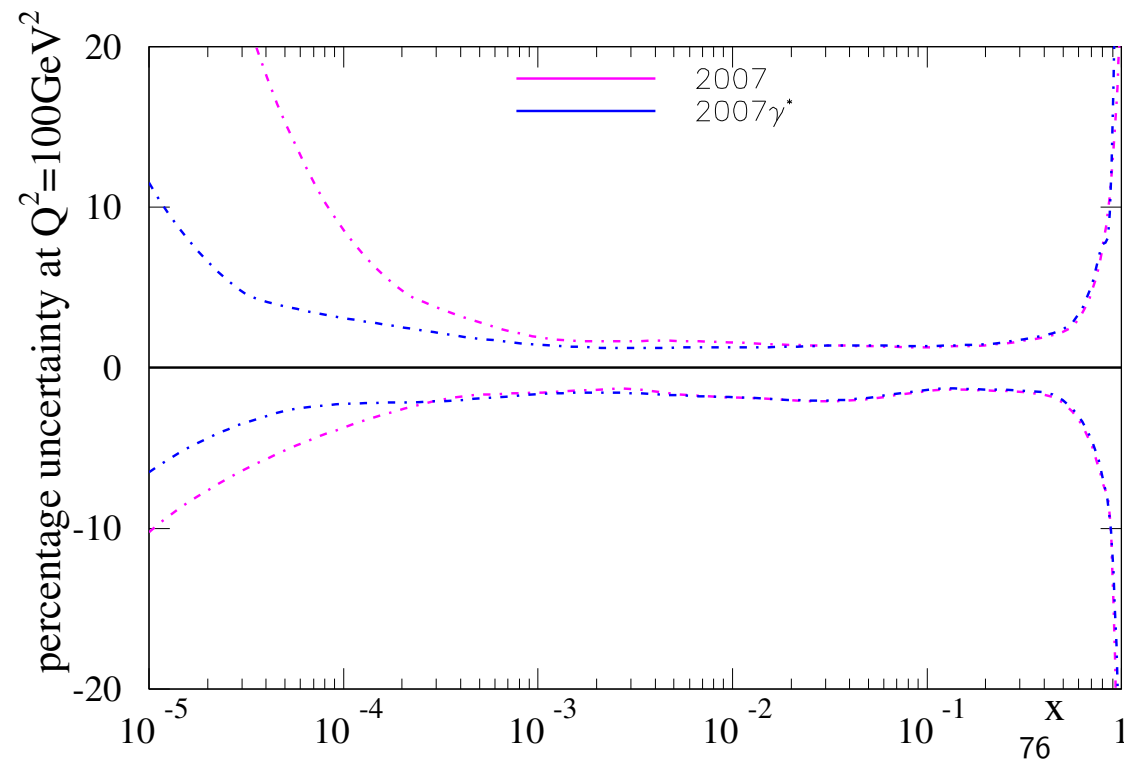
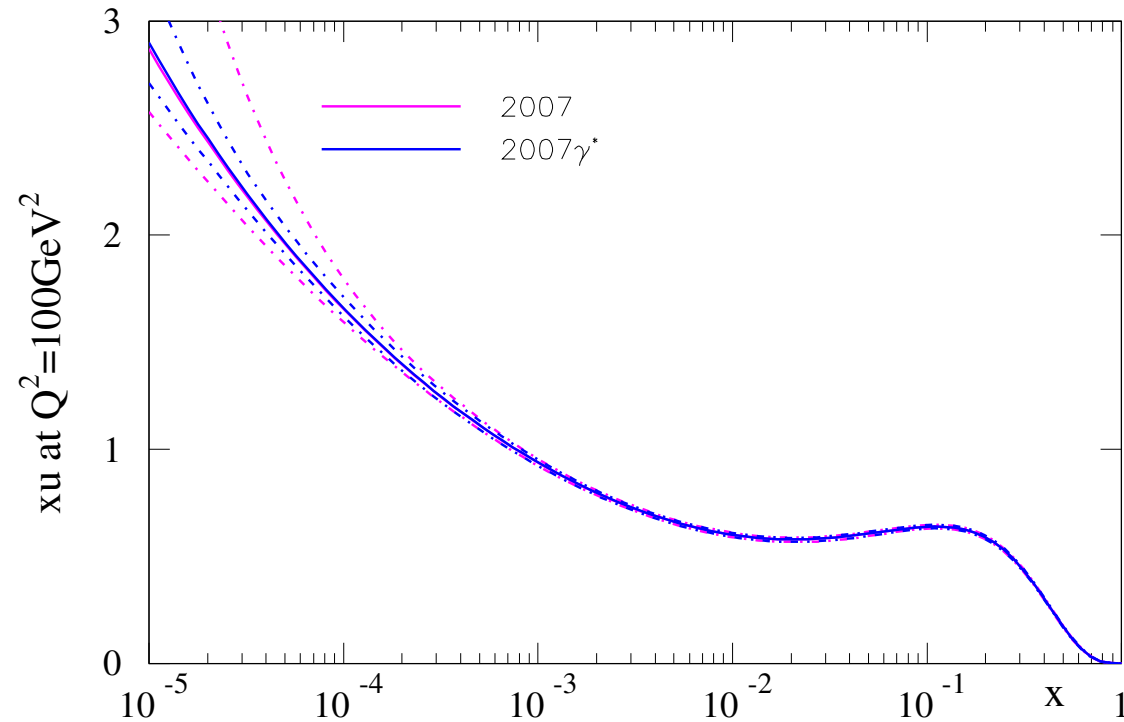
Data compared with prediction shown.



This time data most sensitive to very low- $x$  quark distributions.

Very significant reduction in uncertainty.

Immediately just about main constraint on quarks for  $x \leq 0.0003$ .

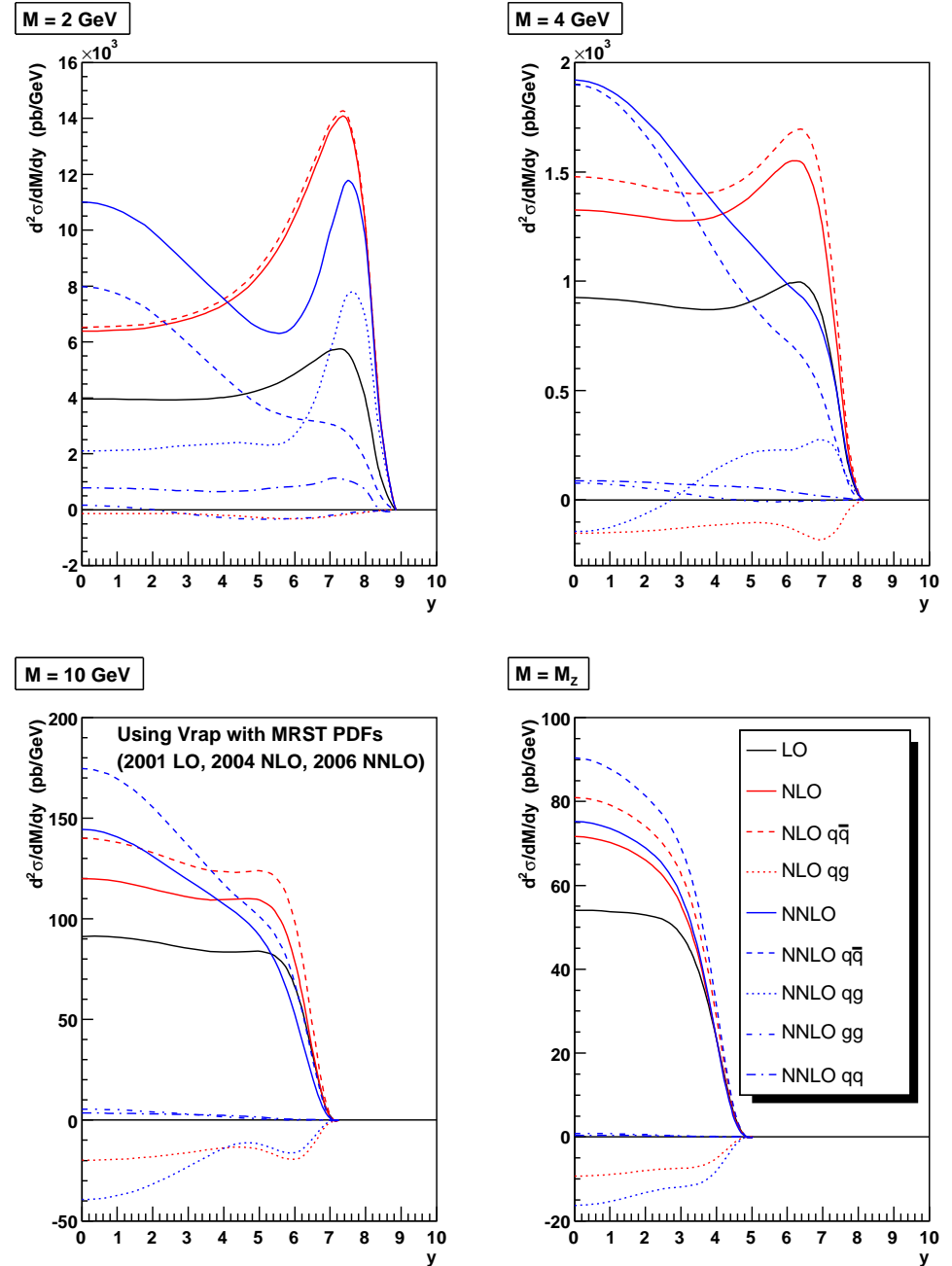


However, this assumes perturbative prediction of Drell-Yan production is reliable.

As seen very large change in prediction from order to order, particularly for low  $M$  and high  $y$ .

Problem with perturbative stability. Is this due to partons or cross-sections?

## $\gamma^*/Z$ rapidity distributions at LHC



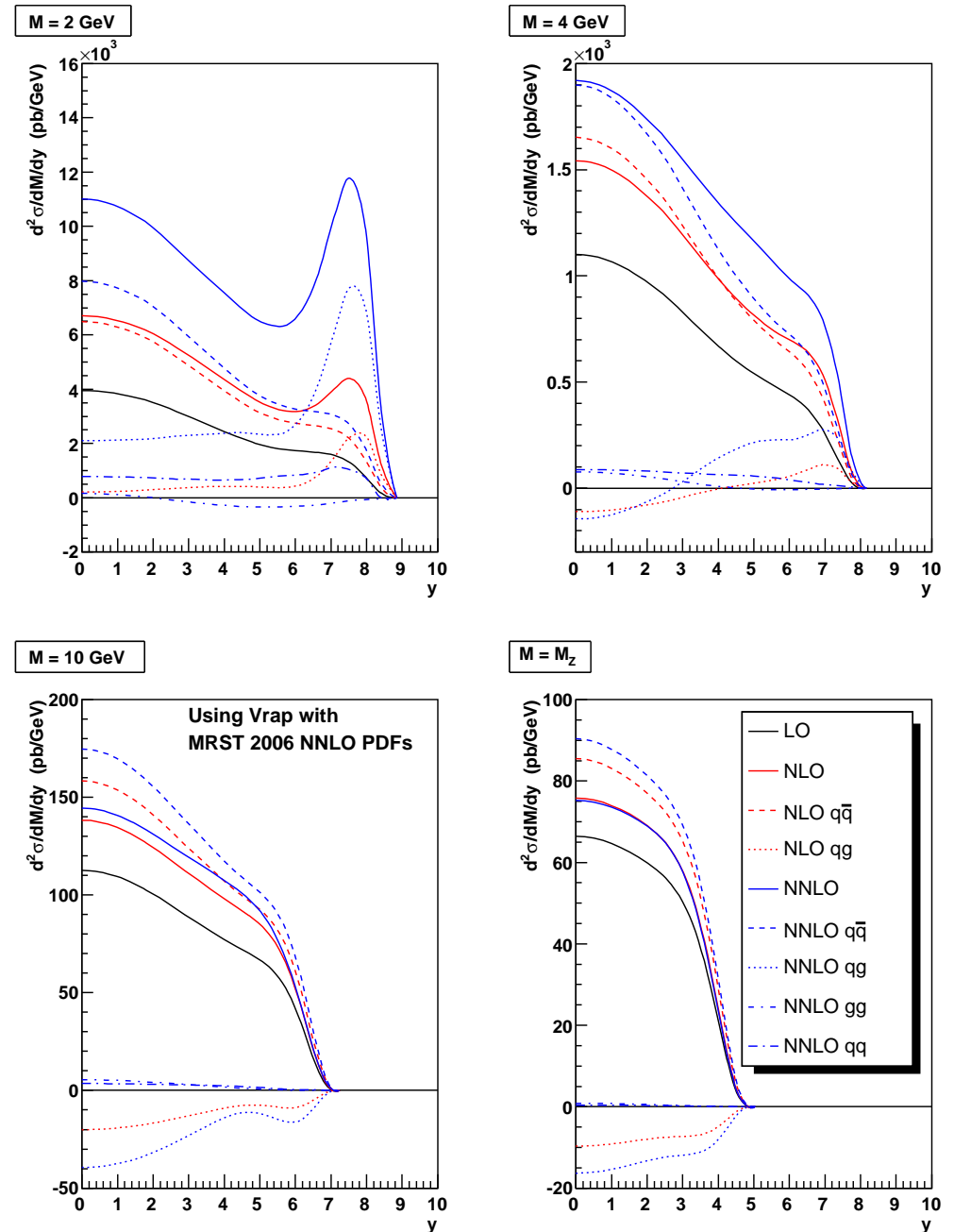
## $\gamma^*/Z$ rapidity distributions at LHC

Keeping partons fixed while changing cross-sections (using MRST2006 NNLO partons) shows part of instability due to partons. Unusual behaviour in very small  $x$  partons at NNLO.

However, large change in quark-gluon (and quark-quark) contributions at NNLO due to  $1/z$  divergences in cross-sections appearing at this order.

Reminiscent of behaviour of  $F_L(x, Q^2)$ . As in this case further  $\ln(1/z)$  divergences at higher orders.

may be sensitive to resummations (amongst other things) at lowest  $M$  and highest  $y$ . In region where measurements can be made?



# Conclusions

**NNLO** partons exist now. Provisional update of partons **MRST06**, need to input full data sets. Main difference due to better **NNLO** heavy flavour prescription. This is important. Change in  **$W, Z$**  cross-section predictions.

Inclusion of new data. Neutrino structure function data inconsistent at high  $x$ . Cut at  $x = 0.5$ . Important constraint at lower  $x$ . Dimuon data fitted directly. Important constraint on strange, and weak evidence for strangeness momentum asymmetry. New uncertainties on  $s + \bar{s}$  feed into other partons.

**Tevatron  $W, Z$**  data important constraint on quarks – constraining for  $d_V$  and to some extent  $\bar{d}$ . Slightly different shape for  $d_v(x, Q^2)$ . Better fits at **NNLO**.

**HERA** and **Tevatron** jets now fit using **fastNLO**. Works well and fit good. New run II **CDF** jet data included in fit. Slightly smaller high- $x$  gluon  $\rightarrow$  lower  $\alpha_S$ .

Will have full updated **NLO** and **NNLO** partons for **LHC** complete with experimental uncertainties with weeks. Theoretical uncertainties require more work.

Looking forward to having **HERA** data on  $F_L(x, Q^2)$  to help determine small- $x$  dynamics and “averaged” **HERA** structure function data to help determine uncertainties on quarks and gluon.



Vector boson production at the LHC good constraint on parton distributions. In some cases HERA has helped pin down partons so that uncertainties of  $\sim 2\%$  are possible (in principle).

Fairly central rapidity measurements at ATLAS and CMS will help verify our current partons. Asymmetries will provide info on valence quarks at smallish  $x$ .

High rapidity measurements at LHCb will constrain high- $x$  down quarks, and test small- $x$  extrapolations. Lower mass  $\gamma^*$  measurements will potentially probe quarks and gluons at lower  $x$  than even HERA – particularly in perturbative range.

However, perturbation series not that convergent for predictions at lowish scales and small  $x$ , similar to  $F_L(x, Q^2)$ .

Neither standard LO and NLO partons ideal for LO generators. Comparison with processes where NLO known suggests modified LO partons, momentum violation plus NLO coupling constant, usually provides most reliable results. Additional partons allowed by extra momentum compensate semi-universally for higher orders.

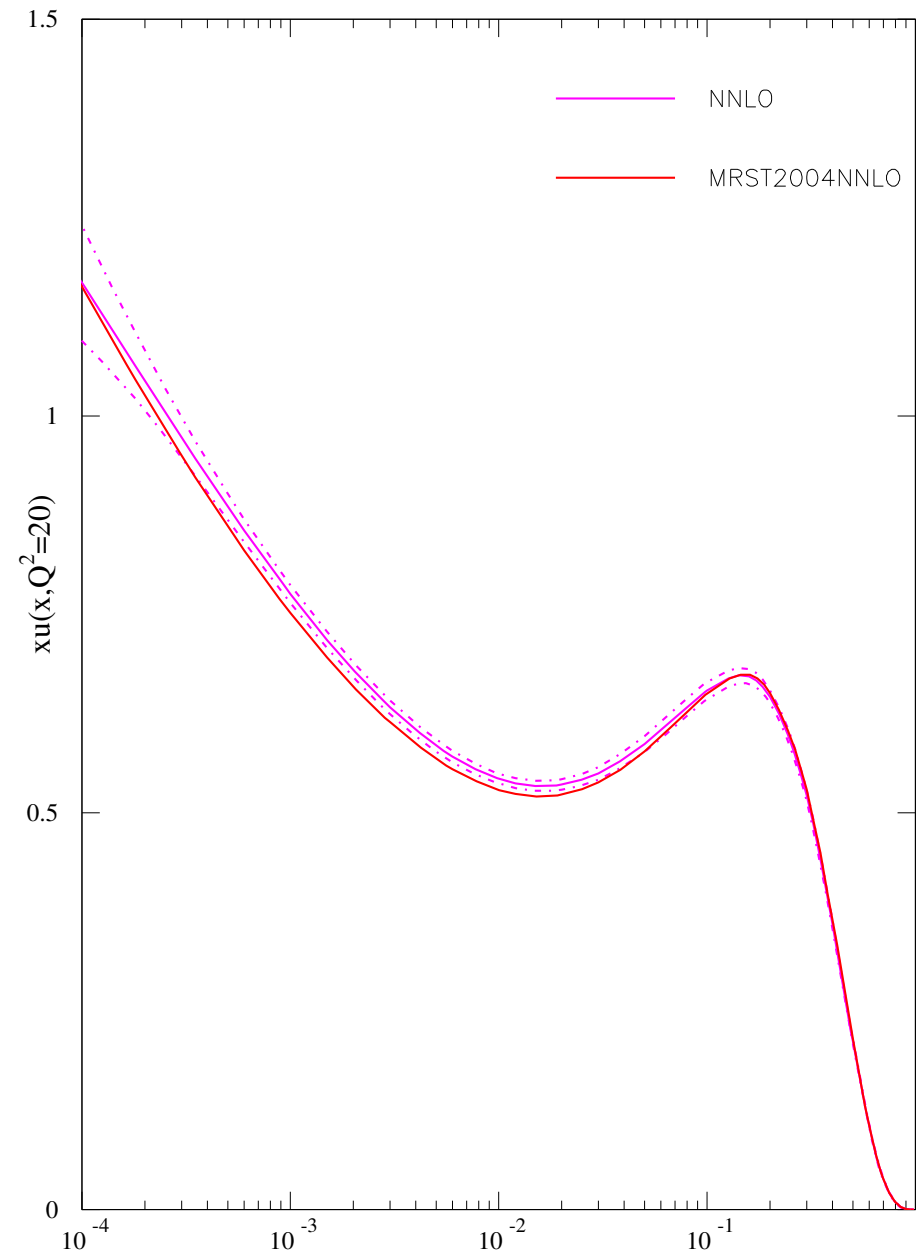
Structure of the proton incredibly well-constrained by lots of different data sets, many of the most important from HERA. Still lots to test/check at LHC and quite a few uncertain realms for predictions. Plenty of scope for surprises.

Not much change in light quarks due to these to theoretical updates.

Minor change – bit bigger than **MRST2004** at small  $x$ .

Slightly lower  $s(x, Q^2) \rightarrow$  more  $u(x, Q^2)$ .

Also slightly higher  $\alpha_S(M_Z^2)$ . Negative **NNLO** correction bigger  $\rightarrow$  more  $u(x, Q^2)$ .

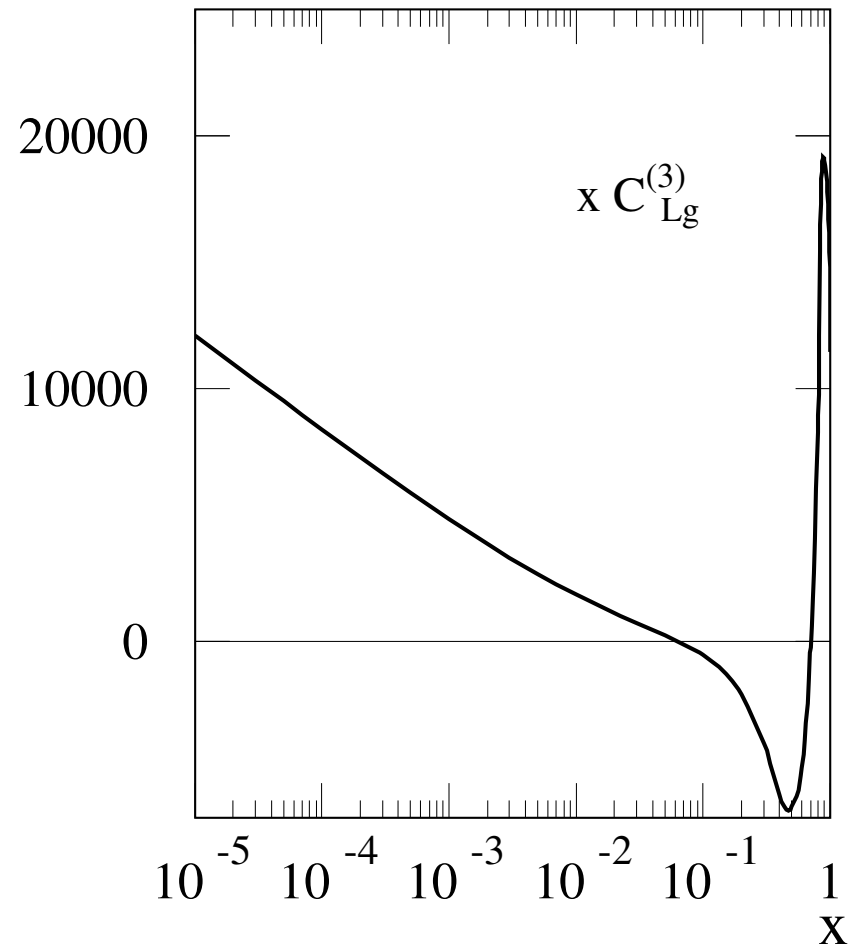


The NNLO  $\mathcal{O}(\alpha_s^3)$  longitudinal coefficient function  $C_{Lg}^3(x)$  given by

$$C_{Lg}^3(x) = n_f \left( \frac{\alpha_s}{4\pi} \right)^3 \left( \frac{409.5 \ln(1/x)}{x} - \frac{2044.7}{x} - \dots \right)$$

Clearly a significant positive contribution at small  $x$ .

Counters decrease in small- $x$  gluon.



## Comparisons

Compare with only other NNLO partons on market – Alekhin2002.

Nothing from CTEQ?

Much larger  $\alpha_S(M_Z^2)$  in this fit than that of Alekhin ( $\alpha_S(M_Z^2) = 0.119$  compared to 0.114).

Not much difference in high- $x$  valence quarks, except than explained by difference in  $\alpha_S(M_Z^2)$ . Very well-constrained.

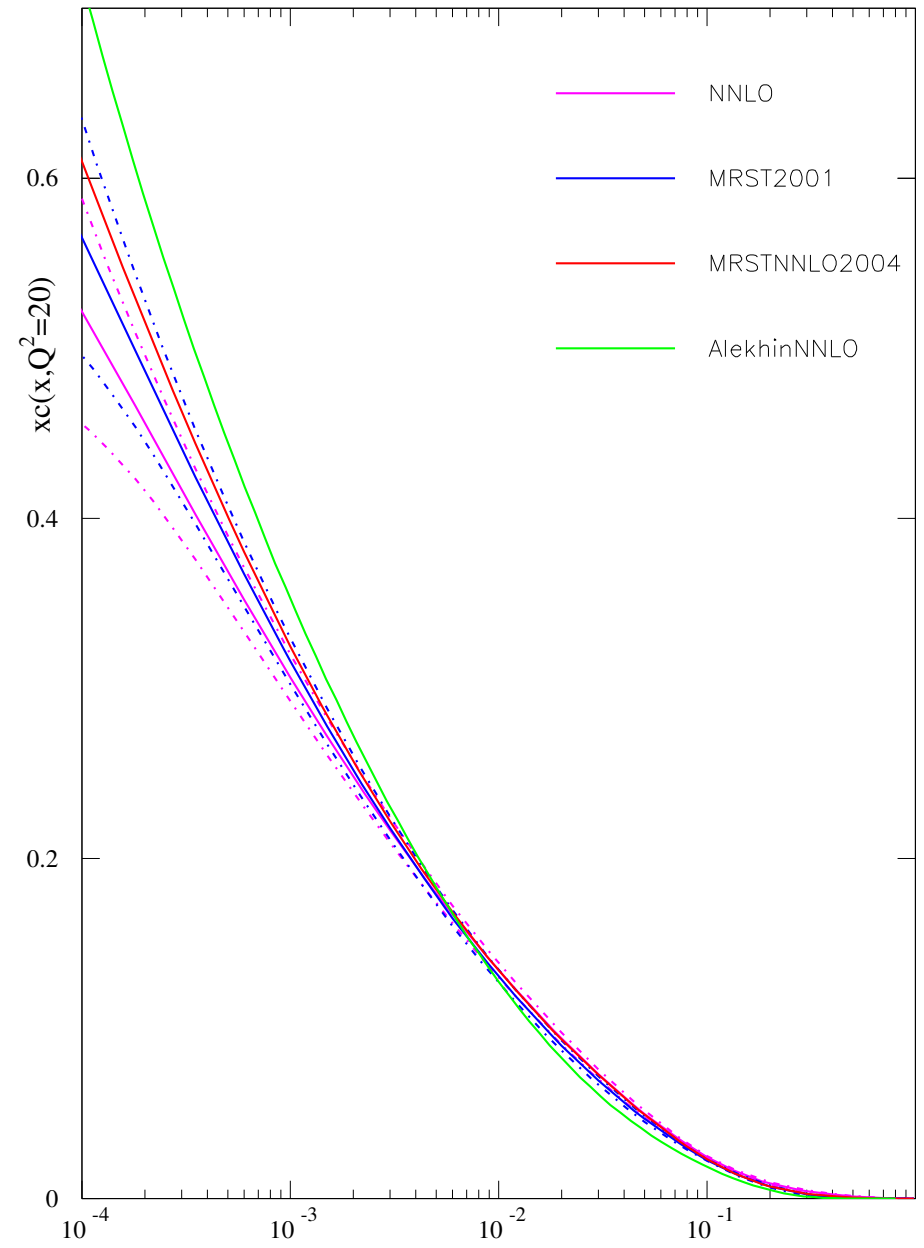
Differences in low- $x$  sea quarks. Swamped by differences in flavour treatments –  $\bar{u} - \bar{d}$  and  $s(x, Q^2)$ .

Main difference in gluon distribution.

Difference in gluon feeds through to charm.

Alekhin2002 much bigger at small  $x$ .

Starts from zero as with MRST2004NNLO.

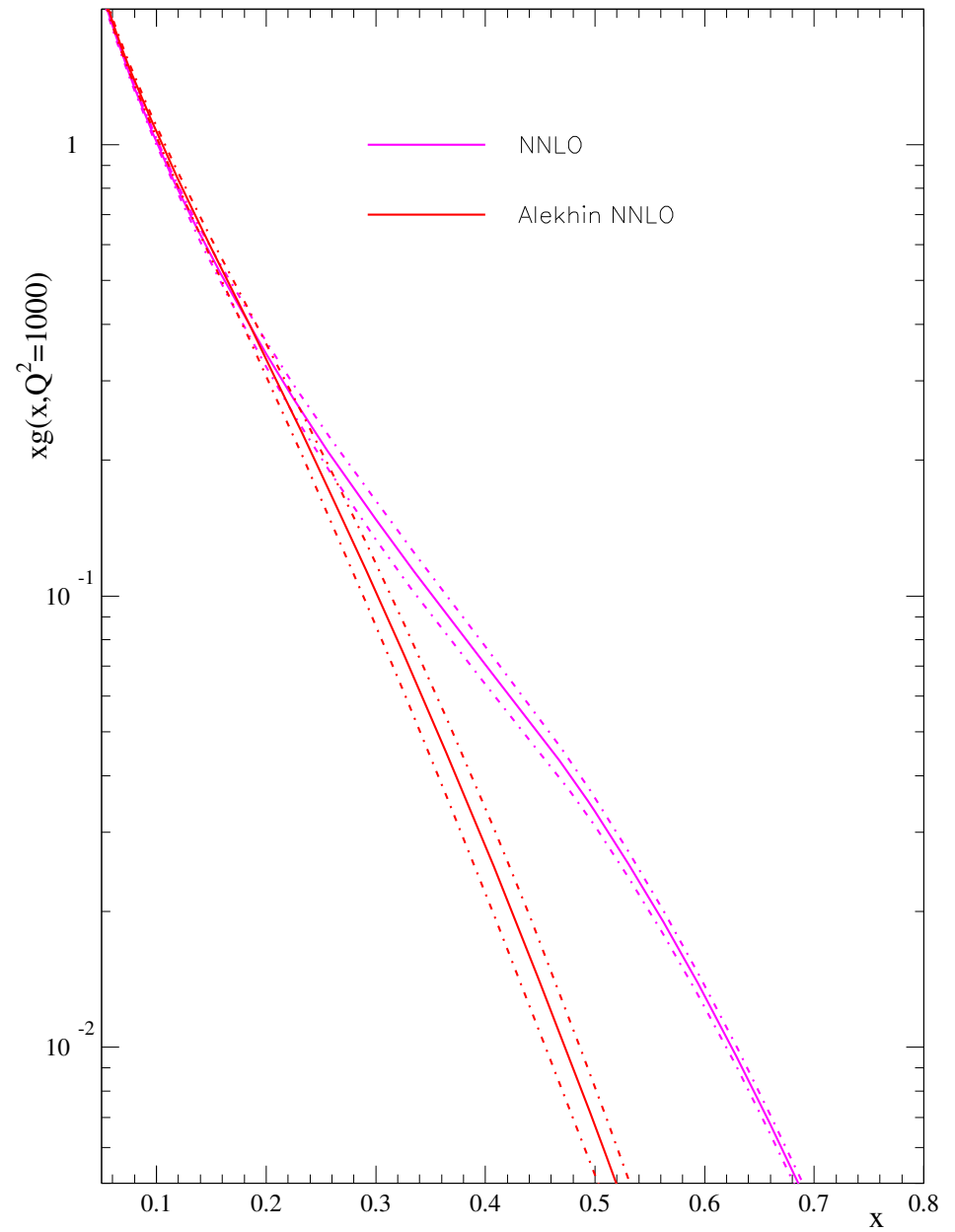


Big difference at high  $x$  and  $Q^2$ .

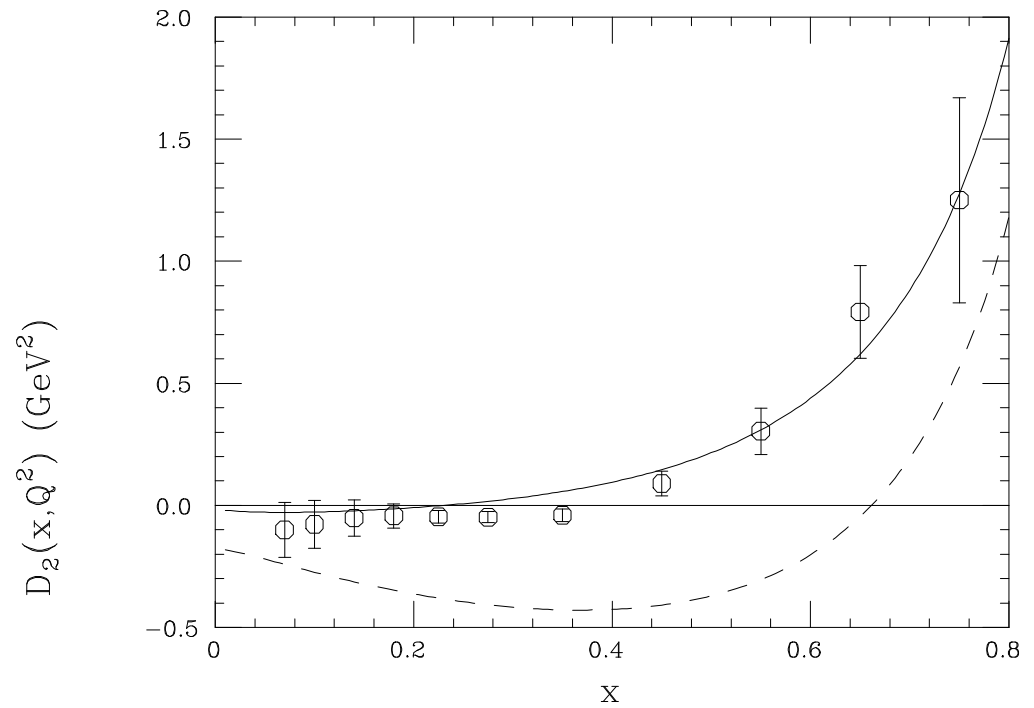
Determined by Tevatron jet data for MRST. Fit now excellent.

Divergences at  $x = 0.25$  corresponds to  $E_T \sim 225\text{GeV}$ .

In  $\overline{MS}$  scheme gluon more important for jets at high  $x$  at NNLO because high- $x$  quarks smaller.



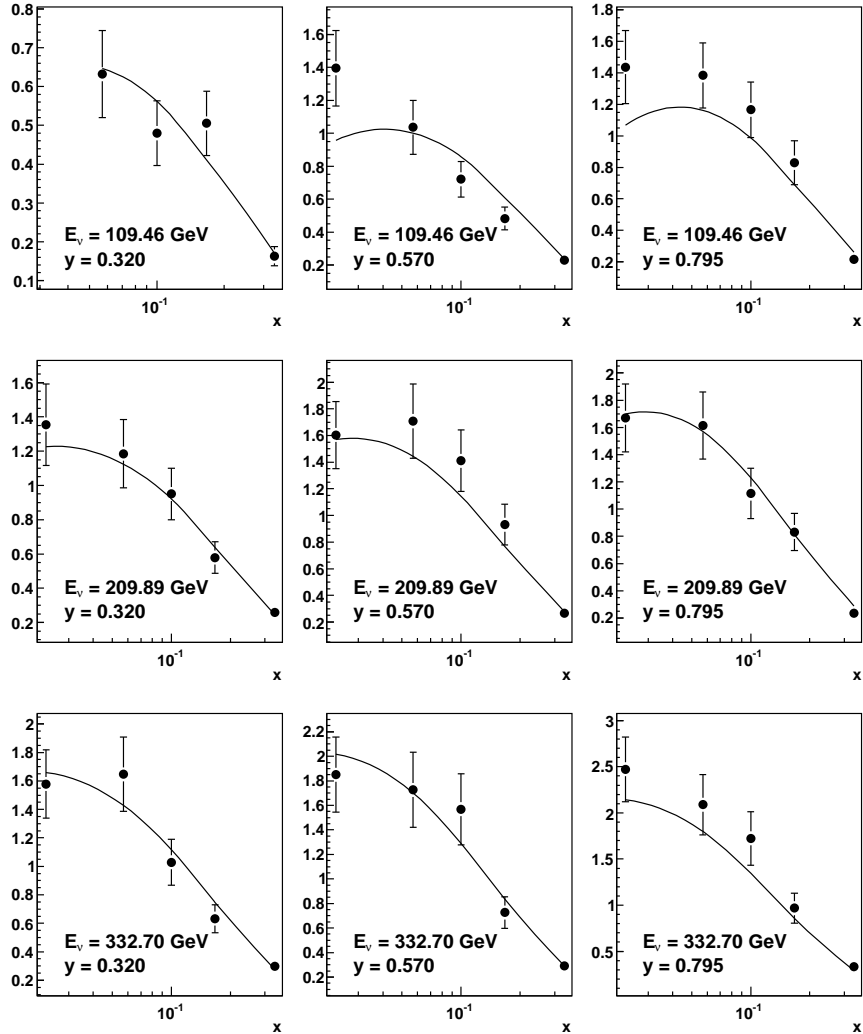
Renormalon prediction for  $1/Q^2$  corrections for  $F_2(x, Q^2)$  (solid line) and  $xF_3(x, Q^2)$  (dashed line)  
Dasgupta and Webber.



Fit to data clearly very good.

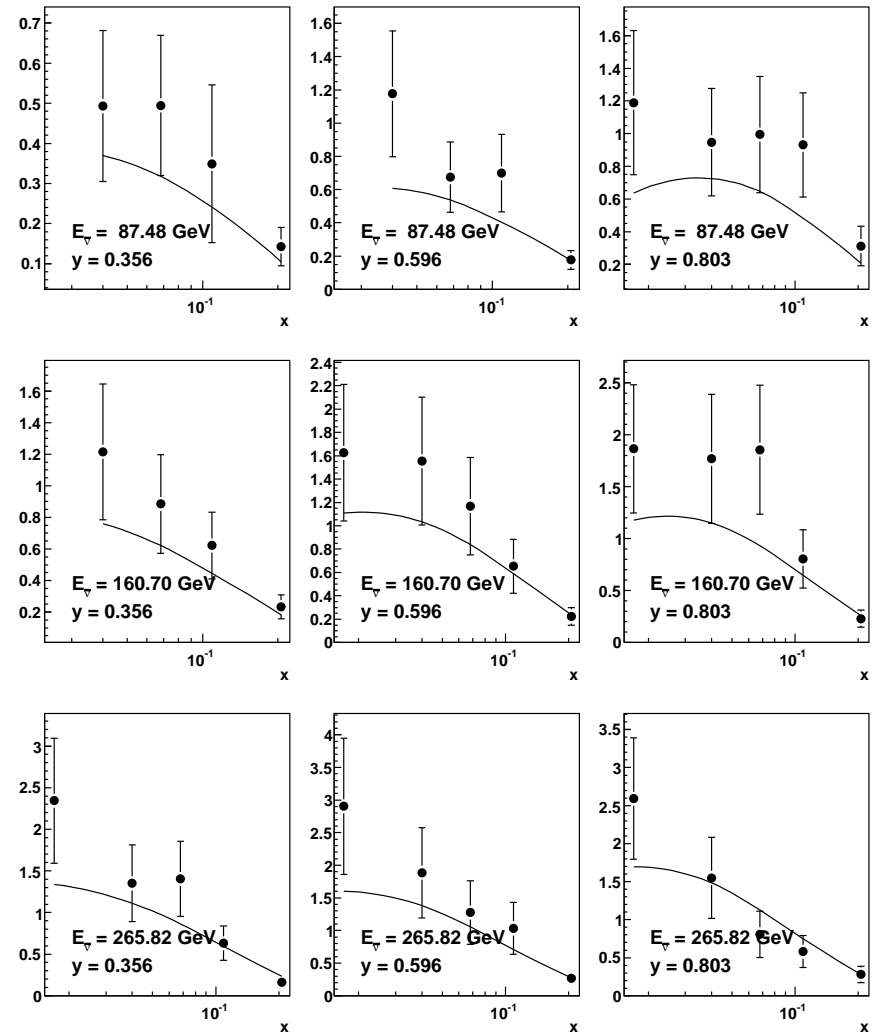
$$\text{CCFR } \frac{100\pi}{G_F^2 M_N E_\nu} \frac{d\sigma}{dx dy} (\nu_\mu N \rightarrow \mu^+ \mu^- X) \text{ in } \text{GeV}^{-2}, \chi^2 = 34/44 \text{ pts.}$$

MSTW NLO PDF fit (preliminary, 17/10/2007)



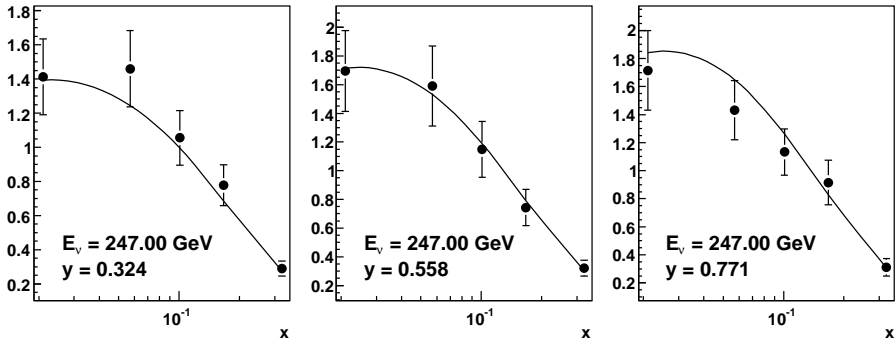
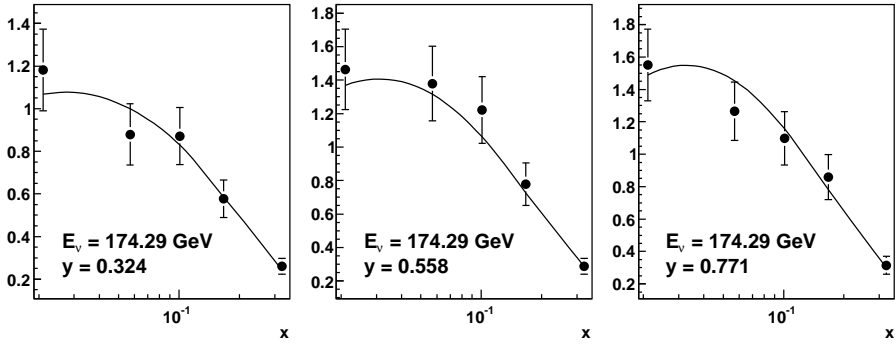
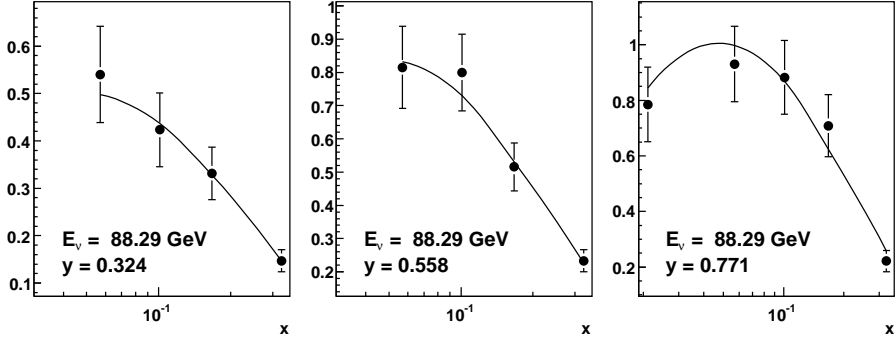
$$\text{CCFR } \frac{100\pi}{G_F^2 M_N E_\nu} \frac{d\sigma}{dx dy} (\bar{\nu}_\mu N \rightarrow \mu^+ \mu^- X) \text{ in } \text{GeV}^{-2}, \chi^2 = 34/42 \text{ pts.}$$

MSTW NLO PDF fit (preliminary, 17/10/2007)

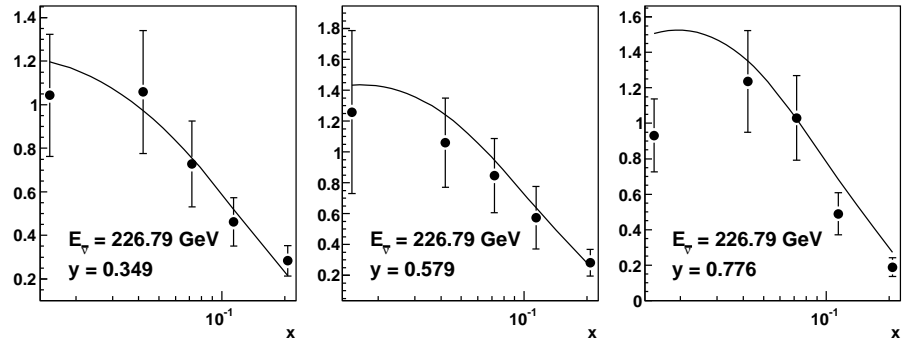
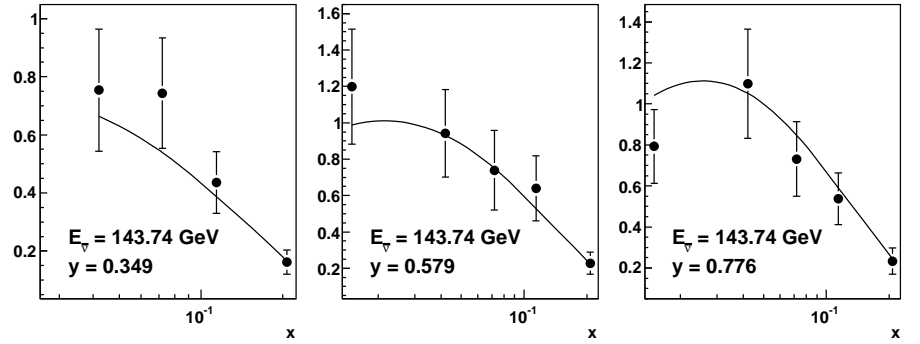
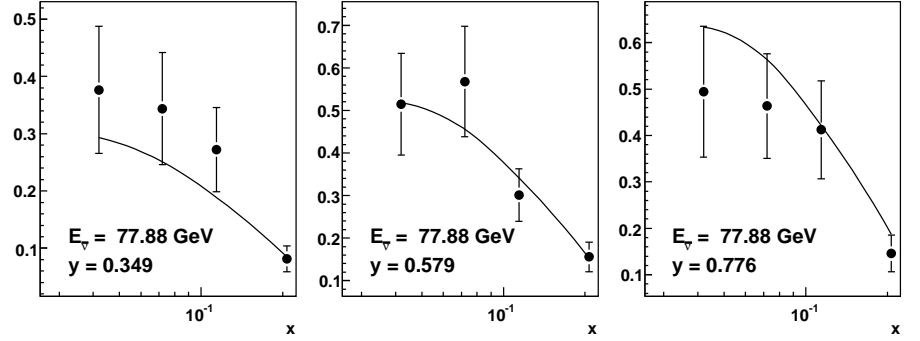




$\text{NuTeV } \frac{100\pi}{G_F^2 M_N E_\nu} \frac{d\sigma}{dx dy}(\nu_\mu N \rightarrow \mu^+ \mu^- X) \text{ in } \text{GeV}^{-2}, \chi^2 = 11/21 \text{ DOF}$   
MSTW NLO PDF fit (preliminary, 17/10/2007)



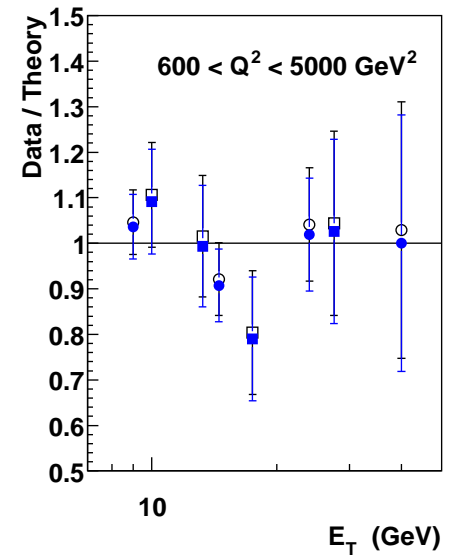
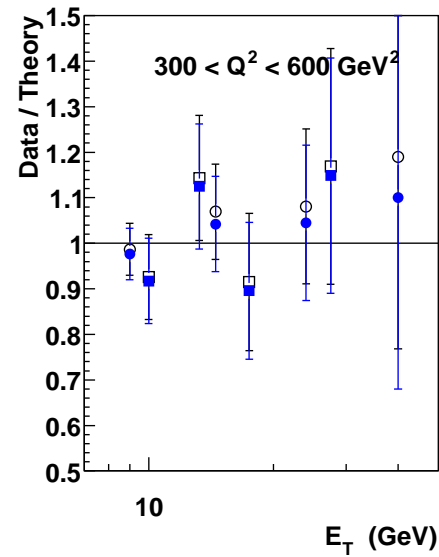
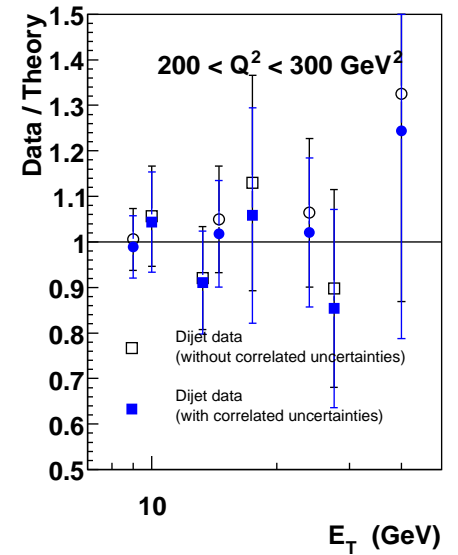
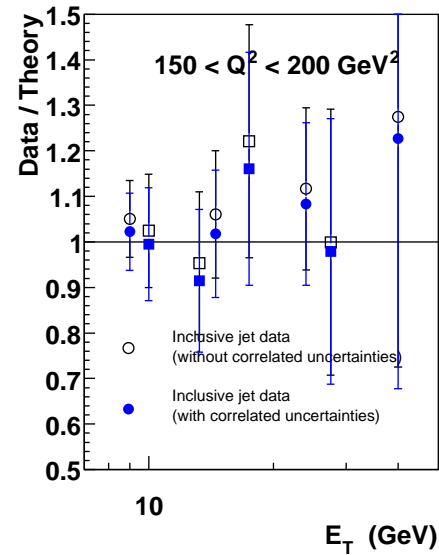
$\text{NuTeV } \frac{100\pi}{G_F^2 M_N E_\nu} \frac{d\sigma}{dx dy}(\bar{\nu}_\mu N \rightarrow \mu^+ \mu^- X) \text{ in } \text{GeV}^{-2}, \chi^2 = 28/19 \text{ DOF}$   
MSTW NLO PDF fit (preliminary, 17/10/2007)



Fit to HERA inclusive and dijet DIS data using fastNLO at NNLO using NLO cross-section.

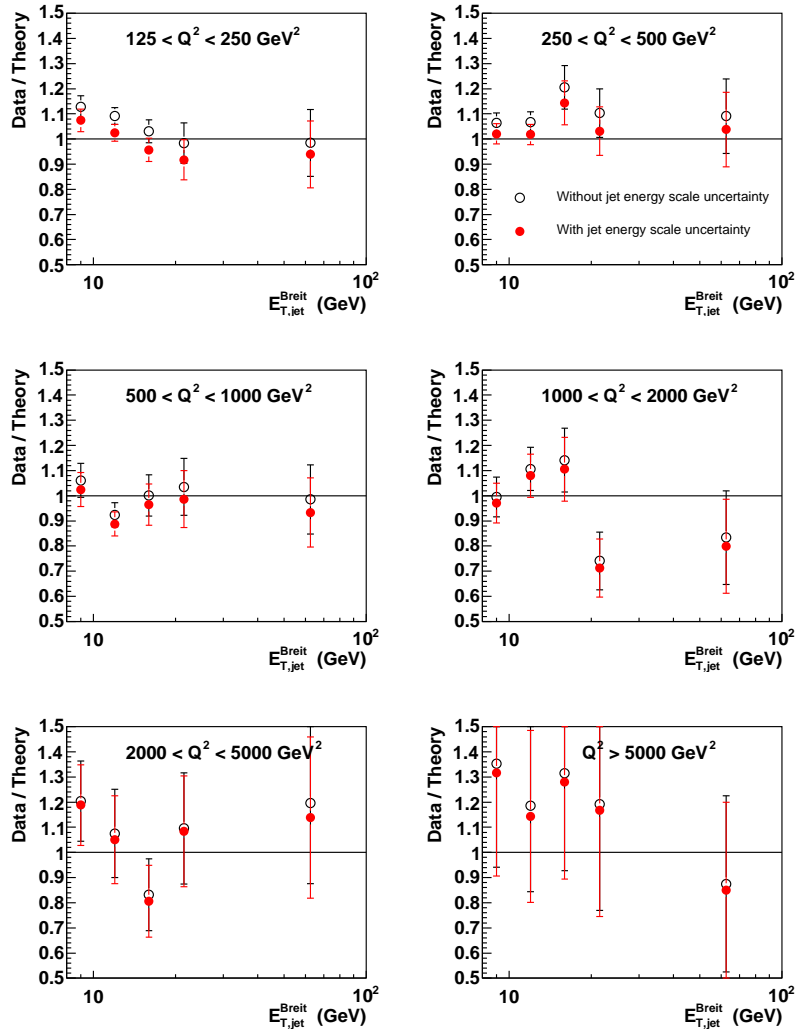
Fit generally excellent.

# H1 95-97 incl. jet and dijet data, $\chi^2 = 11/32$ pts. MSTW NNLO PDF fit (preliminary, 21/10/2007)



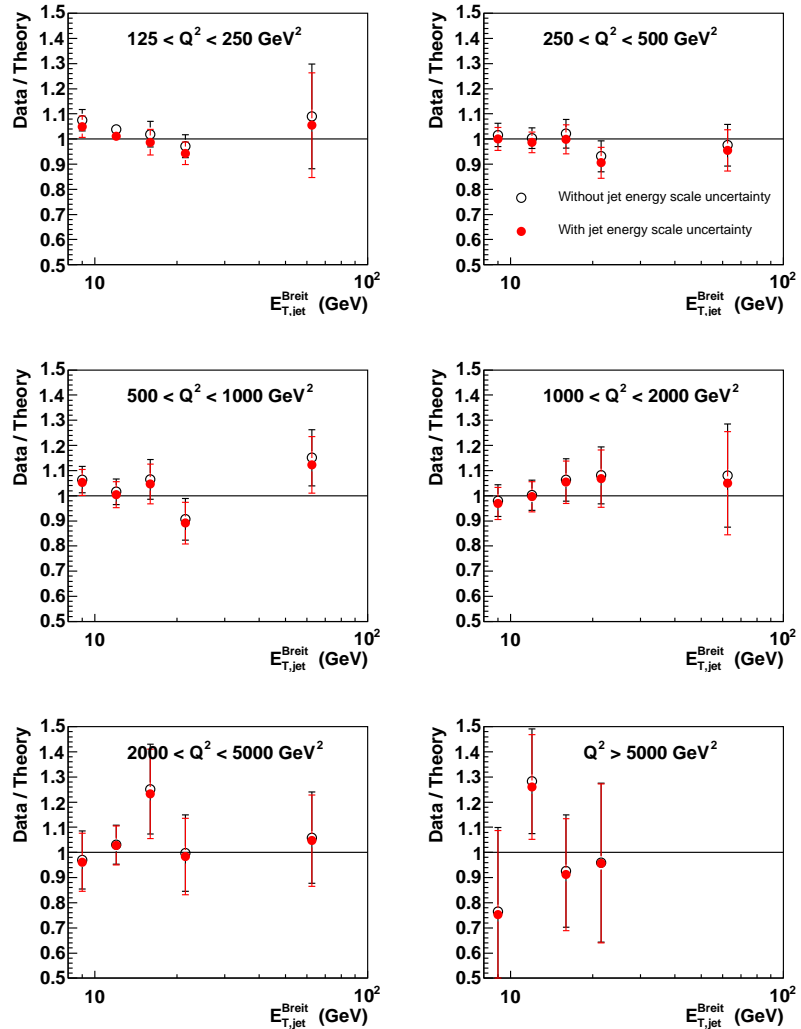
# ZEUS 96-97 inclusive jet data, $\chi^2 = 31/30$ pts.

MSTW NNLO PDF fit (preliminary, 21/10/2007)



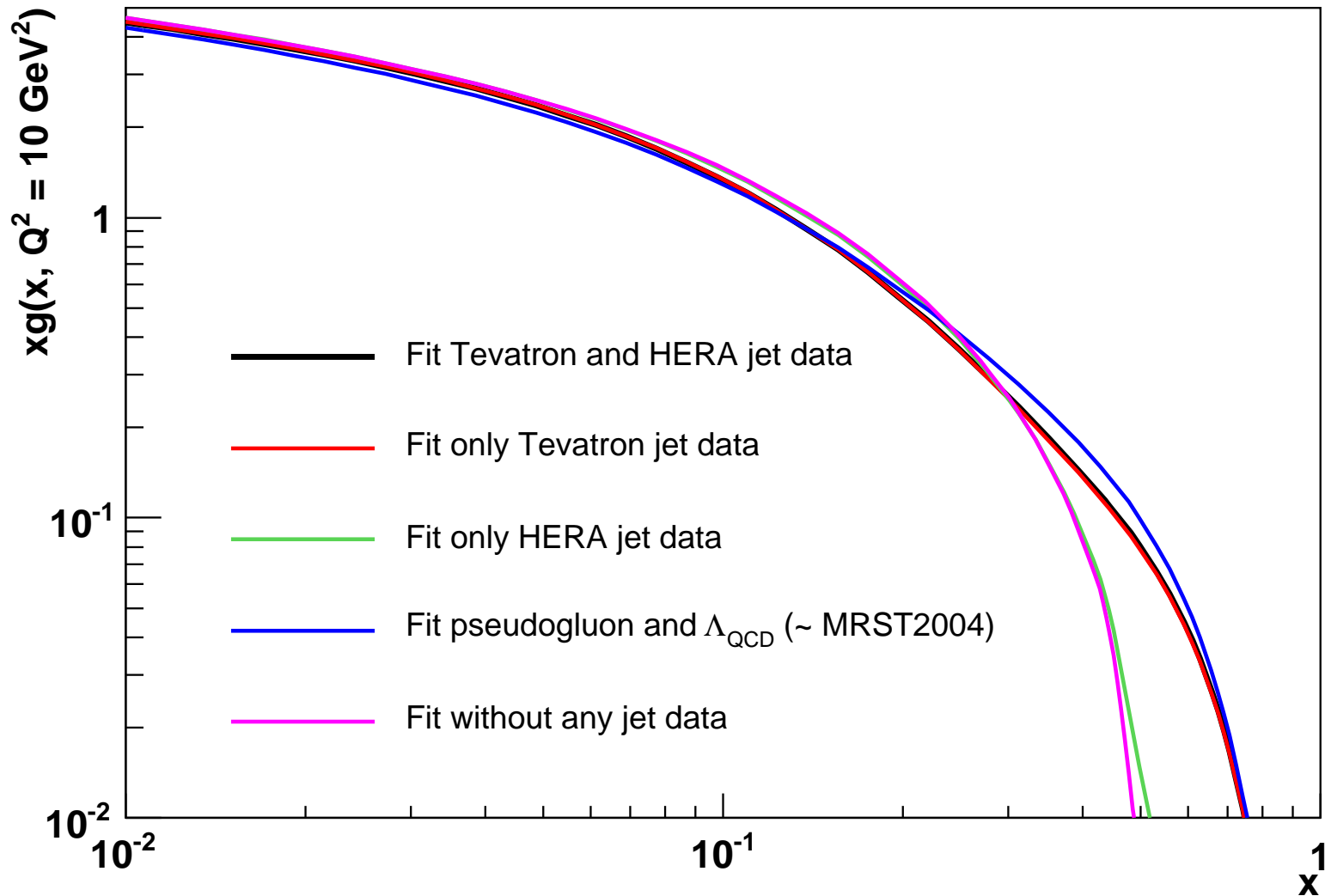
# ZEUS 98-00 inclusive jet data, $\chi^2 = 17/30$ pts.

MSTW NNLO PDF fit (preliminary, 21/10/2007)



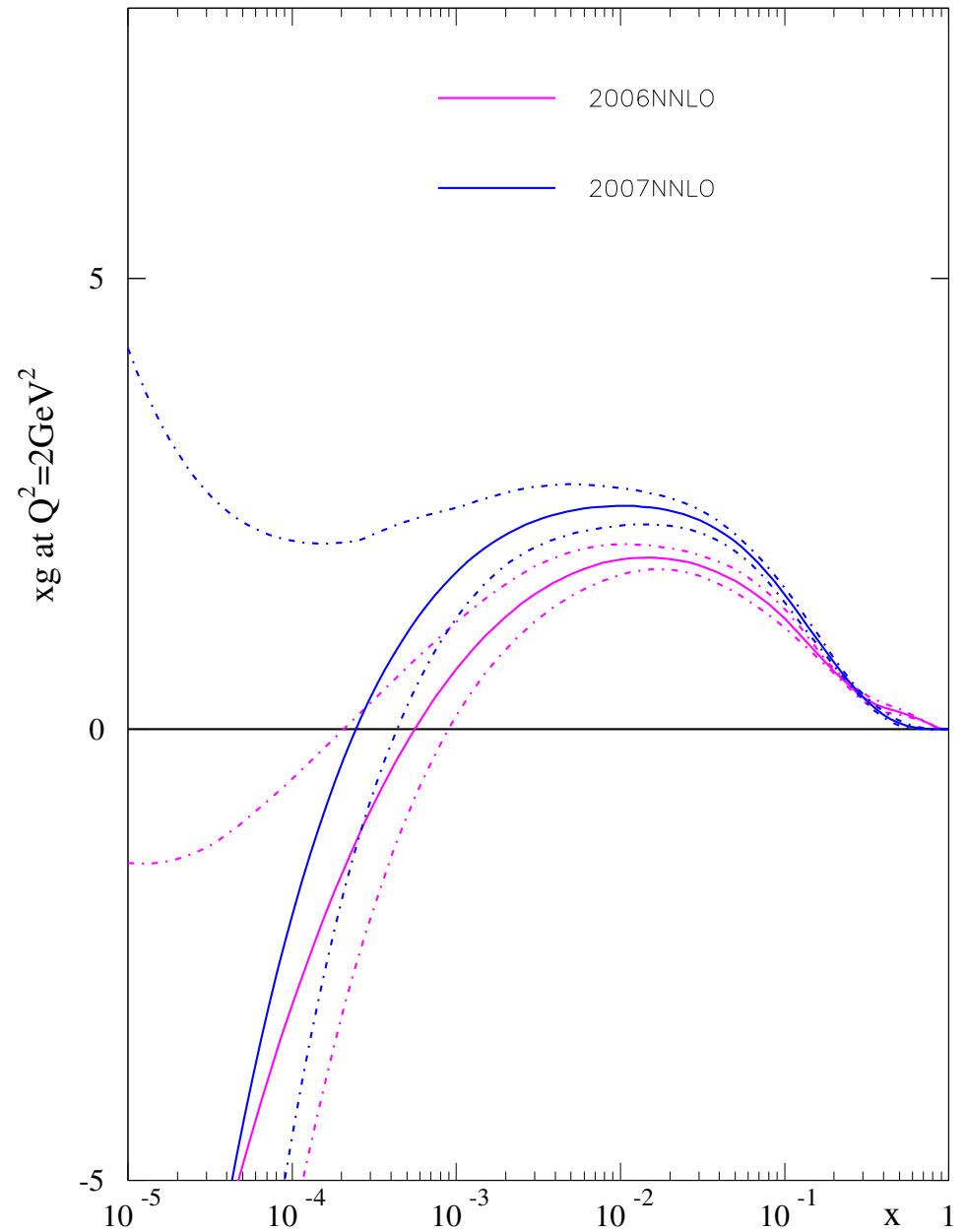
Same for **ZEUS** data.

Tevatron jet data are essential for constraining high  $x$  gluon – HERA jet data not sensitive to these  $x$  values and have much less pull.



Comparison of most up-to-date gluon distributions at **NNLO** and **MRST06**.

New **CDFII** jet data  $\rightarrow$  smaller very high- $x$  distribution at low  $Q^2$ . Due to different couplings washes out at higher  $Q^2$ .

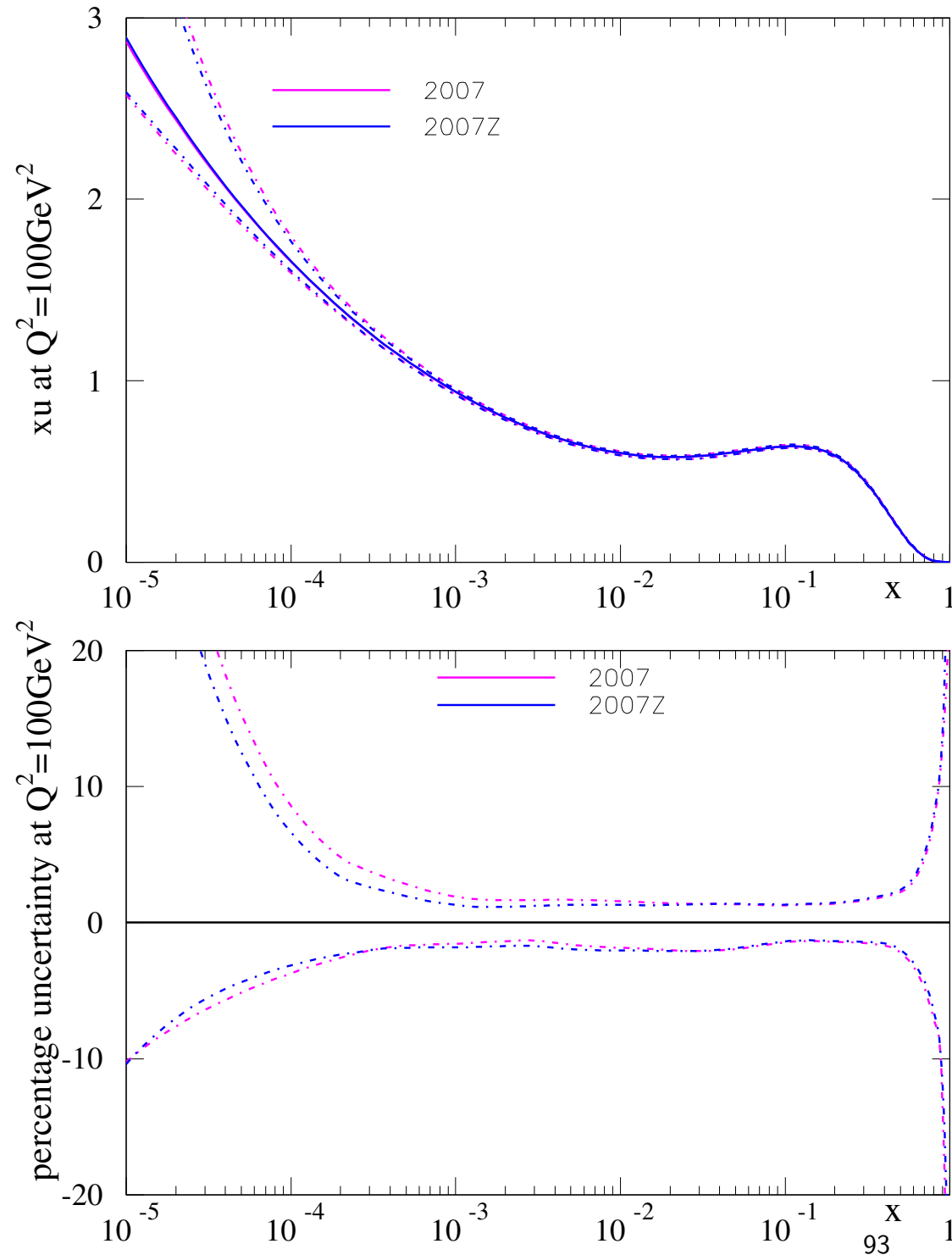


Constrains parton distributions almost entirely at small  $x$ .

With previous data improvement on uncertainty on  $u(x, Q^2)$  shown. Essentially identical for  $d(x, Q^2)$ .

Definite narrowing of uncertainty band for  $x < 0.01$ .

Maximum reduction in uncertainty of  $\sim 20\%$ . However, can improve to perhaps  $\sim 50\%$  with  $10fb^{-1}$  data.

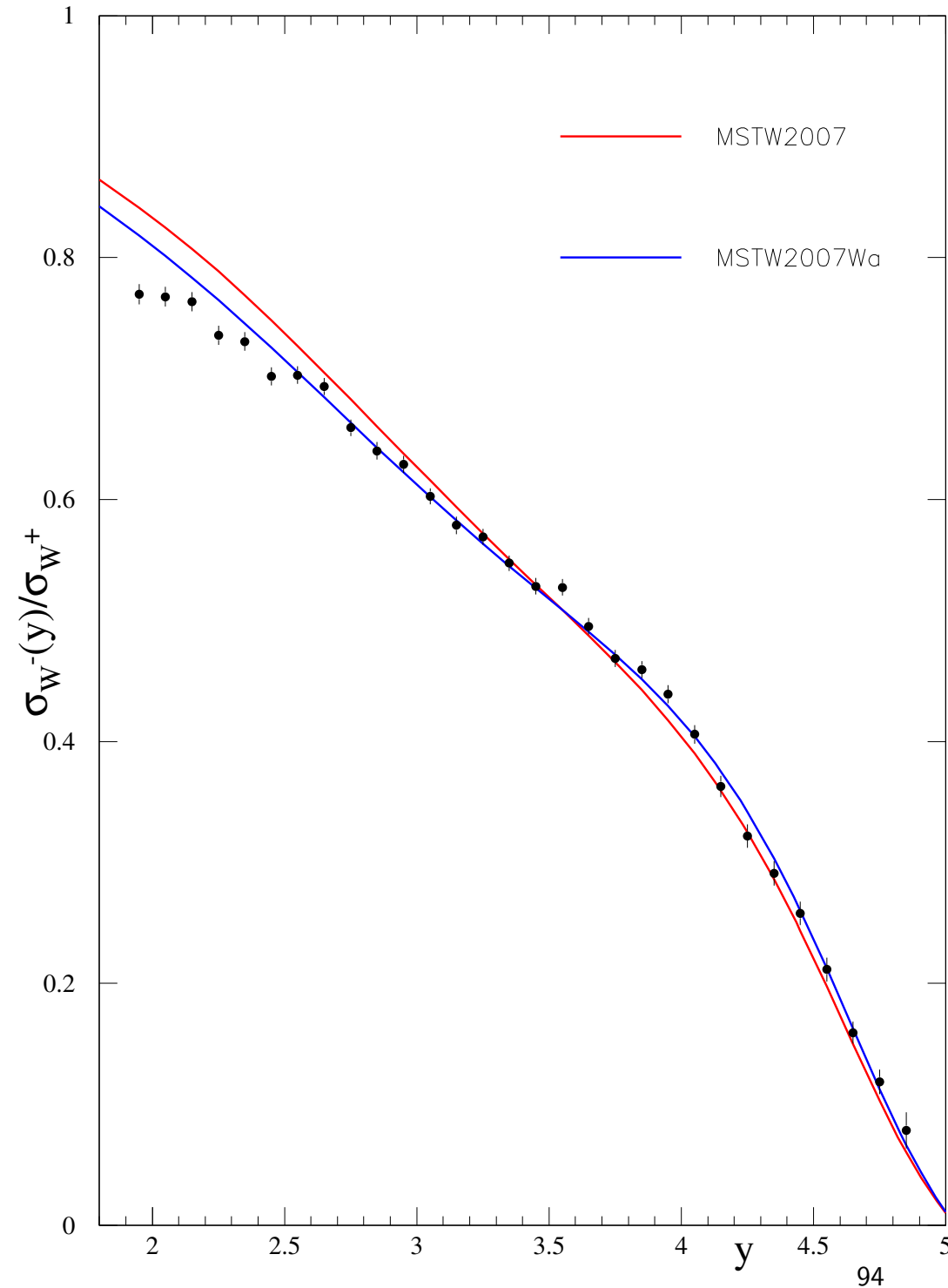


Again we obtain even more information if the measurement is not as predicted.

As before shift predicted data by by factor  $0.05(y - 3.4)$ .

Comparing to prediction  $\chi^2 = 338/30$ .

Blue line shows result of new fit. Not possible to obtain good agreement  $\chi^2 = 109/30$ .



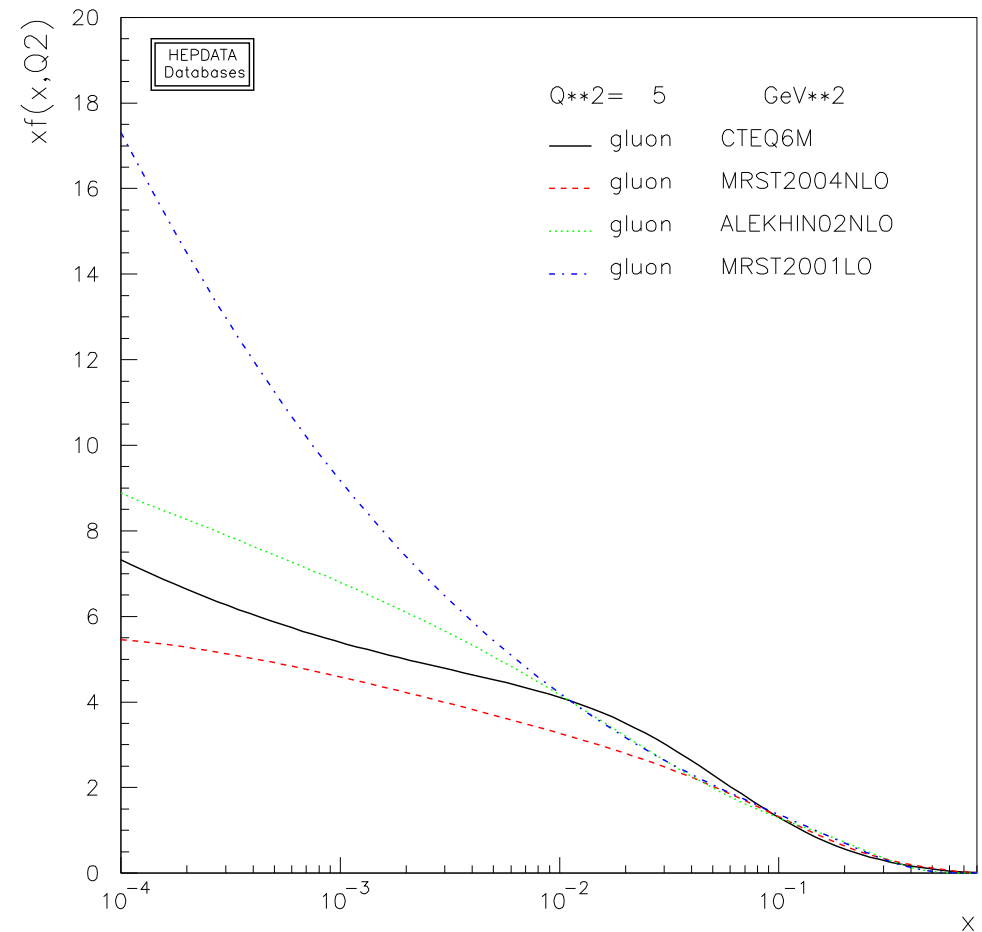
Which order of partons should be used in **LO** Monte Carlo generators.

Enormous change in partons, especially gluon when going from **LO** → **NLO**.

**LO** partons are the usual one used with many **LO** Monte Carlo programs.

All such results should be treated with care.

Not **NLO** partons? Not a trivial issue.

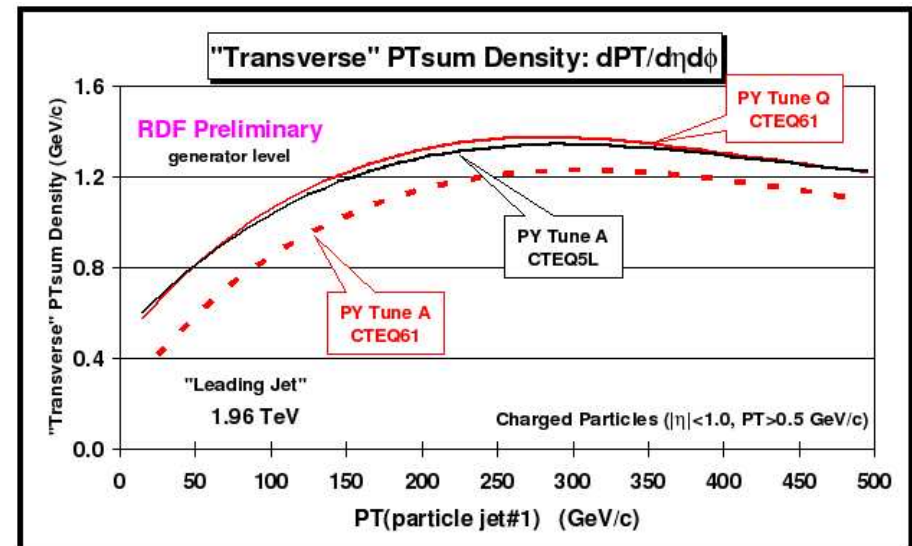
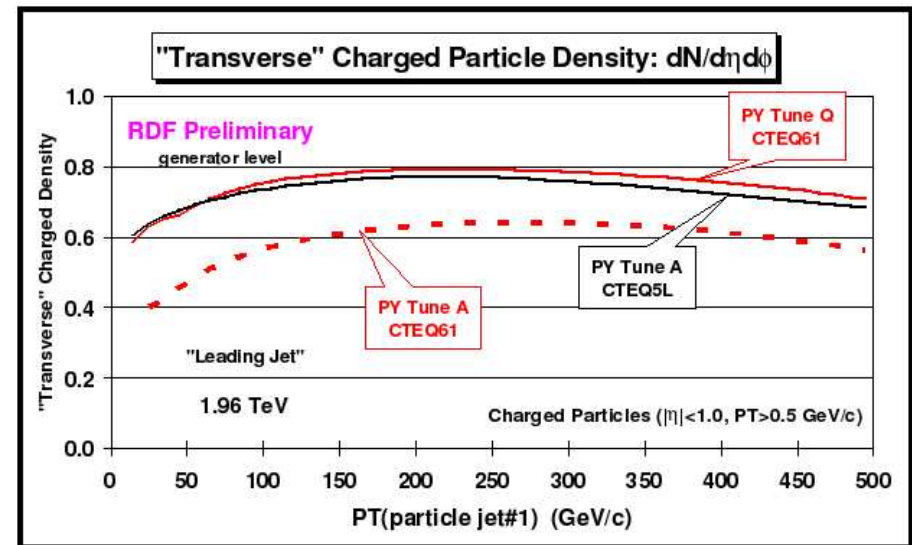




Already investigated in terms of tuning for underlying event ([Field](#)). See big difference between using [CTEQ6L](#) and [CTEQ6.1M](#) partons, mainly due to gluon.

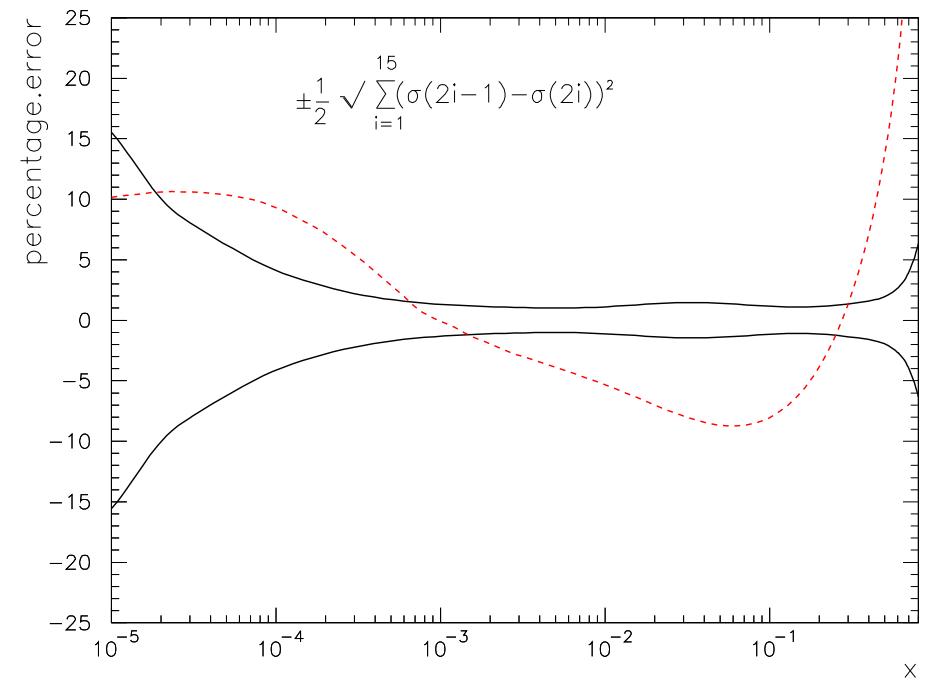
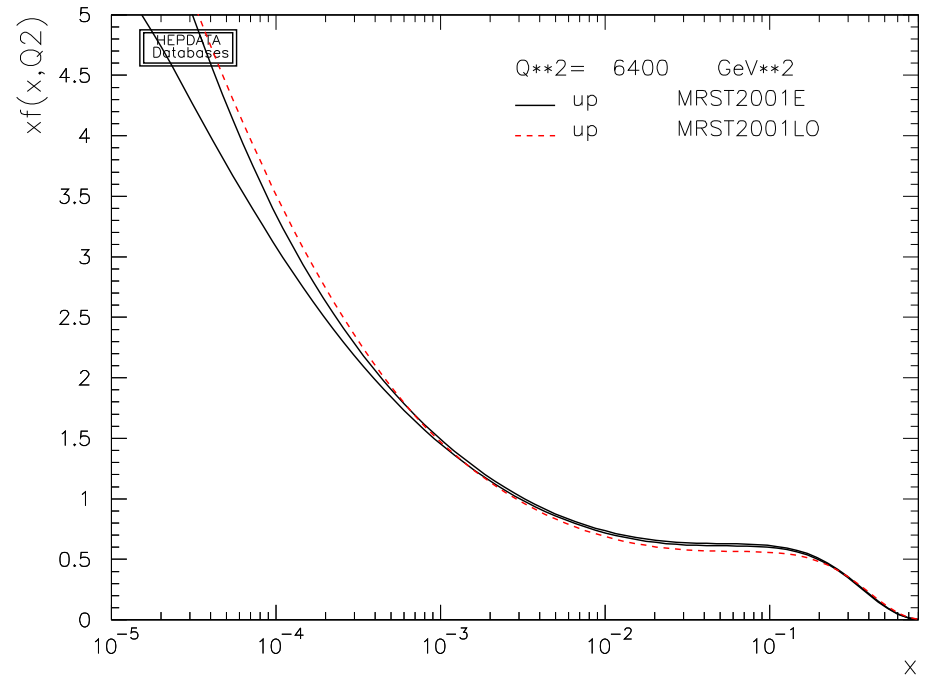
Agreement can be reached by retuning. Will affect predictions for other quantities. Want universality.

In order to investigate this look at indications from well-understood (simple) processes.



First note that the **LO** quarks over wide region of smaller  $x$  qualitatively smaller than **NLO**. Lack of additional quark evolution at **NLO**.

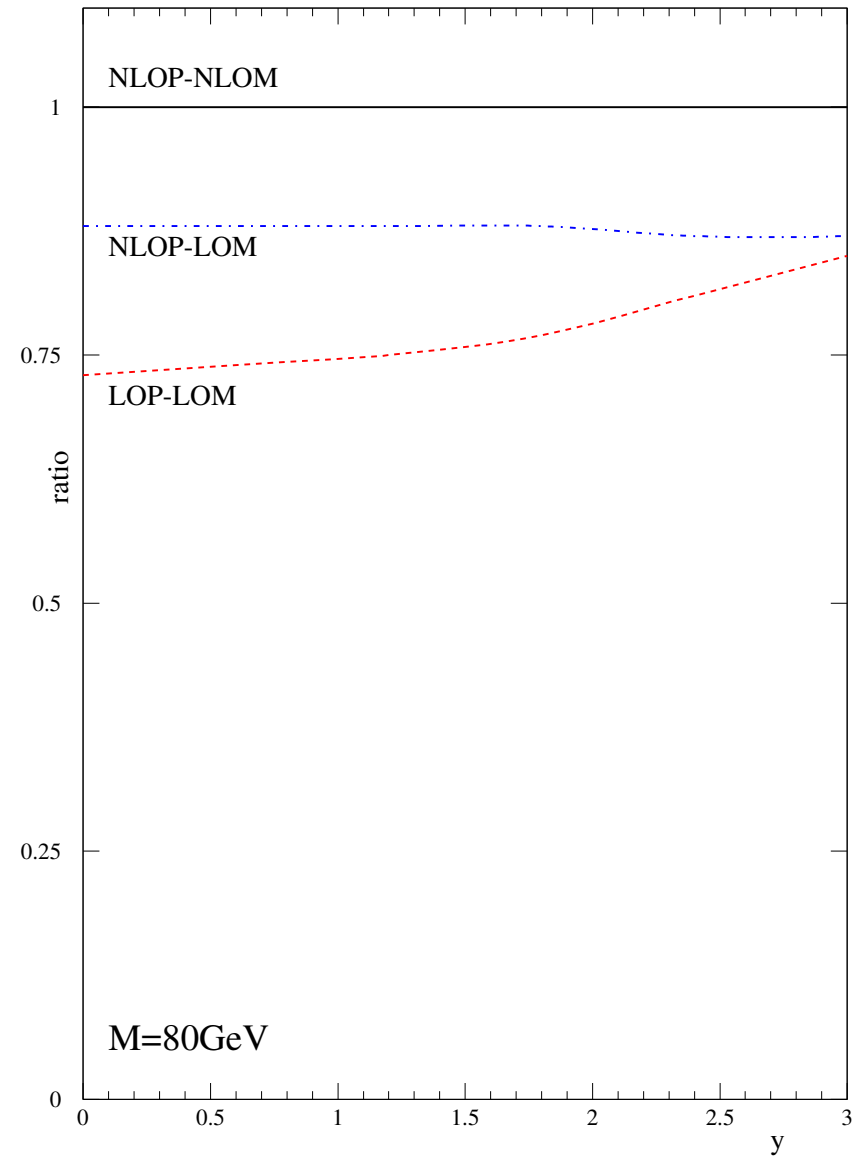
At high  $x$   $\ln(1 - x)$  terms in **NLO** matrix elements lead to **NLO** quarks being smaller.



NLO partons lead to best shape for inclusive fixed order heavy boson production at the LHC.

Has lead to the proposal that NLO partons should always be used.

Drell-Yan Cross-section at LHC for 80 GeV with Different Orders



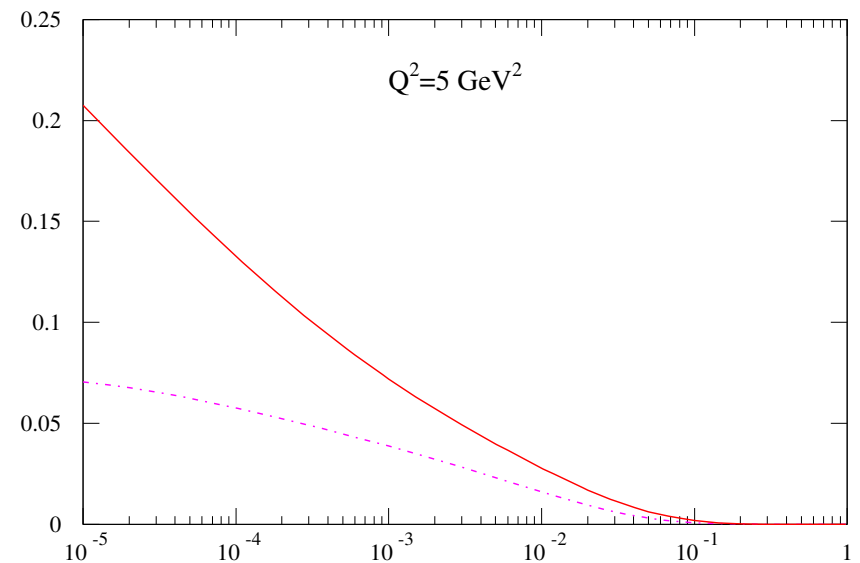
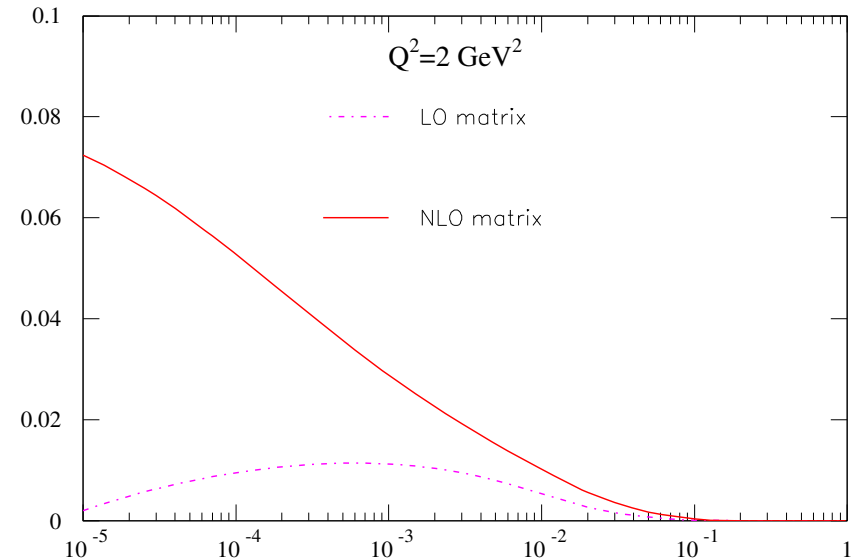
Small  $x$  counter-example. Consider production of charm in DIS. All charm produced in final state (FFNS).

NLO matrix element contain divergence at small  $x$  not present at LO.

Same issues in heavy flavour hadro-production.

Using NLO partons the LO matrix element result is well below the truth at low scales. Shape totally wrong.

$F_2^c$  NLO partons LO/NLO Matrix element



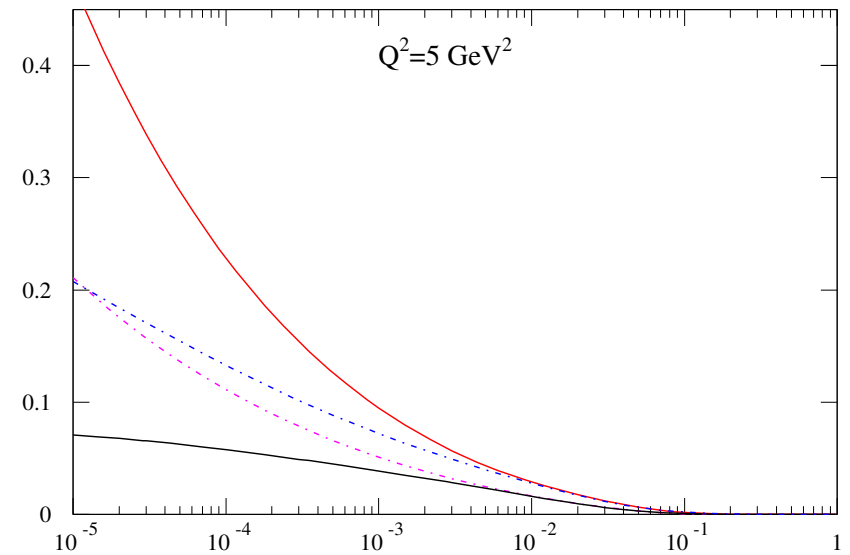
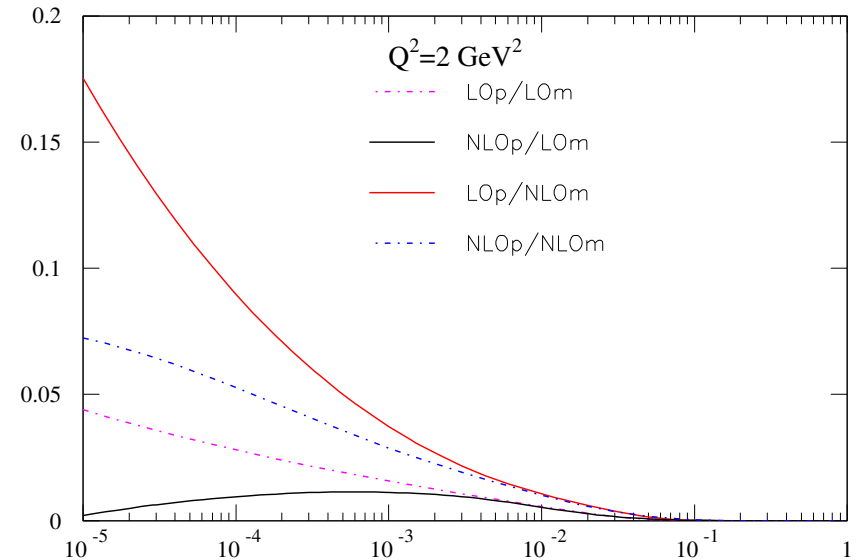
Consider using LO partons.

Using LO partons the NLO matrix element result is extremely large.

LO gluon is very large at small  $x$  since it has been extracted with missing enhancements at small  $x$ .

LO partons and LO matrix element more sensible. compensation between failings in both.

$F_2^e$  LO/NLO partons LO/NLO Matrix element



## Conclusions - so far

Sometimes **NLO** partons better to use if only **LO** matrix elements are known.

Can get significant problems with shape if **LO** partons used.

**But** can be completely wrong at small  $x$  using **NLO** partons due to *zero*-counting of  $\ln(1/x)$  terms.

Can we find some optimal partons which have most desirable features?

Need to understand difference between **LO** and **NLO** partons better.

At LO compared to NLO (and higher orders) missing terms in  $\ln(1-x)$  and  $\ln(1/x)$  in coefficient functions and/or evolution.

→ partons at LO bigger at  $x \rightarrow 1$  and at  $x \rightarrow 0$  in order to compensate.

From momentum sum rule not enough partons to go around.

Leads to bad global fit at LO – partially compensated by LO extraction of  $\alpha_S(M_Z^2) \geq 0.130$ .

However, leads to suggestion (Sjostrand) that relaxing momentum sum rule at LO could make LO partons rather more like NLO partons where they are normally too small.

Resulting partons would still be bigger than NLO where necessary.

Also useful to use **NLO** definition of coupling constant.

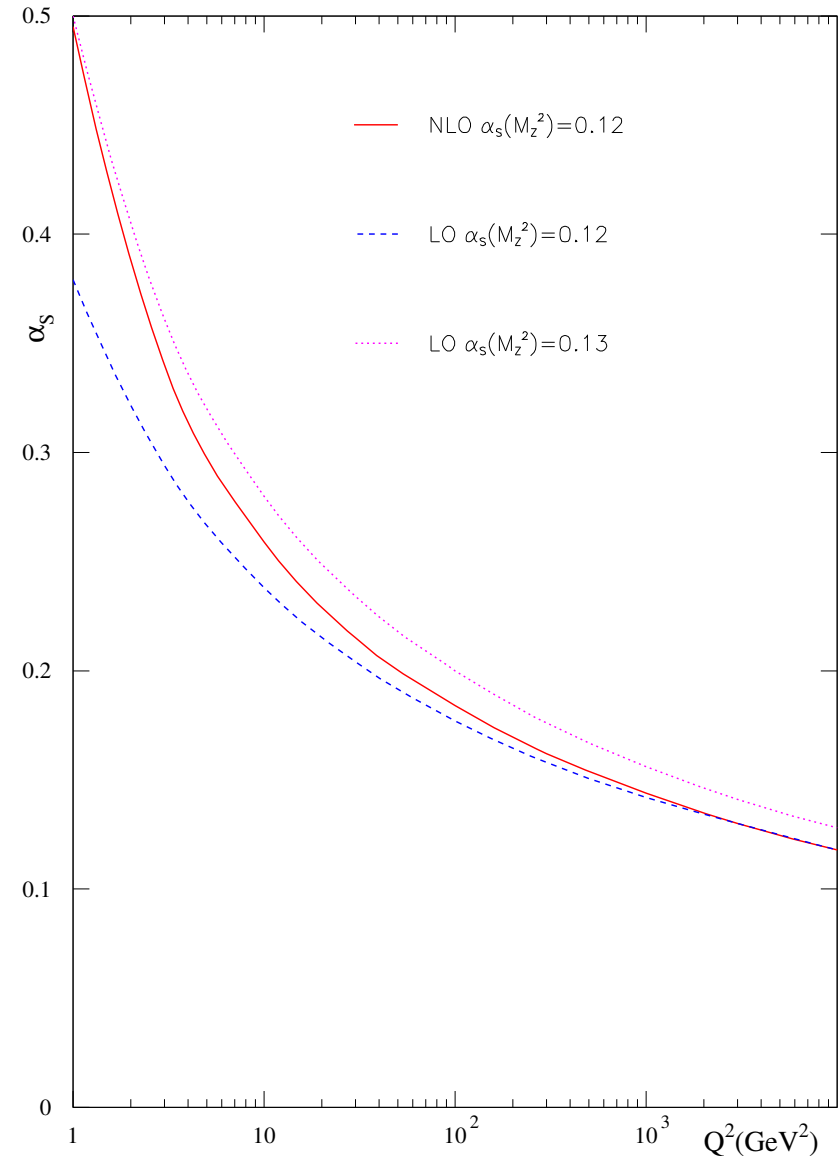
Because of quicker running at **NLO** couplings with same value of  $\alpha_S(M_Z^2)$  very different at lower scales where **DIS** data exists.

Near  $Q^2 = 1\text{GeV}^2$  **NLO** coupling with  $\alpha_S(M_Z^2) = 0.120$  similar to **LO** coupling with  $\alpha_S(M_Z^2) = 0.130$ .

Use of **NLO** coupling helps alleviate discrepancy between different orders.

**NLO** coupling already used in **CTEQ** **LO** partons and in Monte Carlo generators.

Comparison of  $\alpha_S$  at LO and NLO





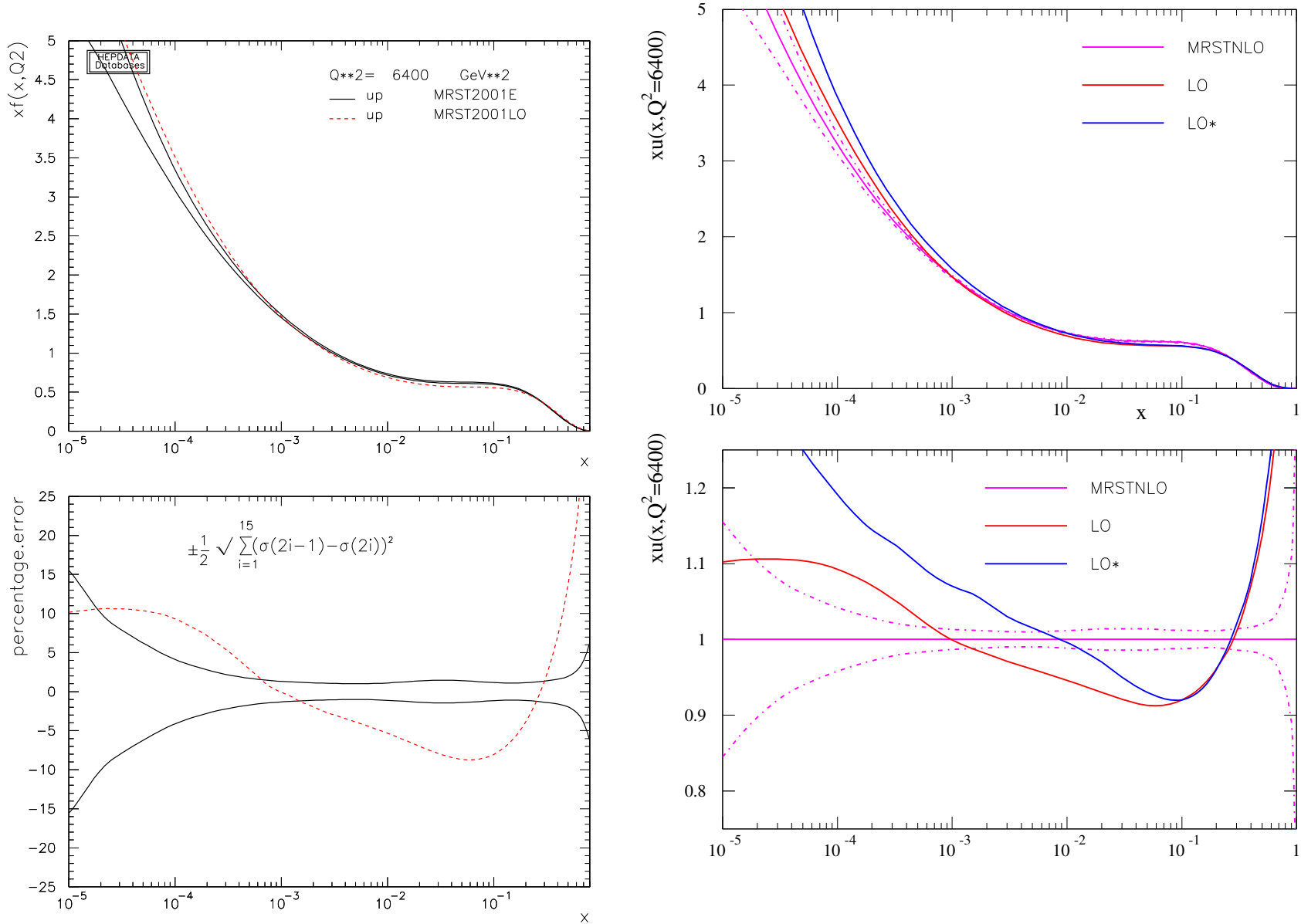
Relaxing momentum violation and allowing NLO definition of coupling does dramatically improve quality of LO global fit (K-factor of 1.3 necessary for fixed target Drell-Yan data).

$\chi^2 = 3066/2235$  for standard LO fit becomes  $\chi^2 = 2691/2235$ . Big improvement in HERA data.

Momentum carried by input partons goes up to 113%. Much more similar to NLO partons, in particular at small  $x$  LO quark distributions evolve as quickly at NLO partons.

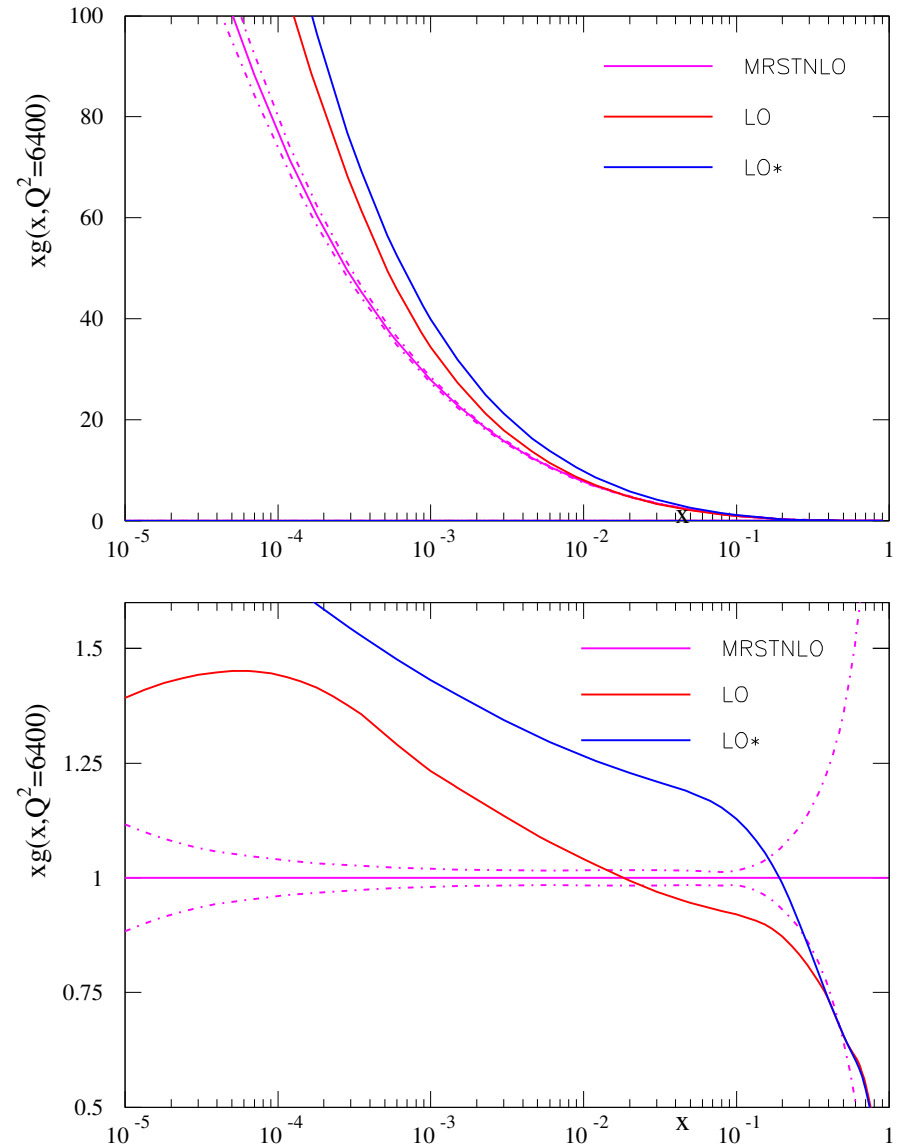
Using NLO definition  $\alpha_S(M_Z^2) = 0.121$ .

The **LO\*** and **NLO** partons are more similar in this case, particularly for  $x \sim 0.001 - 0.01$ . (**LO\*** often bigger – compensates for smaller cross-section at **LO**).



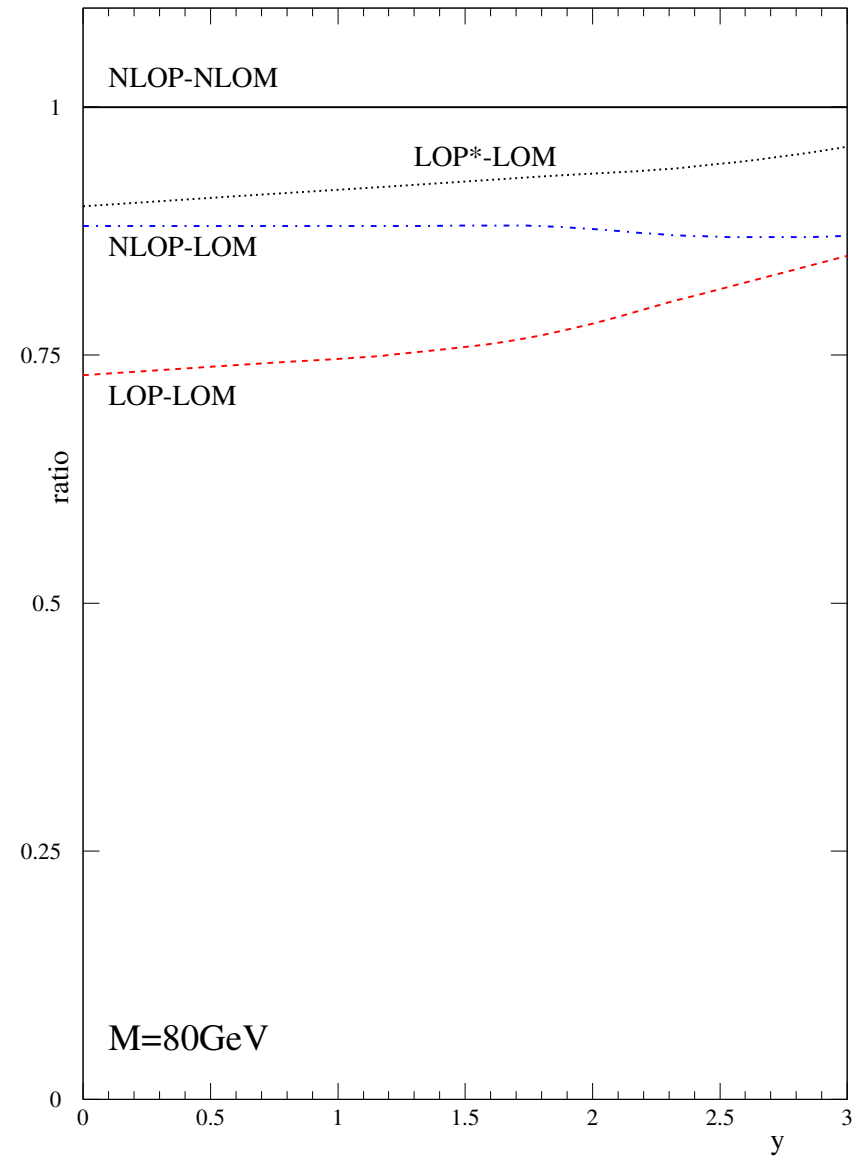
Similarly  $g(x, Q^2)$  is significantly bigger at **LO\*** than at **LO**, and much bigger than **NLO** at small  $x$ .

Should do better for gluon-gluon initiated processes (e.g. **Higgs** production where  $K$ -factors are often much greater than unity).

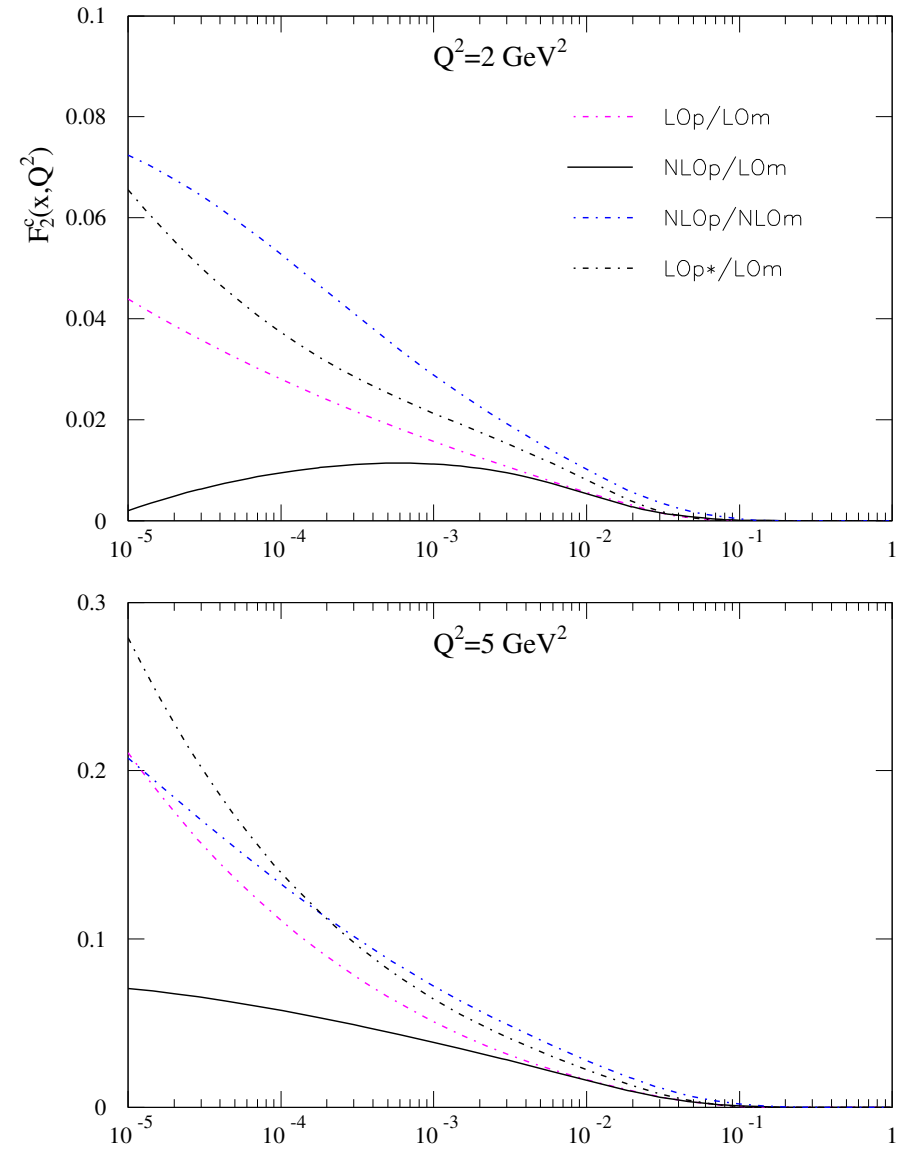


For LHC  $LO^*$  partons lead to shape of comparable quality as NLO partons. Normalization better.

Drell-Yan Cross-section at LHC for 80 GeV with Different Orders



For charm structure function comparing all possibilities  $\text{LO}^*$  partons and  $\text{LO}$  matrix element is indeed nearest to *truth* at low scales.



These are for totally inclusive, strictly fixed order calculations. Consider using generators (work with/by [A Sherstnev](#)) and include parton showering (i.e. use [MC@NLO](#) at [NLO](#)).

Consider first  $Z \rightarrow \mu^+ \mu^-$  production at the LHC with  $p_T > 10\text{GeV}$  and  $|\eta| < 5$

$$\text{NLO}(\text{ME}) \otimes \text{NLO}(\text{pdf}) = 2.40\text{nb}.$$

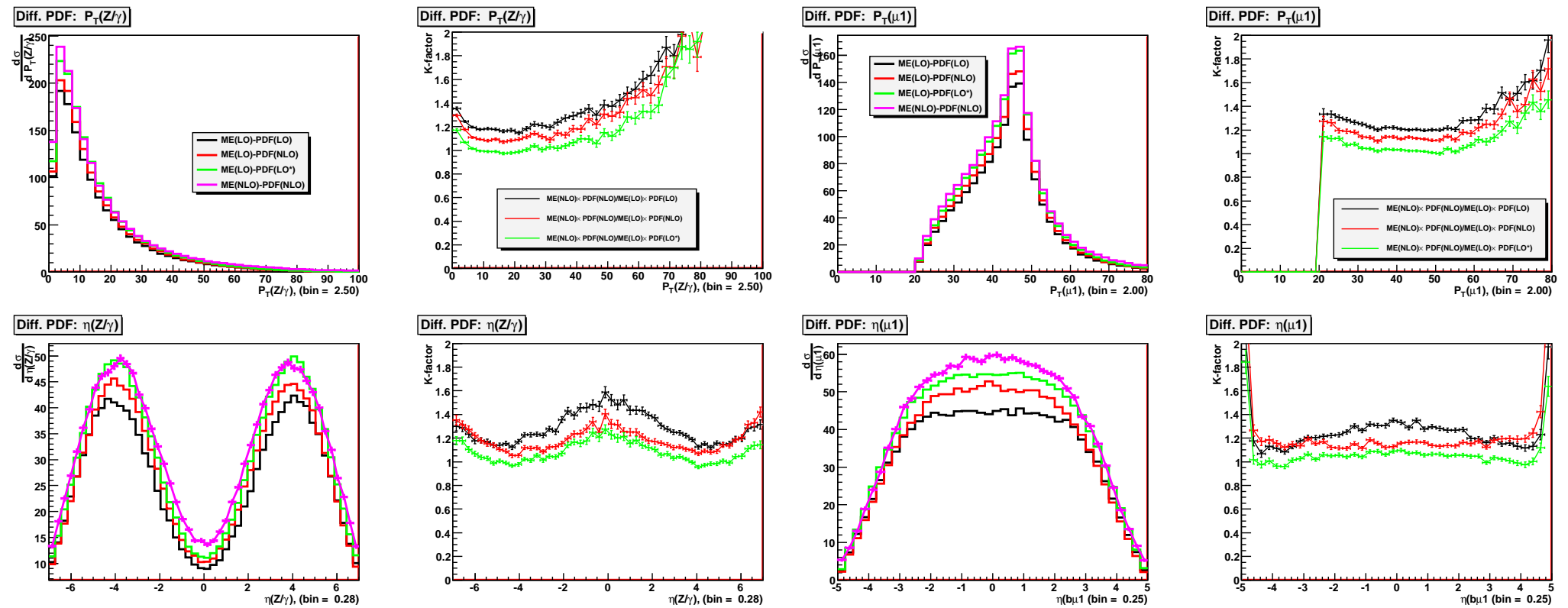
$$\text{LO}(\text{ME}) \otimes \text{NLO}(\text{pdf}) = 1.98\text{nb}.$$

$$\text{LO}(\text{ME}) \otimes \text{LO}(\text{pdf}) = 1.85\text{nb}.$$

$$\text{LO}(\text{ME}) \otimes \text{LO}^*(\text{pdf}) = 2.19\text{nb}.$$

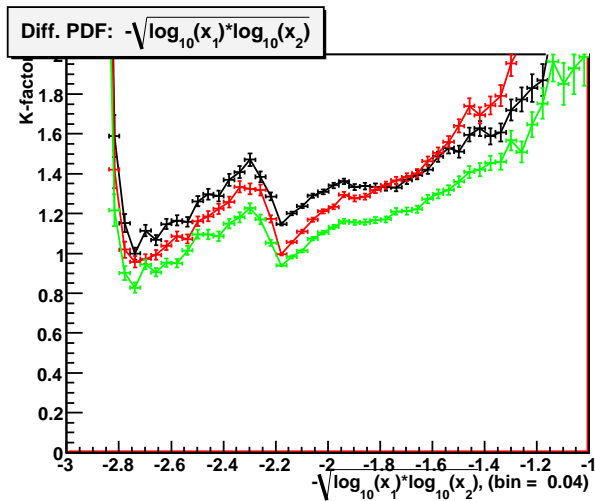
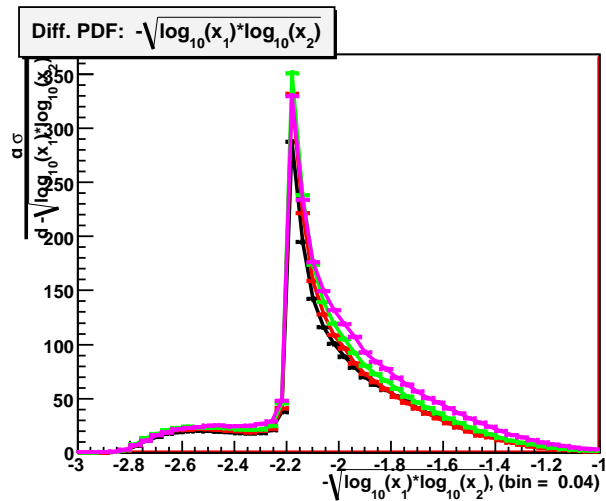
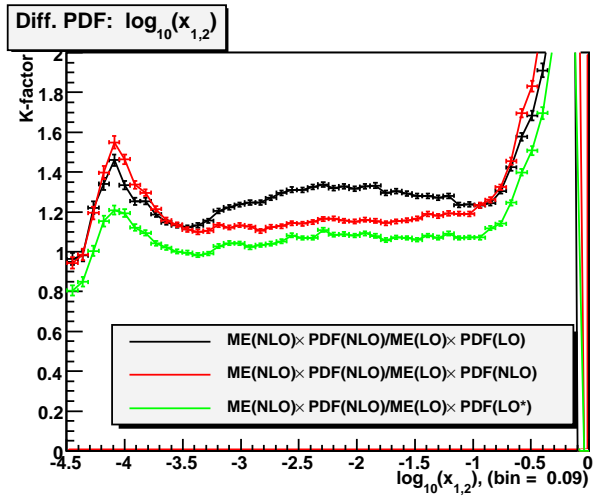
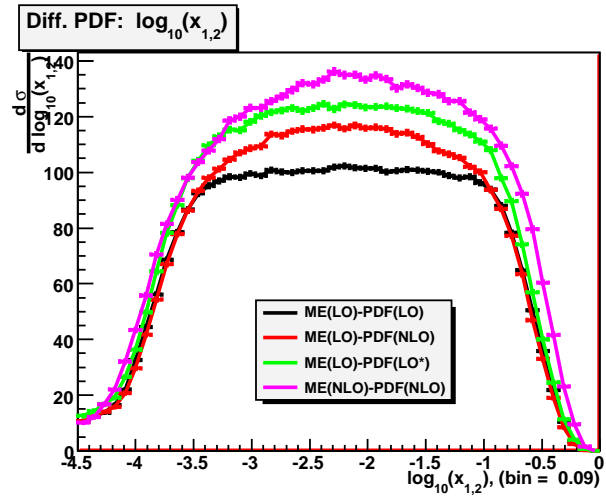
With very similar relative results for  $W \rightarrow \nu\mu$ .

Also look at distributions for  $Z$  boson and final state muon.



Results using **LO\*** partons clearly best. No parton can account for details of  $p_T$ -distribution due to hard emissions at **NLO**.

Examination of values of  $x$  sampled in cross-section shows that deficit in **LO** rates due to lack of partons for  $x \sim 0.01$ .



**NLO** partons have better distribution, but **LO\*** are good in normalization and shape.



Consider also single top production with  $t \rightarrow \mu + \nu + b$  production at the LHC.

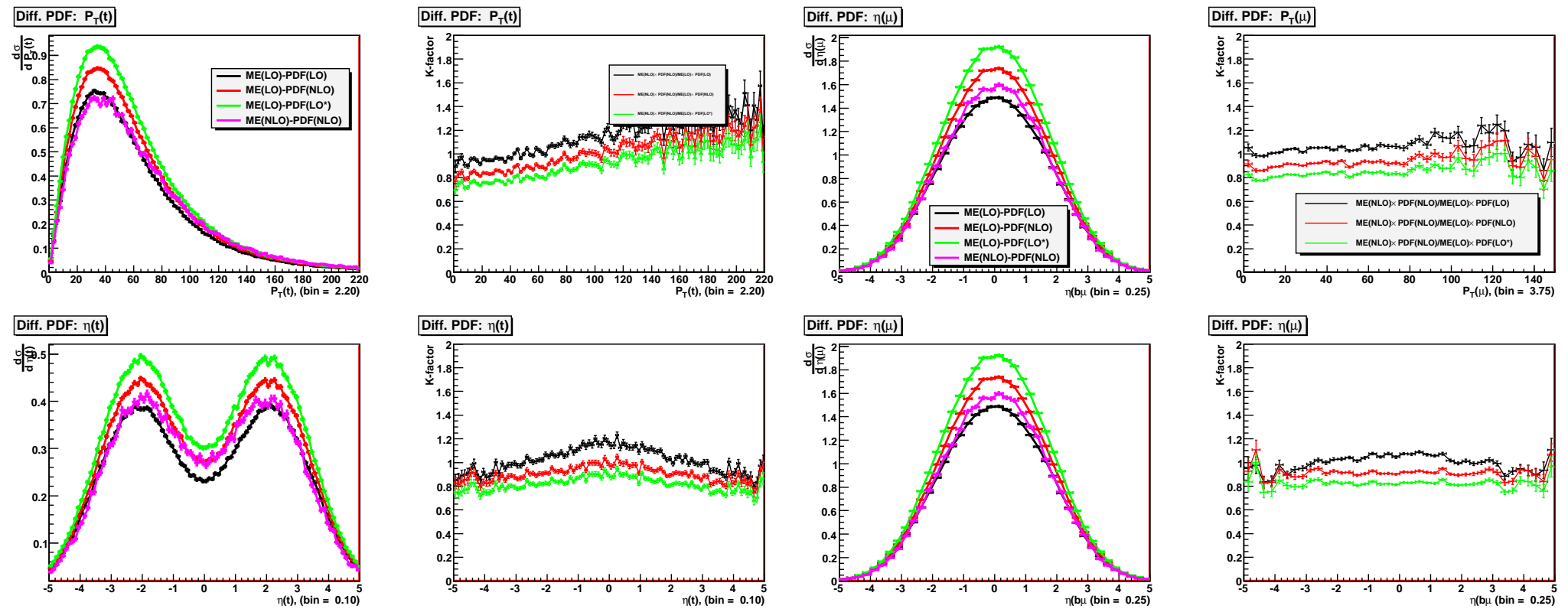
$$\text{NLO(ME)} \otimes \text{NLO(pdf)} = 27.6 \text{ pb.}$$

$$\text{LO(ME)} \otimes \text{NLO(pdf)} = 30.0 \text{ pb.}$$

$$\text{LO(ME)} \otimes \text{LO(pdf)} = 26.4 \text{ pb.}$$

$$\text{LO(ME)} \otimes \text{LO}^*(\text{pdf}) = 33.1 \text{ pb.}$$

Also look at distributions for  $t$  and final state muon.



Results using **LO\*** partons a bit high in normalization, but a better shape than **LO** which has the best normalization. No parton can account completely for details of  $p_T$ -distribution due to hard emissions at **NLO**.

Consider Higgs (130GeV) production at the LHC.

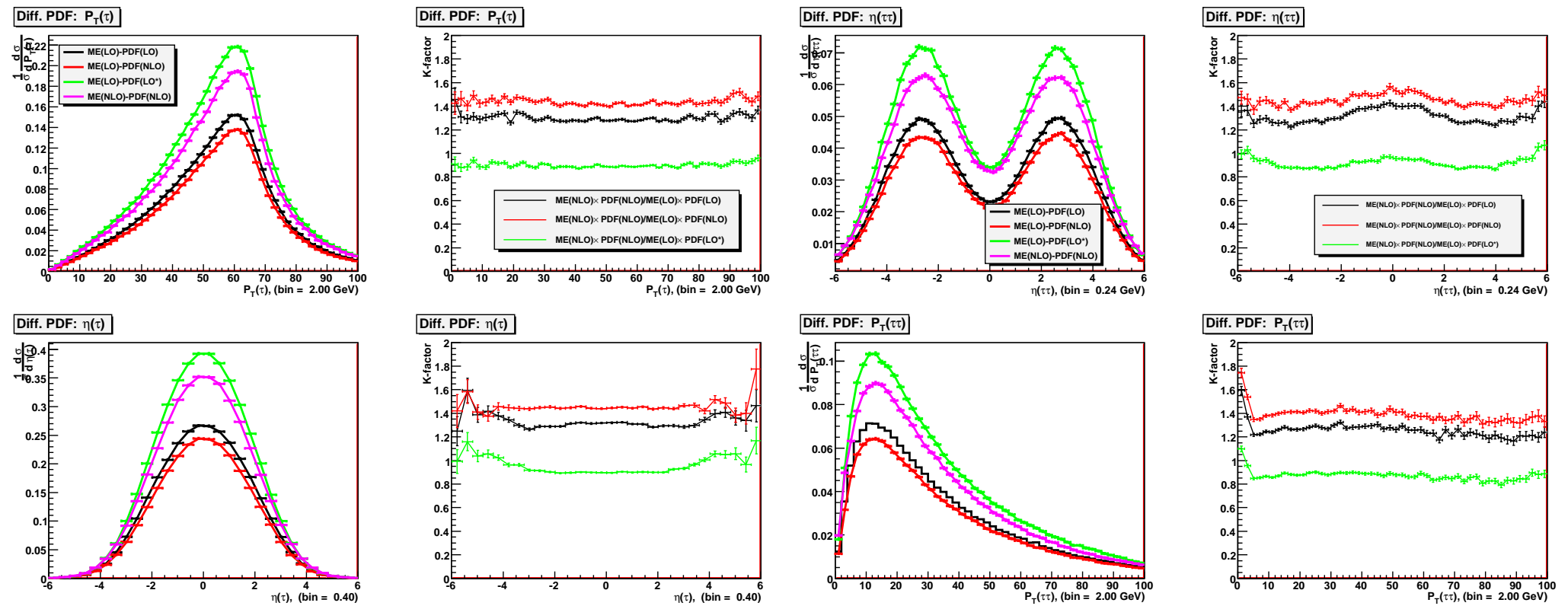
$$\text{NLO(ME)} \otimes \text{NLO(pdf)} = 38.0 \text{ pb.}$$

$$\text{LO(ME)} \otimes \text{NLO(pdf)} = 20.3 \text{ pb.}$$

$$\text{LO(ME)} \otimes \text{LO(pdf)} = 22.4 \text{ pb.}$$

$$\text{LO(ME)} \otimes \text{LO}^*(\text{pdf}) = 32.4 \text{ pb.}$$

Also look at distributions with  $H \rightarrow \tau^+\tau^-$  for single  $\tau$  and  $\tau^+\tau^-$  pair.



Results using LO\* partons clearly best in normalization. All reasonable in shape.

Consider  $b\bar{b}$  production with the included contribution for radiated  $g \rightarrow b\bar{b}$  at the LHC. Noted contribution strictly **NLO** but vital for  $p_T$ -distribution and included in **LO** generators. Cuts  $p_t > 20\text{GeV}$ ,  $|\eta(b)| < 5$   $\Delta R(b, b) > 0.5$ .

$$\text{NLO(ME)} \otimes \text{NLO(pdf)} = 2.76\mu b.$$

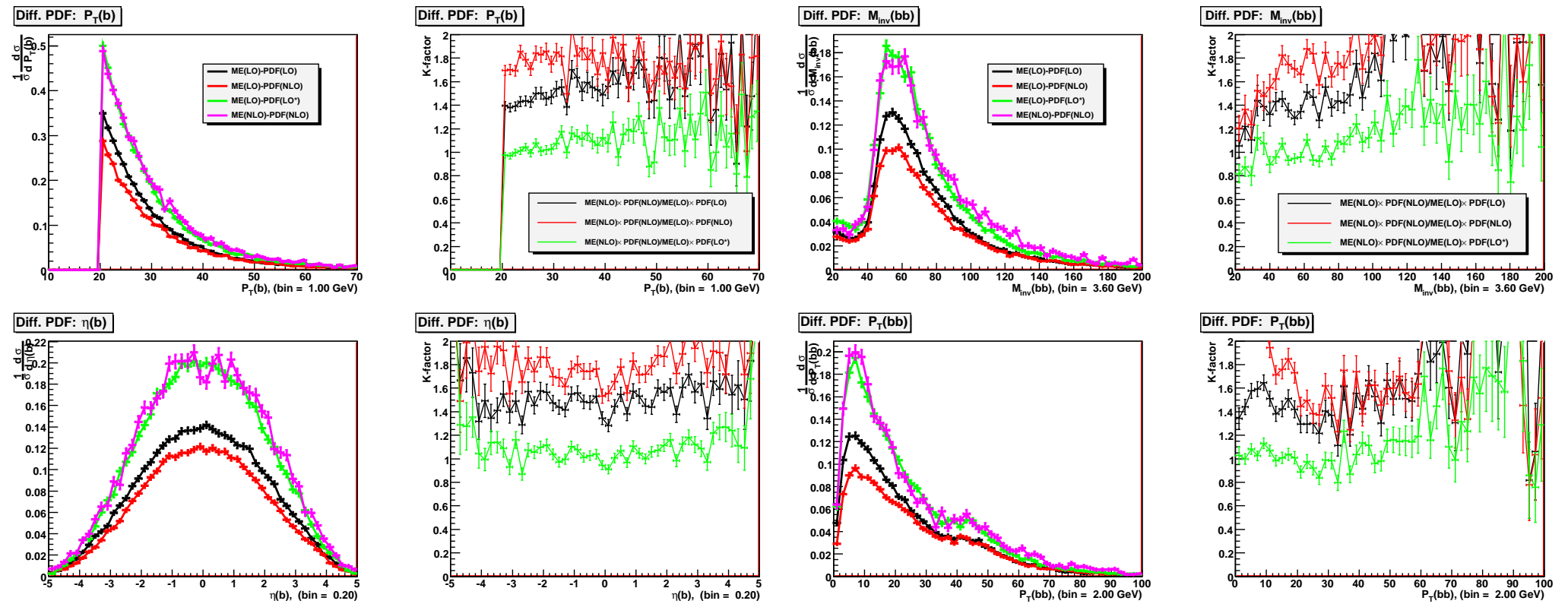
$$\text{LO(ME)} \otimes \text{NLO(pdf)} = 1.56\mu b.$$

$$\text{LO(ME)} \otimes \text{LO(pdf)} = 1.85\mu b.$$

$$\text{LO(ME)} \otimes \text{LO}^*(\text{pdf}) = 2.63\mu b.$$

This process probes the fairly small  $x$  gluon, i.e.  $x \sim 0.001$ , so **NLO** partons are worst due to small gluon at small  $x$ .

Also look at distributions for single  $b$  and  $b\bar{b}$  pair.



Results using **LO\*** partons clearly best in normalization. **NLO** worst and problems with shape at low scales (i.e. small  $x$ ).

Finally consider vector boson production of Higgs + two jets using NLO code VBFNLO (Zeppenfeld *et al*).

$$\text{NLO}(\text{ME}) \otimes \text{NLO}(\text{pdf}) = 4.52 \text{pb}.$$

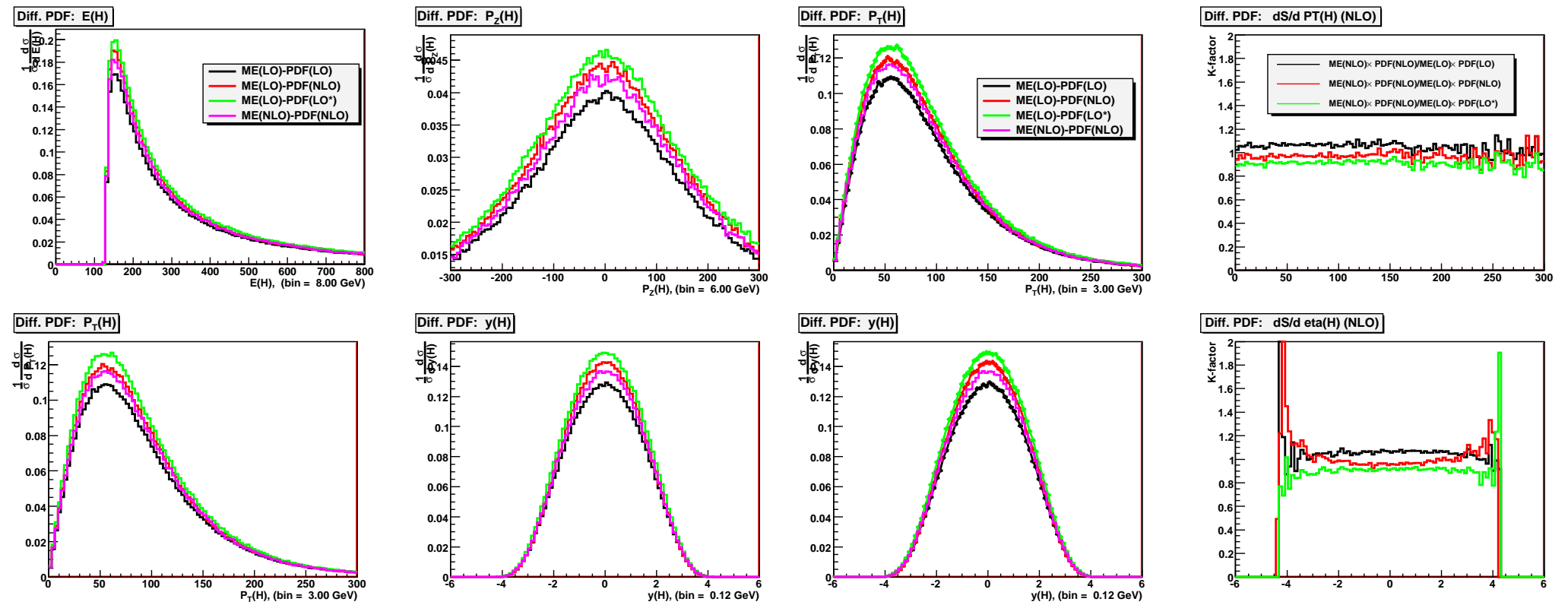
$$\text{LO}(\text{ME}) \otimes \text{NLO}(\text{pdf}) = 4.65 \text{pb}.$$

$$\text{LO}(\text{ME}) \otimes \text{LO}(\text{pdf}) = 4.26 \text{pb}.$$

$$\text{LO}(\text{ME}) \otimes \text{LO}^*(\text{pdf}) = 4.95 \text{pb}.$$

This process probes the fairly high- $x$  quarks, i.e.  $x \sim 0.1$ , and in this case the LO\* partons lead to a slight overestimate of the results.

Also look at distributions for Higgs.



Results using LO\* partons a bit high in normalization. NLO partons a little off in rapidity distribution.



## Conclusions

Neither standard LO and NLO partons ideal for LO generators.

NLO gluon much smaller at small  $x \rightarrow$  qualitative changes. LO quarks usually too small.

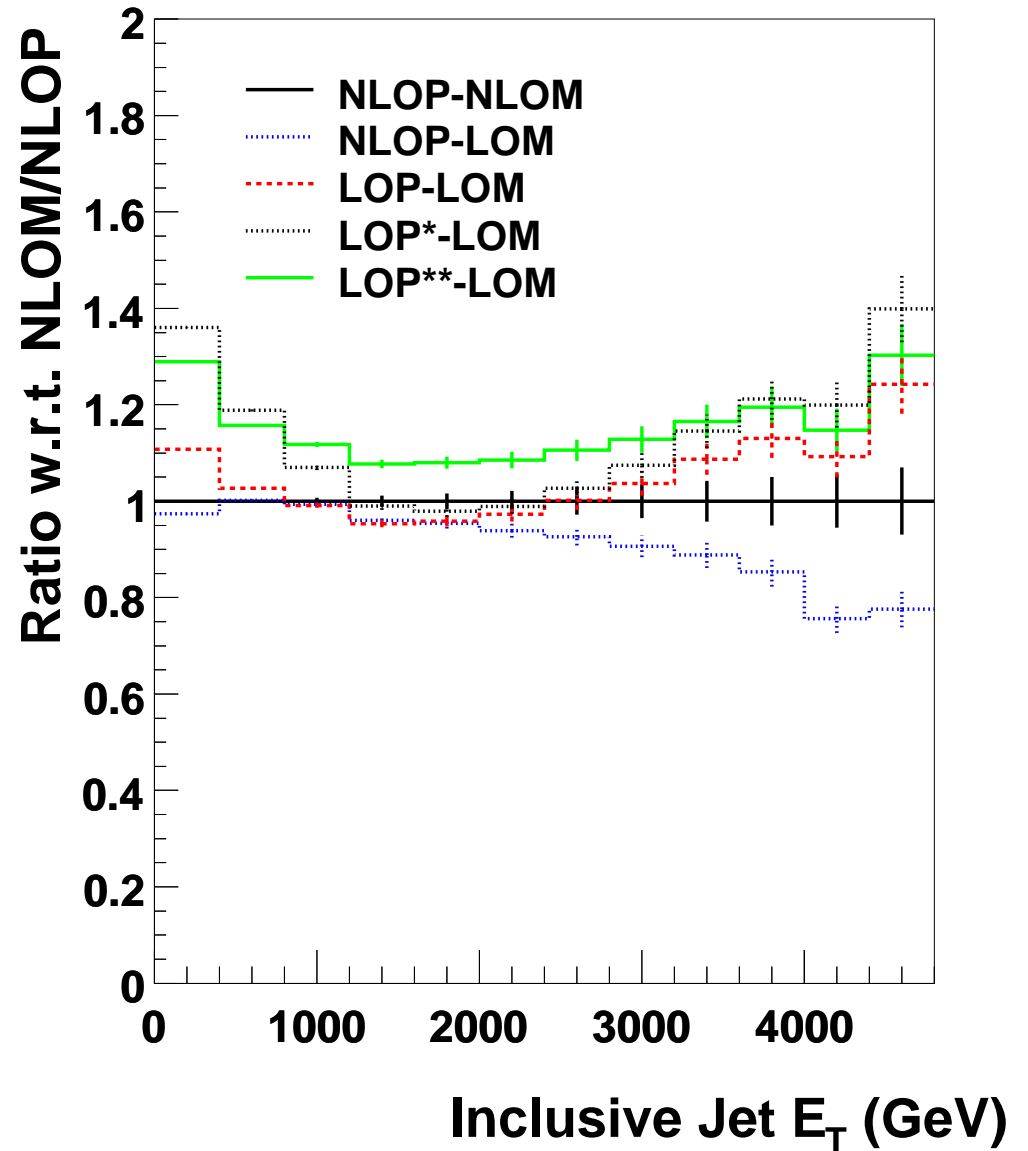
Introduce modified LO partons, i.e. momentum violation plus NLO coupling constant.

Comparison with processes where NLO known suggests modified LO partons usually provides most reliable results – especially if sensitive to smallish  $x$ . Additional partons allowed by extra momentum compensate semi-universally for higher orders.

Never badly wrong for any particular parton in any particular range, unlike standard fixed order.

Also look at other quantities, e.g. very high- $E_T$  jets at [ATLAS](#) (thanks to [Claire Gwenlan](#)).

In this case **LO** and **NLO** partons deviate in shape in opposite directions.



Situation for hadro-production of  $b$  quarks at LHC using strict LO cross-section.  
 (Some bugs here -general features hold).

Particularly large matrix element effect for  $p_T$  distribution in this case.

